



University of Sussex

A University of Sussex DPhil thesis

Available online via Sussex Research Online:

<http://sro.sussex.ac.uk/>

This thesis is protected by copyright which belongs to the author.

This thesis cannot be reproduced or quoted extensively from without first obtaining permission in writing from the Author

The content must not be changed in any way or sold commercially in any format or medium without the formal permission of the Author

When referring to this work, full bibliographic details including the author, title, awarding institution and date of the thesis must be given

Please visit Sussex Research Online for more information and further details

**Multi-electrode analysis of pattern
generation and its adaptation to reward**

Christopher A. Harris

Submitted for the degree of Doctor of Philosophy

School of Life Sciences

University of Sussex

June 2012

Associated journal articles:

Harris C.A., Passaro P.A., Kemenes I., Kemenes G., O'Shea M. (2010) Sensory driven multi-neuronal activity and associative learning monitored in an intact CNS on a multielectrode array. *Journal of Neuroscience Methods* 186(2): 171-178.

Harris C.A., Buckley C.B., Nowotny T., Passaro P.A., Seth A.K., Kemenes G., O'Shea M. (2012) Multi-neuronal refractory period adapts centrally generated behaviour to reward. *PLoS ONE* 7(7): e42493.

I hereby declare that this thesis has not been and will not be submitted in whole or in part to another University for the award of any other degree.

.....

Christopher Harris

Abstract

Much behaviour is controlled by neural circuits known as central pattern generators (CPGs). The aim of the work presented in this thesis was to uncover general mechanisms that modify the behavioural output of CPGs in ways that maximise adaptive fitness. To achieve this aim it was necessary to monitor populations of neurons associated with a CPG that responds to changes in sensory reward. I used multi-electrode arrays (MEAs) to monitor neuronal populations in semi-intact preparations of the snail *Lymnaea stagnalis*. Spike patterns associated with cycles of the feeding CPG were readily recorded in the buccal, cerebral and pedal ganglia. A sensory food stimulus accelerated the CPG and this acceleration was shown to depend on dopamine. Single-trial conditioning on the MEA allowed fictive feeding to be induced by a previously neutral taste stimulus. In addition to the activity of the feeding CPG the MEA also revealed a second neuronal population that had not previously been characterized. This population fires continuously in-between the cycles of the feeding CPG but becomes quiescent for a variable period following each cycle. The duration of this quiescent period often predicted the timing of the next activation of the CPG. Stimulation of a nerve associated with food reward failed to activate the CPG during the quiescent period, indicating that it reflects a 'network refractory period' (NRP) of the kind previously observed in locomotor CPGs. The sucrose and dopamine stimuli both significantly shortened the NRP. These results show that the MEA recording method can identify distinct populations of neurons associated with adaptive feeding behaviour, and suggest a general mechanism that allows a CPG to adapt its behavioural output to maximise reward.

Table of Contents

Acknowledgements	1
List of Figures	2
List of Abbreviations	4
1 Introduction	5
1.1 Central pattern generators (CPGs)	8
1.2 Reward and dopamine signalling	16
1.3 The molluskan feeding CPG	22
1.4 Multi-electrode array (MEA) technology	30
1.5 Aim and thesis structure	33
2 Materials and methods	35
2.1 Animals	35
2.2 Semi-intact preparations	35
2.3 MEA recording equipment	38
2.4 Stabilizing the brain on the array	41
2.5 Microscopy and perfusion	43
2.6 Electrical stimulation techniques	45
2.7 Recording software and settings	46
2.8 Protocols	46
2.9 Monitoring the stomatogastric ganglion on the MEA	47
2.10 Using laser to record neural activity on the MEA	47
3 Results: Spike sorting	50
3.1 Pre-processing	54

3.2	Estimating the spatial origin of spikes	56
3.3	Distinguishing spikes by location and amplitude	57
3.4	Quality control	59
4	Results: Fictive feeding and experimental perturbations	61
4.1	Fictive feeding induced by depolarization of a cerebral neuron	61
4.2	Fictive feeding induced by a chemosensory sucrose stimulus	64
4.3	Dopamine is necessary and sufficient for rapid fictive feeding	71
4.4	Locating identified motoneurons in the buccal ganglia	78
4.5	Cerebral and pedal activity associated with sensory feeding	81
4.6	Classical reward conditioning on the MEA	83
5	Results: A reward-sensitive network refractory period	86
5.1	Feeding cycles are followed by a period of quiescence	86
5.2	The quiescent period is a network refractory period (NRP)	89
5.3	Sensory sucrose and dopamine shorten the NRP	92
5.4	The NRP predicts future activation of the feeding CPG	95
6	Discussion	100
6.1	The MEA recording method	103
6.2	Spike sorting	104
6.3	Feeding cycles	107
6.4	The NRP	108
6.5	Conclusion	113
	References	115
A	Science communication	126
A.1	Communicating dopamine and reward neuroscience	126
A.2	The iPlant project	127
A.3	References	130

Acknowledgements

This thesis represents four years of research carried out at the University of Sussex and would not have been possible without the support of a number of exceptional individuals. My supervisors and mentors Michael O'Shea and George Kemenes, whose outstanding guidance, dedication and clear thinking has been fundamental to my development both as a scientist and as a person. Peter Passaro, who taught me to use and appreciate multi-electrode arrays. Christopher Buckley, who wrote the spike sorting code, taught me MATLAB and provided inspiration and good cheer along the way. Thomas Nowotny, Anil Seth, Ildiko Kemenes, Paul Benjamin, Vincenzo Marra, Zsolt Pirger and Lucas Wilkins, whose experience and assistance greatly improved both my research and my time in Brighton. Ele Wood, who gave me the energy to keep going, and who first realized that the data was suggestive of a refractory period. Finally my family, especially my parents, whom, for their extraordinary example and unfailing love and support, I owe everything.

Thank you all.

Christopher Harris

Stockholm, 29 June 2012

List of Figures

1.1	General framework for brain-based intelligent behaviour	7
1.2	Pattern generation by recurrent excitation	10
1.3	Pattern segmentation by reciprocal inhibition	11
1.4	Rewarding brain stimulation and the reward pathway	18
1.5	The <i>Lymnaea</i> brain	24
1.6	Feeding in <i>Lymnaea</i> is a rhythmic 3-phase pattern	25
1.7	The MEA dish	31
2.1	Semi-intact preparations of <i>Lymnaea</i> stabilized on the MEA	36-37
2.2	Buccal ganglia on the MEA	39
2.3	Entire brains on the MEA	40
2.4	MEA recording rig	44
2.5	The stomatogastric ganglion on the MEA	48
3.1	Voltage spikes recorded on the MEA	51
3.2	Summary of the spike sorting process	52-53
3.3	Spike amplitude at different electrodes indicate neuronal location	55
3.4	Delineating spike clusters	58
3.5	Validating the spike sorting process	60
4.1	Fictive feeding induced by depolarisation of a cerebral interneuron	62-63
4.2	Fictive feeding induced by a sensory stimulus	65-66
4.3	Phase structure of 3-phase feeding cycles	68
4.4	Sensory sucrose stimulus induces fictive feeding	69-70
4.5	Dopamine induces fictive feeding	72-73

4.6	Spontaneous and stimulus-driven feeding cycles are similar in a preparation	74
4.7	Excessive concentrations of dopamine induce expanding cycles	76
4.8	Dopamine antagonist prevents sucrose-induced CPG acceleration	77
4.9	Putatively identified neurons	79
4.10	Local field potentials	80
4.11	Cerebral and pedal activity associated with fictive feeding	82
4.12	Withdrawal-associated activity recorded throughout the brain	84
4.13	<i>In vitro</i> classical reward conditioning on the MEA	85
5.1	Feeding cycles are followed by a period of quiescence	87
5.2	Stimulation of a nerve that mediates food stimuli fails to activate the feeding CPG during the quiescent period	90-91
5.3	Sucrose and dopamine stimuli shorten the refractory period	93-94
5.4	The duration of the NRP predicts the interval to next feeding cycle	96-97
5.5	Inter-cycle interval (ICI) distributions	99
6.1	Partial spike sorting failure during certain bursts	106
6.2	NRP-based mechanism for adapting CPG output to reward	110
6.3	NRP vs. remaining ICIs, all durations and conditions	112
A.1	Public opinion about medical application of RBS	128

List of Abbreviations

CNS	Central nervous system
CPG	Central pattern generator
ICI	Inter-cycle interval
LFP	Local field potential
MEA	Multi-electrode array
NRP	Network refractory period
STG	Stomatogastric ganglion

Chapter 1

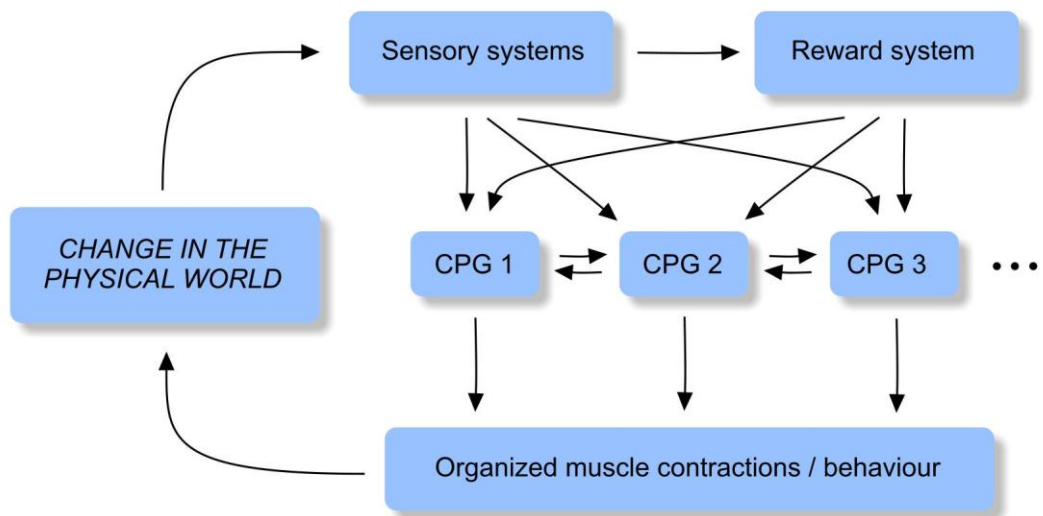
Introduction

Brains are complex neural networks evolved to generate behaviours that maximize reproductive success: breathing, feeding, locomotion, self-defence, mating, cooperation, imitation, communication, altruism, tool use and so on. Motor behaviours are muscle contractions organized into meaningful sequence by the electrical activity of dedicated neural circuits. The rhythmic contractions of the diaphragm that drive breathing for example are driven by a neural circuit in the hindbrain and brain stem (Smith et al., 2009). If excised and kept alive *in vitro* this circuit continues to generate rhythmic bursts of electrical activity - so called 'fictive breathing'. Neural tissue from the region of the spinal cord that controls walking similarly continues to generate alternating bursts of electrical activity *in vitro*, but only if the circuit is activated by an electrical or chemical stimulus (Streit et al., 2006). This is because the 'walking circuit', like most motor circuits, is only active *in vivo* while disinhibiting commands from other brain regions act on it, i.e. while the brain chooses to walk. In addition to such on-off commands, neural circuits that drive behaviour respond to a range of modulatory signals by adjusting the rate, intensity and pattern of the behaviour they control. This allows the brain to fine-tune behaviour to changing circumstances. But how do brains decide when and how to perform different behaviours? How do they determine precisely which patterns of activity will maximise reproductive success in an unpredictable environment? What, in short, is the neural basis of intelligent behaviour? This is a fundamental question facing the neurosciences today.

In this thesis I consider two features of the brain that are of particular importance for the generation of intelligent patterns of behaviour: central pattern generator (CPG) circuits and dopamine signalling. CPGs, described in Section 1.1, are neural circuits whose anatomical and physiological properties allow them to generate

repeating, precisely timed patterns of electrical activity. A range of behaviours, including locomotion, feeding and mating, have been associated with specific CPGs in a number of species (Grillner, 2006; Marder and Bucher, 2001; Selverston, 2010; Wagenaar et al., 2010). Dopamine signalling, discussed in Section 1.2, is involved in the detection and acquisition of ‘rewards’, such as food or mates. In a range of species dopamine signalling adapts neural and behavioural activity in ways that maximise adaptive fitness (Barron et al., 2010; Schultz, 2007; Wise, 2006). Specifically, dopamine facilitates at least three brain processes that are fundamental to intelligent behaviour: *classical learning*, in which the association between a stimulus and a reward is stored in memory (Kemenes et al., 2011; Lisman and Grace, 2005; Wise, 2006); *operant learning*, in which the association between a stimulus, a behaviour and a reward is stored in memory (Lindskog et al., 2006; Wise, 2006); and *free operant behaviour*, where dopamine adapts the rate and vigour of behaviour to reward (Cools and Robbins, 2004; Niv et al., 2007). We can think of CPGs as defining key components of an animal’s behavioural repertoire and of dopamine as acting on CPGs to facilitate the selection and effective execution of behaviours that maximise reward acquisition in a given environment. This general model of the neural basis of intelligent behaviour is summarized in Figure 1.1.

Our ability to understand and computationally model CPGs, dopamine signalling and their interaction is limited by our inability to identify, monitor and manipulate the activity of many neurons simultaneously. Dye imaging can resolve the simultaneous activity of hundreds of neurons (Ahrens et al., 2012; Briggman and Kristan, 2006) but is associated with poor temporal resolution (<1 kHz, although see (Miller et al., 2012)), neurotoxic and other unwanted effects on the activity of neurons, photo-bleaching and poor uptake of the dye resulting in low signal-to-noise. Microelectrodes on the other hand have a very high temporal resolution (≥ 40 kHz) and can both deliver and record electrical current, but have a spatial resolution that is limited by the size and shape of the electrodes. Since the advent of multi-electrode array (MEA) recordings in the 1950s the number of neurons that can be simultaneously monitored by electrodes has doubled every 7 years (Stevenson and Kording, 2011). In cortical recordings that number now approaches 500 – a small fraction of the total number of neurons present in most model nervous systems.



1.1 General framework for the neural basis of intelligent behaviour

Central pattern generator circuits (CPG 1, 2, 3 etc.) organize muscle contractions into meaningful behaviours that change the physical world. The changes are monitored by sensory systems that modulate CPG activity. Patterns of CPG activity that become associated with reward are reinforced in order to maximise the adaptive fitness of the animal.

Invertebrate brains contain fewer neurons than vertebrate brains, and their analysis has led to key breakthroughs in neuroscience (Hodgkin and Huxley, 1939, 1952; Kandel, 2001), including the detailed characterization of different CPGs and their adaptive mechanisms (Brembs, 2011; Brembs et al., 2002; Marder and Bucher, 2007; Selverston, 2010). However, although two early studies showed that MEAs can be used to record voltage spikes in intact invertebrate ganglia (Gross, 1979; Novak and Wheeler, 1986) this experimental approach has remained largely unexplored.

This thesis introduces an MEA method for locating and recording the simultaneous activity of many neurons in intact invertebrate brains with active sensory organs (Harris et al., 2010). The method involves the stabilization of the brain on a flat MEA (Chapter 2) and the triangulation of neuronal activity by means of a custom-made spike sorting procedure (Chapter 3). The aim of the thesis is to show how this technique can be used to better understand the neural basis of the adaptive feeding behaviour of the snail *Lymnaea stagnalis*. To this end, I monitor populations of neurons associated with the feeding CPG while using a range of sensory, pharmacological and electrical stimulation techniques to manipulate the output of the CPG (Chapter 4). This analysis shows how two neuronal populations interact to adapt feeding behaviour to changes in dopamine and the availability of food (Chapter 5).

In the first Section of this introduction I review research on CPGs. In the second Section I discuss our current understanding of how dopamine signalling optimises the activity of neural circuits associated with reward-seeking behaviours such as feeding. In the third Section I describe the feeding CPG of *Lymnaea*. In the fourth Section I describe the MEA recording technology. Finally I outline my research aims and the structure of the thesis.

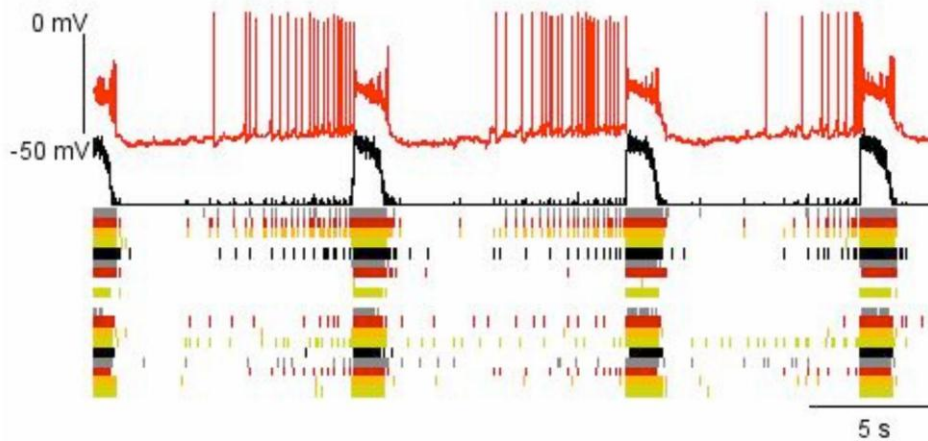
1.1 Central pattern generators (CPGs)

To control behaviour neural circuits must generate intricately structured bursts of electrical activity that contract the various muscles involved in different behaviours. These burst patterns must moreover be adjustable to allow optimal performance in changing environments. Neural circuits employ a number of anatomical and physiological mechanisms to achieve these goals. ‘Pacemaker currents’ for example allow neurons to generate ‘plateau potentials’, either spontaneously or in response to

activating commands. Such neurons have two relatively stable states: a hyperpolarized 'down-state' and a depolarized 'up-state' that often involves rapid spiking. By oscillating between these two states pacemaker neurons can drive a basic pattern of rhythmic activity in a neural circuit (Grillner, 2006; Selverston, 2010). Many continuously active motor circuits, such as those controlling heartbeat, breathing and mastication, derive their motor pattern from pacemaker neurons and continue to fictively 'beat', 'breathe' and 'digest food' for hours *in vitro*.

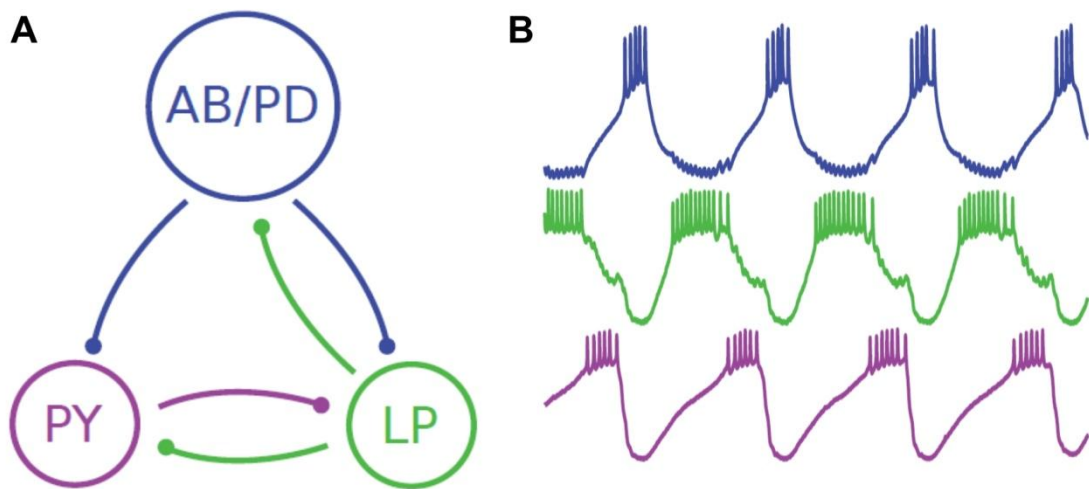
Also the synaptic properties of a circuit can generate rhythmic patterns of electrical activity. For example, spontaneously firing neurons connected by excitatory synapses can gradually depolarize each other and activate other, otherwise silent neurons, resulting in a spread of activity that culminates in a synchronized network-wide burst (Streit et al., 2006). Such connectivity is called 'recurrent excitation' and can generate rhythmic activity in a network if a burst-terminating mechanism, such as activity-dependent up-regulation of the Na/K-pump, is also present. Figure 1.2 shows a pattern of rhythmic bursting generated by a population of recurrently excitatory neurons from the spinal locomotor CPG of the rat. Here, intrinsically spiking neurons in the population gradually recruit other neurons, triggering population-wide bursts of spikes that drive contraction of the hind legs *in vivo*. Each burst up-regulates the activity of the Na/K-pump in neurons, which eventually terminates the burst and produces a 'network refractory period' during which neurons are transiently hyperpolarized and the CPG refractory to further activation (Darbon et al., 2002; Darbon et al., 2003; Streit et al., 2006).

Most behaviours involve consecutive contraction of different muscles and therefore require specific motor neurons to fire in sequence. Neurons that are reciprocally connected by inhibitory synapses can generate such multi-phase patterns (Selverston, 2010). Figure 1.3 shows the alternating pattern of bursting generated by mutually inhibitory neurons in the stomatogastric ganglion. The two neuronal populations that control the hind legs in vertebrates are similarly connected, across the spinal midline, by inhibitory synapses that organize locally generated bursts (Figure 1.2) into an alternating pattern of bursting that drives sequential contraction of the left and right leg (Streit et al., 2006). Such pattern segmentation by 'reciprocal inhibition' requires an activity-dependent mechanism that allows neurons to escape from



1.2 Pattern generation by recurrent excitation

Rhythmic bursting in a population of neurons from the spinal locomotor CPG of the rat. An intracellular recording of an intrinsically spiking neuron (red trace) is shown together with the total spike rate of the population (black trace) and the spiking activity of many individual neurons (raster plot). Intrinsically active neurons in the population recruit other neurons through recurrent excitation, resulting in population-wide bursts. Each burst activates a burst-terminating mechanism that hyperpolarizes neurons and causes a transient cessation of intrinsic spiking. During this quiescent period the network is refractory to further activation. Adapted from Streit et al., 2006.



1.3 Pattern segmentation by reciprocal inhibition

A: Key neurons in the pyloric CPG, which controls mastication in crustaceans. The AB/PD neuron is a pacemaker neuron, whereas the LP and PY neurons fire on post-inhibitory rebound. All chemical synapses in the CPG are inhibitory. **B:** The reciprocally inhibitory connectivity of the pyloric CPG results in a 3-phase pattern of sequential bursting. Three complete cycles of the pyloric rhythm are shown. Adapted from Kispersky et al., 2011.

inhibition after a delay. Such mechanisms include spike-frequency adaptation, synaptic depression and ‘post-inhibitory rebound’, which refers to the generation of a transient plateau potential in a neuron following a period of hyperpolarization (Selverston, 2010). Mixed circuits, in which one neuron excites a second neuron which in turn inhibits the first neuron, can also generate multi-phase patterns. The feeding CPG of the snail *Lymnaea* is one such circuit (see Section 1.3).

Even the properties of individual neurons can introduce multi-phase structure into the bursting activity of a neuronal circuit. Membrane and synaptic properties can for example delay the onset of spiking in a postsynaptic neuron by several seconds, and activity-dependent synaptic processes can modulate the strength of a synapse over time or induce a switch from excitation to inhibition or vice versa (Selverston, 2010). For a comprehensive discussion of pattern generating mechanisms, see (Grillner, 2006; Selverston, 2010).

CPGs are neuronal circuits that instantiate one or more of the mechanisms of pattern generation for the purpose of driving a specific motor behaviour. For a circuit to be defined as a CPG the pattern generating mechanisms must be local to the circuit so that the complete pattern can be generated without additional patterned input. To verify that a circuit is a CPG it is therefore often necessary to isolate the circuit by severing afferent axons, by excising or reconstructing the circuit *in vitro* or by creating a computational model of the circuit. The definition of a CPG does allow however for a constant input to drive patterned activity, since many CPGs are under tonic inhibition *in vivo* and must receive a disinhibiting command signal to initiate pattern generation (Benjamin et al., 2010).

The first circuit shown to be rhythmogenic in the absence of patterned input was the ‘flight control system’ of the locust (Wilson, 1961). Since that discovery a number of CPG circuits have been characterized in detail. These control a range of rhythmic behaviours, including breathing and feeding in mollusks; heartbeat, swimming, crawling and mating in the leech; heartbeat and mastication in crustaceans; and breathing and locomotion in vertebrates (Benjamin, 2012; Elliott and Susswein, 2002; Grillner, 2006; Marder and Bucher, 2001, 2007; Selverston, 2010; Wagenaar et al., 2010). An important question regarding these CPGs is how similar the spike pattern that the circuit generates in isolation is to the pattern that drives behaviour *in vivo*.

One approach is to compare the duration and timing of the activity phases in a pattern recorded *in vitro* with electromyographic muscle recordings from the intact animal. In the lobster such comparisons have shown a close correspondence between the rhythm generated *in vitro* by the mastication circuit (Figure 1.3) and recordings from electrodes implanted to measure stomach motor patterns (Marder and Bucher, 2001). In other CPGs, such as the one controlling flight in the locust, there are significant differences between the pattern generated by the circuit *in vivo* and in isolation (Marder and Bucher, 2001; Wilson, 1961). This indicates that some CPGs depend more on sensory feedback than others.

Most well-characterized CPGs involve an intricate combination of several pattern generating mechanisms distributed over many neurons. Importantly, this allows CPGs to generate a range of subtly different spike patterns, so that muscle behaviour can be dextrously adapted to changing circumstances. The speed of escape behaviour in the zebrafish is for example modulated both by the variable number of spinal interneurons that participate in generating the behaviour (McLean et al., 2007) and by the variable rate at which those interneurons fire (Bhatt et al., 2007). This allows the zebrafish to adapt the intensity of its escape behaviour to the perceived level of threat.

Sometimes the recruitment of new neurons can add to the frequency or strength of behaviour by introducing new, temporally distinct phases into the circuit's spike pattern. Consider for example the swim CPG of the mollusk *Clione*, which produces alternating contractions of the left and the right wing muscles. Here, two pacemaker neurons with post-inhibitory rebound properties are connected by reciprocal inhibition and generate the basic 2-phase pattern at a low frequency. A third neuron in the circuit is inhibited by the first neuron, which it excites, and excited by the second neuron, which it inhibits. When the third neuron is activated it shortens both phases of the original 2-phase pattern so that faster frequencies and thus faster swimming is possible (Selverston, 2010).

The individual phases of a CPG's spike pattern can in addition often be selectively modified by proprioceptive feedback and other modulatory signals that serve to adapt behaviour to the demands of the moment. Consider again the swim CPG of *Clione*. Here the firing rates of neurons that control the left and right wing muscles

are modulated by a gravity-sensing organ that ensures the animal's upright posture in the water (Levi et al., 2004). Interestingly, 'cerebral hunting neurons' are able to 'hijack' this sensory organ by exciting its sensory neurons to the point of triggering a chaotic output pattern. This chaotic pattern is communicated to the swim circuit and causes it to generate an unpredictable pattern of movement that allows the animal to capture nearby prey (Levi et al., 2004, 2005).

In some cases the spike pattern of a motor CPG can be modified to such an extent that a single circuit is able to drive functionally distinct behaviours (Briggman and Kristan, 2008). Such CPGs are said to be 'multi-functional'. Crawling and swimming behaviour in the leech is for example generated by a multi-functional circuit that can generate either a slow 'crawling rhythm' or a fast 'swimming rhythm' (Briggman and Kristan, 2006). The two behaviours are generated by two overlapping populations of neurons. Fewer neurons are involved in swimming than in crawling and more than 90% of the swim-neurons are phase-locked also to the crawling rhythm, suggesting that the ability to swim evolved in this circuit after the ability to crawl (Briggman and Kristan, 2008). Whether a leech decides to crawl or swim away from a touch to the skin depends on sensory neurons that monitor the amount of water surrounding the animal and modulate the multi-functional locomotor CPG accordingly (Briggman and Kristan, 2008).

Traditionally the concept of the CPG has only been used in reference to motor circuits that drive rhythmic behaviours. Recently however the concept has been broadened in two important ways (Grillner, 2006; Yuste et al., 2005). First, many non-rhythmic behaviours such as reflexes, defensive postures and emotional expressions depend on the same pattern generating mechanisms that underlie rhythmic behaviours (Grillner, 2006). The difference is that non-rhythmic behaviours are generated by neural circuits that respond to activating input with one rather than repeated instances of their activity pattern, perhaps due to an absence of burst-terminating mechanisms. It may therefore be appropriate to refer to these circuits as 'non-rhythmic' CPGs.

Second, circuits have now been identified throughout the mammalian brain that share many biophysical and dynamic properties with rhythmically active CPGs, but which are not directly involved in the organization of muscle contractions. Cortical

microcircuits for example generate rich spontaneous patterns (Ikegaya et al., 2004), include numerous pacemaker neurons and are characterized anatomically by recurrent excitation within and reciprocal inhibition between functionally distinct neuronal populations (Yuste et al., 2005). It has been argued that a single set of mechanisms guide the development of functional circuits throughout the brain (Edelman, 1993) and that the evolution of brains should be understood as progressive complexification or ‘encephalization’ of basic rhythmic motor circuits (Yuste et al., 2005). Much theoretical neuroscience rests on the concept of dynamic, functionally distinct neural populations, variously called ‘neuronal groups’ (Edelman, 1993), ‘cell assemblies’ (Cools and Robbins, 2004), ‘neural ensembles’ and attractors (Djurfeldt et al., 2001; Stringer et al., 2003). The identification and characterization of CPG-like circuits that control specific behaviours and span multiple brain regions in the mammalian CNS is therefore a key challenge for research in the neurosciences.

Identifying such circuits is not an easy task. As mentioned previously, current electrophysiological recording techniques do not allow us to record more than a fraction of the many neurons expected to contribute to the control of specific behaviours in the mammalian brain. This makes it difficult to estimate the size and dynamics of putative CPG circuits in the higher regions of the mammalian brain. We should also assume significant overlap between functionally distinct circuits (Yuste et al., 2005), especially those that activate comparable sets of muscles. However, as we have seen, even simple invertebrate CPGs overlap (i.e. some neurons are phase-locked to more than one motor pattern) and can vary considerably in size (Briggman and Kristan, 2008, 2006). Another factor that makes it difficult to determine the structure of putative CPGs in the mammalian brain is that some neurons will likely be more essential to the generation of a specific behaviour than others. However, this too is something we see in invertebrate CPGs, where neurons vary both in terms of their participation in successive repetitions of a motor pattern (Hill et al., 2009) and in terms of the impact their deletion has on the pattern. These observations suggest that the concept of distinct CPGs or CPG-configurations controlling specific behaviours may be useful in understanding complex mammalian behaviours, especially rhythmic behaviours. To this end, I will use the term CPG to refer not only to the core group of essential pattern-generating neurons, but to all neurons whose activity is phase-locked

with or otherwise predicts a specific recurring behaviour (see Section 1.3).

Numerous questions about the nature of CPGs remain. For example, what anatomical and physiological principles distinguish CPGs that control different behaviours? How do CPGs change over time and with training? What neural mechanisms are required for the generation of intricate patterns of muscle contraction, such as those involved in playing tennis or making pancakes?

1.2 Reward and dopamine signalling

As we saw in the previous Section, CPGs allow for the generation of a range of repeating neural and behavioural patterns, which can be fine-tuned to facilitate successful performance in a constantly changing environment. The questions regarding the neural basis of intelligent behaviour that were posed at the beginning of the Chapter can therefore be re-formulated and stated as questions about how brains control their CPGs. For example, how does a brain choose which CPGs should be active at any given time? How is the precise activity pattern and performance of a CPG evaluated and improved? How do different sensory and cognitive states change the activity of CPGs? We can imagine how CPG circuits that drive adaptive muscle contractions, such as breathing, walking and feeding, might evolve in a species by genetic combination of different pattern-generating mechanisms in the brain, and how genes for particularly useful CPGs might spread through the gene pool. We can also imagine the evolution of hard-wired activation of specific CPGs in response to specific sensory cues, i.e. unconditioned responses such as feeding in response to food stimuli, sexual display in the presence of attractive mates, escape behaviour in response to perceived threats, and so on. But behaviours and their underlying CPGs also adapt during the life-time of an animal. In particular, brains continually check whether the patterns of neural and behavioural activity that they have evolved to generate in different situations in fact increase their access to primary rewards, such as food and mates, or learned rewards such as money. Crucially, brains then selectively reinforce and repeat patterns of activity that appear to increase adaptive fitness. Understanding this process of evaluation and selective reinforcement is a fundamental prerequisite for any comprehensive understanding of the neural basis of intelligent behaviour.

Neuroscientific research into the link between behaviour and reward began in

earnest in the 1950s and 1960s following the discovery that animals, including humans, work extremely hard to have electrical current applied to certain regions of the midbrain, hypothalamus or striatum (Bishop et al., 1963; Johansen, 2005; Olds and Milner, 1954; Wise, 1996). This technique, called ‘rewarding brain stimulation’ (RBS), was shown to depend on the activation of dopaminergic neurons in the midbrain, and pre-treatment with dopamine receptor antagonists strongly attenuated the rewarding effect (Fouriez and Wise, 1976). Since then, dopamine has been shown to play a crucial role in various forms of reward-seeking and reward-learning across animal phyla (with the possible exception of arthropods) (Barron et al., 2010). Even in the simple worm *C. elegans* dopamine facilitates basic forms of food-seeking behaviour and learning (Hills et al., 2004; Qin and Wheeler, 2007). Dopamine also plays an important role in motor-control and in the initiation of voluntary movement, although pharmacological blockade of dopamine signalling impairs reward-seeking and reward-learning before it impairs motor-control (Wise, 2006). In the mammalian brain, these dual aspects of dopamine function appear to depend on distinct pathways (Figure 1.4), with one dopaminergic projection from the substantia nigra to the dorsal striatum mainly subserving motor functions and a second pathway from the ventral tegmental area to the ventral striatum, hippocampus and frontal cortex mainly subserving reward-associated functions. This latter pathway is often called the ‘reward pathway’ and is the target of electrical stimulation in RBS.

The definition of the term ‘reward’ is controversial. I define a reward as an object or event that induces approach and consummatory behaviour, and produces short- or long-term learning of that behaviour. This definition differs in two ways from a more restrictive definition, such as Wolfram Schultz’s (Schultz, 2007). First, whereas Schultz holds that rewards must induce long-term memory, I argue that a stimulus-induced increase in the rate and intensity of approach and consummatory behaviour can be thought of as a reward-response regardless of whether it produces lasting behavioural change. This distinction has physiological consequences: as I discuss below, both classical and operant conditioning involve brief bursts of spikes in dopaminergic neurons (Kim et al., 2012; Tsai et al., 2009), whereas the rate and intensity of ongoing behaviour, and the stability of working memory representations, are regulated by the

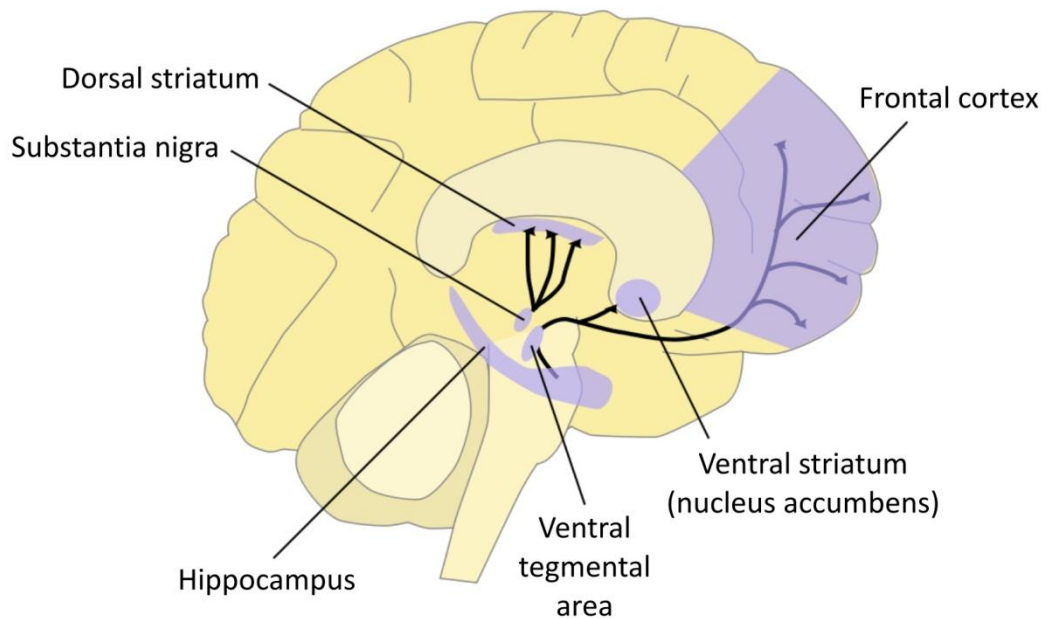


Figure 1.4. Dopamine pathways in the human brain

The human brain contains two primary dopaminergic pathways. One projects from the substantia nigra to the dorsal striatum and mainly subserves motor functions. The second projects from the ventral tegmental area to the ventral striatum, hippocampus and frontal cortex. This second pathway is called the 'reward pathway' and subserves reward-seeking and reward-learning functions (see text).

tonic background concentration of dopamine (Cools and Robbins, 2004; Niv et al., 2007), which is set by the number of tonically active dopamine neurons. Schultz only considers the burst pattern a reward-response, whereas I think of both firing patterns as signalling reward. In this I follow for example Yael Niv, who has shown that, at least in the case of foraging behaviour, the average rate of reward adapts the rate and intensity of approach and consummatory behaviour by modulating the tonic concentration of dopamine in the brain (Niv et al., 2007). This view is also in accordance with Norman White's, who writes that rewards are stimuli that elicit approach behaviour whereas 'reinforcers' induce memory consolidation (White, 1989). Roy Wise similarly points out that 'priming' is an important energizing effect of rewards, but one which does not find its way into long-term memory (Wise, 2009).

My second disagreement with Schultz is that, unlike him, I do not think a reward must be a consequence of decision making. I base this view on two arguments. First, many cases of classical conditioning where a neutral stimulus is paired with for example food, producing a subsequent preference for the neutral stimulus, do not involve any decision making and so cannot according to Schultz be said to involve reward. This however is in stark contrast to numerous papers that describe such experiments as 'classical reward conditioning', and the food stimuli used as rewards (e.g. (Kim et al., 2007)). Second, assume a hungry rat is given a food pellet, either at a randomly chosen time or as a consequence of the rat wandering into a pre-defined section of its cage. Do we really want to say that the pellet is a reward in the latter case but not in the former? Physiologically there will be no difference: the dopaminergic burst response and its effect on synaptic plasticity and memory (described below) will be the same in both cases. In my view brains achieve adaptive behaviour by responding to *correlations* between their own activity states (be they sensory- or motor states) on the one hand and varying concentrations of dopamine on the other. Whether or not a reward is in fact the causal outcome of a decision is irrelevant from the perspective of the brain. My definition of a 'reward' therefore does not require that a reward be the consequence of some specific choice or action, though the majority of the rewards that brains encounter in the real world probably are.

The dopaminergic neurons of the reward pathway are large, electrically coupled cells that fire synchronously and release dopamine homogeneously into very wide

regions of tissue (Glimcher, 2011). The transmitter diffuses rapidly from the synaptic cleft and often acts extrasynaptically (Schultz, 2007). It is therefore common to think of reward-associated dopamine signalling in the brain as a scalar signal. However, as previously mentioned, research on dopamine distinguishes between *phasic* dopamine signalling, which promotes long-term memory formation by changing synaptic connectivity, and *tonic* dopamine signalling, which reinforces on-going neural and behavioural activity. Phasic dopamine refers to the brief (approx. 200 ms) bursts of dopamine neuron spikes that are famously associated with unexpected rewards and conditioned stimuli that predict such rewards (Bayer and Glimcher, 2005; Glimcher, 2011; Schultz, 2007; Schultz et al., 1997). These bursts vary in size proportional to the unexpectedness of the reward, such that completely unpredicted rewards elicit larger bursts than partially predicted rewards (Fiorillo et al., 2003; Glimcher, 2011). Omitted rewards on the other hand are associated with briefly depressed firing at the time the reward was expected (Schultz et al., 1997). These temporal properties suggest that phasic dopamine constitutes a 'reward prediction error signal', a fundamental concept in reinforcement learning theory (Glimcher, 2011). The details of this interpretation are contested (Redgrave and Gurney, 2006) but the ability of phasic dopamine signalling to induce classical and operant conditioning has now been clearly demonstrated using optogenetic techniques (Kim et al., 2012; Tsai et al., 2009).

Phasic bursting in dopaminergic neurons raise concentrations of dopamine transiently above approximately 100 nM, which significantly activates the low-affinity type-1 dopamine receptor (Schultz, 2007). This in turn promotes NMDA receptor activation (Lindskog et al., 2006) and CRE-mediated gene transcription (Dudman et al., 2003), both of which are fundamental components of long-term potentiation and memory formation. Reinforcement of electrical synapses may also play a role in dopamine-dependent memory formation (Nargeot et al., 2009). This ability of the phasic dopamine signal to modify the synaptic structure of neural circuits facilitates two fundamental forms of learning. In classical conditioning, previously neutral stimuli that predict future reward become learned rewards themselves and acquire the ability to activate neural circuits that drive approach and consummatory behaviour. In operant learning, neural circuits whose behavioural output appear to bring about reward are reinforced and become more likely to drive behaviour in the future, especially in

situations similar to the one in which the reward was obtained.

Tonic dopamine signalling refers to the continuous firing, at about 2-3 Hz, of midbrain dopamine neurons. This tonic firing works to maintain baseline concentrations of dopamine in target tissues (e.g. 5-10 nM in the striatum (Schultz, 2007)), although the presynaptic action of glutamate on dopaminergic synaptic terminals also contribute to the regulation of baseline concentrations (Schultz, 2007). Rewards, even the anticipation of future rewards, increase this tonic firing rate (Fiorillo et al., 2003), as do certain intense or novel stimuli. High baseline concentrations of dopamine seem to reinforce on-going patterns of neural and behavioural activity, and it has been argued that whereas phasic dopamine signals the surprise associated with rewards, tonic dopamine signals the average rate of reward that the brain expects if on-going behaviours continue (Niv et al., 2007). Dopamine agonists such as amphetamine decrease the latency of behavioural responses, while increasing the speed and intensity with which those behaviours are performed (Niv et al., 2007). Dopamine agonists are also associated with repetitive, stereotyped behaviour and attentional and behavioural inflexibility (Cools and Robbins, 2004). Dopamine antagonism and depletion on the other hand increase response latency, decrease the speed and vigour of behaviour and increases both distractibility and the capacity to shift attention between different rewarding stimuli (Crofts et al., 2001). Thus the relationship between baseline dopamine concentrations and task performance follows a \cap -shaped curve, where optimal dopamine concentrations decrease with increasing task complexity (Cools and Robbins, 2004; Ljungberg and Enquist, 1987).

A number of models have been proposed to explain the 'energizing' and stereotyping effects of tonic dopamine on ongoing behaviour. At the core of these theories is the idea that tonic dopamine stimulates the activity of neural circuits that drive ongoing behavioural activity, and inhibits the activity of other circuits that compete for use of the animal's muscles, time and energy (Cools and Robbins, 2004). Mechanisms include dopamine-mediated enhancement of the internal excitatory connections of strongly active circuits (e.g. circuits that are currently engaged in behaviour), decreased dendritic input from sources external to those circuits (such as distracting sensory input), and enhanced GABA signalling resulting in decreased activity in weakly active circuits (Cools and Robbins, 2004). In other words, tonic dopamine

acts to make behaviourally engaged, task-relevant circuits more active, more robust and less sensitive to competing signals and information. Among other things, this model explains the seemingly paradoxical observation that stimulants have a calming effect on persons with attention deficit hyperactivity disorder. Disorders of attention are associated with impaired dopamine signalling (Volkow et al., 2007) and stimulants, which enhance dopamine signalling, compensate for this deficit, presumably by allowing weakly rewarding neural circuits, such as those involved in reading an unengaging text, to remain active for longer periods of time.

Our inability to monitor many neurons simultaneously leaves us with several unanswered questions about how dopamine affects behaviour at the level of neuronal populations. For example, at which neurons are circuits that control different behaviours most affected by tonic and phasic dopamine signalling? How are the network properties of such circuits modified by dopamine? Why do some circuits adapt more efficiently in the context of dopaminergic reward than others? What factors determine the extent to which a circuit can be modified by dopaminergic reward and how can we quantify and visualize such modifications?

1.3 The molluskan feeding CPG

The feeding behaviour and circuitry of gastropod mollusks (snails and slugs) offer an excellent model system for exploring pattern generation and its adaptation to dopaminergic reward at the level of many individual neurons interacting in well-defined CPGs. Mollusks are popular model organisms in neuroscience. Their brains contain on the order of 5.000 to 25.000 large and often brightly coloured neurons, many of which are experimentally accessible on the surface of the brain (Figure 1.5). Every neuron has a more or less fixed location, connectivity and function in all members of the species, making the cells ideal for mapping and electrophysiological characterization. Mollusks (not including cephalopods) moreover have an open circulatory system, which means that complex semi-intact preparations consisting of the brain and attached sensory organs and/or muscle groups remain functional for several hours in physiological saline.

Lymnaea stagnalis, the subject of this thesis, is an air-breathing freshwater snail

found throughout the northern continents (Benjamin, 2008). The animals live in ponds, lakes and rivers, typically close to the water surface, where they feed on floating weeds. Adult snails are 2-5 cm in shell length and weigh 2-3 g. The brain consists of approximately 20,000 neurons organized into 11 ganglia (Figure 1.5A & B). All ganglia except the visceral ganglion exist as symmetrical pairs that have very similar neuronal organization and function (Benjamin, 2008). The visceral and parietal ganglia are involved in respiration and heartbeat. The pedal ganglia control locomotion and are also involved in respiration. The buccal ganglia, which lie somewhat more distant from the rest of the brain, control feeding. The cerebral ganglia are involved in several behaviours including feeding and reproduction, as well as learning and decision-making. The pleural ganglia, finally, have no nerves and their function remains poorly understood. In addition, neuronal circuits that control behaviours that involve the entire body, such as reproduction and defensive withdrawal into the shell, are distributed over several ganglia.

Lymnaea spends most of its time foraging. The animal feeds by protracting a toothed tongue-like organ called the 'radula', rasping the radula against the food substrate and finally swallowing the food by retracting the radula back into the mouth (Figure 1.6A). Each cycle of protraction, rasp and swallow is called a 'feeding cycle'. *Lymnaea* is not able to detect food at a distance (Bovbjerg, 1968). Rather, food must be detected by sampling the environment. Thus the animals crawl around and occasionally ingest bits of material, typically algae. Food deprivation increases the frequency of these spontaneous 'exploratory' feeding cycles (Tuersley and McCrohan, 1987). When a feeding site with high nutritional content is discovered the hungry animal reduces its rate of locomotion and accelerates its feeding behaviour. This ability to adapt foraging behaviour to changing environmental circumstances is a canonical form of intelligent behaviour and is the subject of 'optimal foraging theory' (Emlen, 1966; MacArthur and Pianka, 1966). For a discussion of how general-purpose goal-oriented cognition may have evolved from motor circuits initially in control of foraging, see (Hills, 2006).

The neural circuits that drive foraging behaviour in *Lymnaea* have been well-characterized. They include a feeding CPG located in the buccal ganglia and a locomotor CPG located in the pedal ganglia. The locomotor CPG controls rhythmic

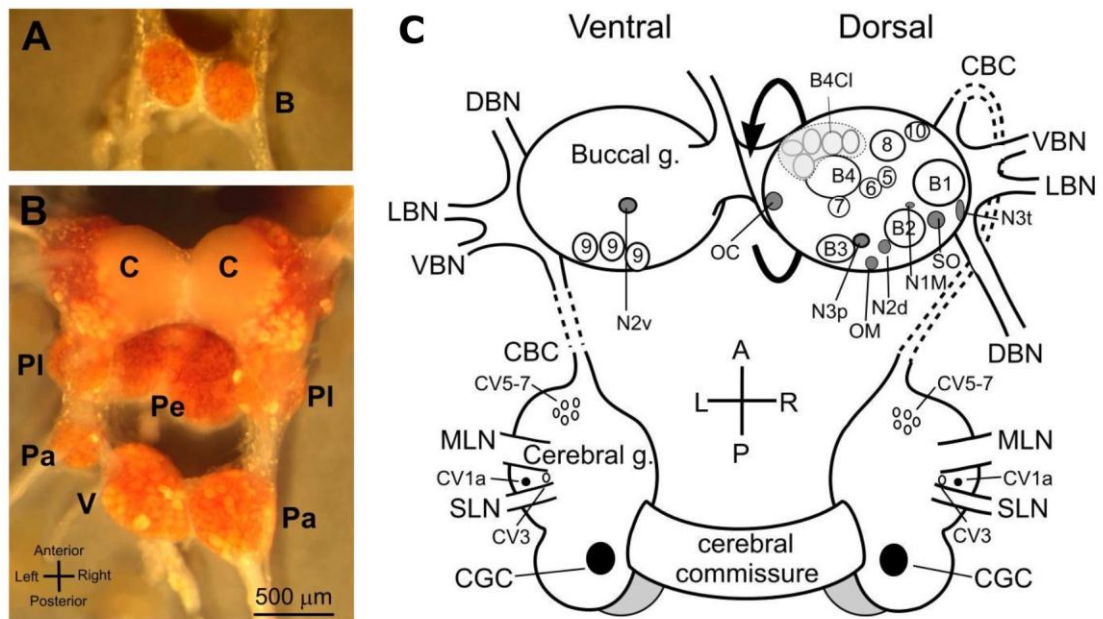


Figure 1.5. The *Lymnaea* brain

A & B: Central nervous system of *Lymnaea*; buccal ganglia (B), cerebral ganglia (C), pedal ganglia (Pe), pleural ganglia (PI), parietal ganglia (Pa) and visceral ganglion (V). Adapted from Benjamin, 2008. **C:** Map of neurons and nerves of the buccal and cerebral ganglia that are associated with feeding behaviour. Adapted from Benjamin, 2012.

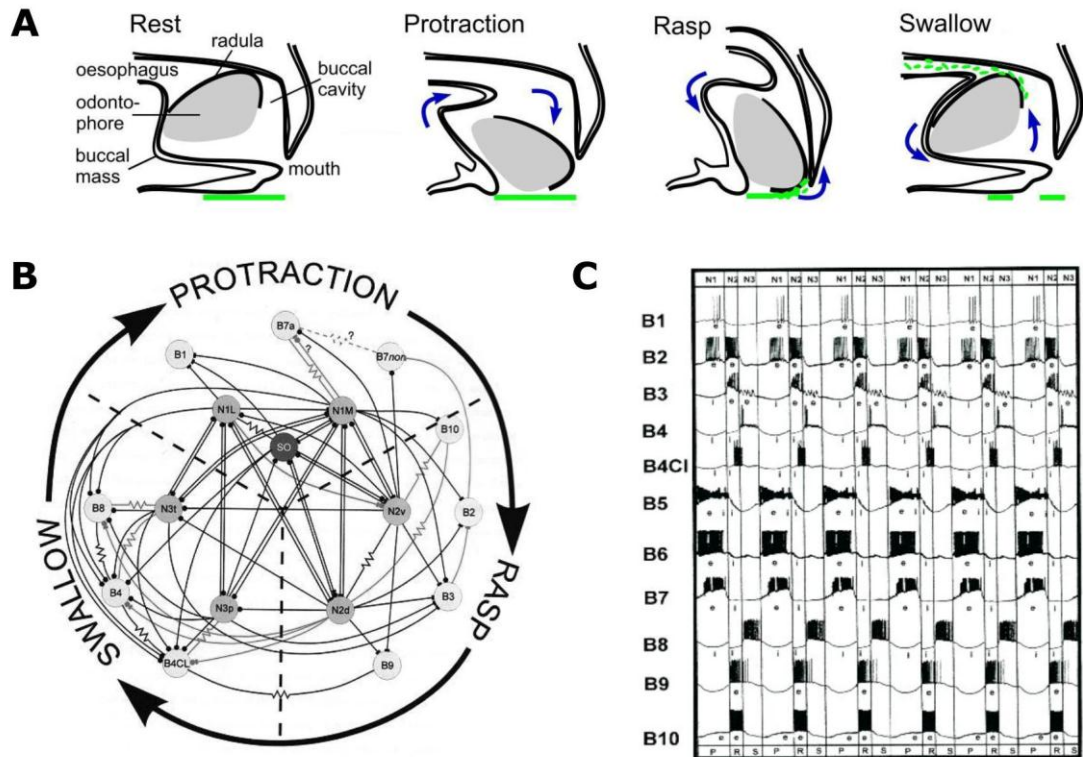


Figure 1.6. Feeding in *Lymnaea* is a rhythmic 3-phase pattern

A: *Lymnaea* feeds by cycles of radula protraction, rasping and swallowing. Adapted from Benjamin, 2012. **B:** Key neurons and connectivity of the *Lymnaea* feeding CPG. Adapted from Straub, 1999. **C:** Firing pattern of identified motorneurons during feeding. Adapted from Straub, 1999.

contractions of the foot and back-to-front beating of foot cilia (Benjamin, 2008; Tsyganov and Sakharov, 2000; Winlow and Haydon, 1986) and is inhibited during feeding (Kyriakides and McCrohan, 1988). The locomotor circuit remains poorly understood however and has not yet been characterized as a CPG in the strict sense of the term (see Section 1.1). The feeding CPG on the other hand is well understood (Benjamin, 2012; Straub, 1999; Vavoulis et al., 2007) (Figure 1.6B). Early research on preparations consisting of the brain attached by motor nerves to the feeding musculature (the buccal mass, Figure 1.6A) showed that each phase in the 3-phase feeding cycle is driven by bursts of spikes in distinct groups of motor neurons located mostly on the dorsal surfaces of the buccal ganglia (Rose and Benjamin, 1979) (Figure 1.5C). These motoneurons are sequentially activated (Figure 1.6C) by a central circuit consisting of three bilaterally paired buccal interneurons (N1M, N2v and N3t). These interneurons form a 'true' CPG circuit, i.e. the membrane properties and synaptic connectivity of the component neurons are sufficient to produce the 3-phase feeding motor pattern (Vavoulis et al., 2007). Generation of the feeding motor pattern is initiated when sufficiently depolarized N1M neurons overcome inhibitory input from the otherwise continuously active N3t neurons that keep the CPG quiescent (Staras et al., 2003). This happens spontaneously, partly due to spontaneous variability in the activity of N1M neurons, and is more common in hungry snails. Having escaped from inhibition, the N1M neurons generate a plateau potential that drives bursting in protraction-phase motor neurons and inhibits N3t neurons. With a delay, this N1M plateau eventually triggers a plateau potential in N2v neurons. The N2v plateau terminates the N1M plateau, drives bursting in rasp-phase motor neurons and further inhibits N3t neurons for about a second before terminating spontaneously. This triggers bursting by post-inhibitory rebound in the newly disinhibited N3t neurons, which drives bursting also in swallow-phase motor neurons and completes the feeding cycle. For a detailed review of the *Lymnaea* feeding CPG see (Benjamin, 2012).

Although the three types of interneuron are able to generate the feeding pattern on their own, motoneurons too play a key role in the generation of the pattern. In particular, motoneurons are electrically coupled to interneurons active in the same phase of the cycle, and hyperpolarization of some protraction-phase motoneurons prevents generation of the feeding motor pattern (Staras et al., 1998).

The feeding CPG also includes interneurons that cannot generate the 3-phase pattern on their own but which are nevertheless significant in the generation of the pattern due to their connectivity within the circuit (Benjamin, 2012). In the following I shall refer to the N1M-N2v-N3t circuit as the 'core CPG' and to the larger population of all neurons that are phase-locked with and significantly contribute to the feeding pattern as the CPG more generally (see Section 1.1). It is estimated that about 100 neurons are members of this larger CPG (Benjamin, 2012). Most of these are motor neurons located in the buccal ganglia. The buccal ganglia contain about 400 cells in total, many of which have not yet been individually characterized.

It should be noted that many CPGs contain a core set of pattern-generating interneurons that communicate a basic pattern to a larger pool of neurons which then refine the pattern and convert it to muscle contractions. This anatomy is presumably a feature also of putative CPGs in the mammalian brain, in which motorneurons of the spinal cord appear to be entrained to the patterns of neuronal circuits in higher brain regions, though the spinal cord, like the motorneurons of the *Lymnaea* feeding CPG, does play a limited role in the shaping of motor patterns (Bizzi et al., 2002; Bizzi et al., 2000).

Like other CPGs the *Lymnaea* feeding CPG has variable dynamics: no two feeding cycles are exactly alike (see Chapter 4). During spontaneous, exploratory feeding the cycle period varies randomly, mainly due to variation in the duration of the final phase of activity (Elliott and Andrew, 1991). The phase duration and firing rate of individual neurons also varies from cycle to cycle, with protraction and swallow phase motor neurons tending to increase their activity as the rate of feeding increases (Elliott and Andrew, 1991). An extensive study of the buccal feeding circuitry in a related mollusk, *Aplysia californica*, showed apparently random variation at the neuronal, neuromuscular and behavioural levels of the system (Horn et al., 2004). Arguably this centrally generated variability is a core component of what in higher animals, particularly humans, is called free will (Brembs, 2011).

Lymnaea detects nutritious food, such as sucrose, by means of chemosensory neurons located in the esophagus and lip. Application of sucrose to these sensory organs induces a dramatic acceleration of the cycling frequency of the feeding CPG (Kemenes et al., 1986), but the precise neuronal mechanisms that mediate this effect

remain poorly understood. Most importantly, general mechanisms that account for the acceleration of this and other goal-oriented CPGs in the presence of reward have not been established. Individual synapses that communicate the presence of nutritious food from chemosensory neurons to the feeding CPG have been identified, including monosynaptic contacts with N1M neurons, and cerebral interneurons, such as the CV1a, that activate N1M neurons (Benjamin, 2012), but these are specific to the feeding CPG of *Lymnaea*, and homologous neurons are difficult to find even in closely related systems such as the buccal ganglia of *Aplysia*. The focus on individual modulatory neurons also does not reflect how modulation occurs *in vivo*, i.e. through the simultaneous activity of a large number of interacting neurons.

In this thesis I attempt to uncover more general, population-level mechanisms of CPG adaptation by using a multi-unit recording method and focusing on the role of dopamine in mediating the effect of food reward. As we saw in the previous Section dopamine acts extra-synaptically and is often released widely and homogeneously into large regions of neural tissue. Similarly in the operation of the feeding circuit the primary source of dopamine appears to be the dopaminergic fibres of the dorsobuccal nerve, which releases dopamine widely in the buccal ganglia (Elekes et al., 1991) and carry information about the nutritional content of ingested food from the esophagus. Dopaminergic neurons in the buccal and cerebral ganglia may also play an important role. Application of dopamine to the isolated brain of *Lymnaea in vitro* induces an acceleration of the feeding CPG similar to that seen following application of sucrose (Kyriakides and McCrohan, 1989). Dopamine was also the only one of a total of 5 putative neuromodulators tested in two studies (serotonin, acetylcholine, dopamine, FMRFamide and octopamine) that could drive rhythmic activation of the feeding CPG *in vitro* (Kyriakides and McCrohan, 1989; Vehovszky and Elliott, 2001). Moreover, methylergonovine, a broad-spectrum dopamine antagonist, blocks sucrose-induced high-frequency feeding (see Chapter 4), indicating that dopamine is both necessary and sufficient for high-frequency activation of the feeding CPG. The *Lymnaea* feeding CPG is thus an example of a well-characterized CPG whose rate of fictive consummatory behavioural output is modulated by dopamine. Since the feeding CPG inhibits the locomotor CPG in the pedal ganglia (Kyriakides and McCrohan, 1988) this model system also provides a concrete example of dopamine-modulated competition

between different CPGs, although the dopamine is not distributed equally between the two CPGs.

Dopamine signalling also plays a central role in the feeding CPG of *Aplysia*. In this CPG, dopamine accelerates fictive feeding at least in part by depolarizing protraction-phase motoneurons, whose activation is associated with initiation of the feeding motor pattern (Kabotyanski et al., 2000). Dopamine also hyperpolarizes B4/5 and B34 type neurons, whose activation is associated with modifying the ingestive feeding pattern into an egestive pattern that drives ejection of unwanted food (Kabotyanski et al., 2000).

In addition to the short-term effects of dopamine on the molluskan feeding CPG, dopamine is also required for classical and operant conditioning of the circuit. Single-trial pairing of sucrose with amyl acetate induces classical conditioning in *Lymnaea*, both *in vivo* and in semi-intact preparations consisting of the intact brain connected to the esophagus and lip (Marra et al., 2010). Prior injection of the dopamine antagonist methylergonovine blocks such conditioning *in vivo* (Kemenes et al., 2011). Methods for operant conditioning of the *Lymnaea* feeding system have not yet been developed. However, the ingestive and egestive motor patterns generated by the multi-functional feeding CPG of *Aplysia* can be selectively reinforced by contingent stimulation of the dopaminergic esophageal nerve (Brembs et al., 2002; Nargeot et al., 1997). This basic form of RBS produces selective generation of the rewarded motor pattern. Prior to training the feeding CPG of *Aplysia* contains several neurons that are able to initiate generation of the feeding pattern; following training only one neuron initiates the pattern, a change that is associated with reinforced electrical coupling within the CPG (Nargeot et al., 2009).

Research on the *Lymnaea* feeding CPG is limited by the near-exclusive use of glass microelectrodes to monitor neural activity. This technique allows detailed recording and manipulation of individual neurons but limits the number of neurons that can be recorded to about four, with each new electrode adding a cost in time and risk of displacing previously positioned electrodes. Of the 200 or so neurons in each buccal ganglion only about 30 have been individually identified and only a small number of these have been characterized in terms of the variability of their firing pattern during spontaneous and food-induced feeding. Patterns of activity that

precede or follow feeding cycles have also not been extensively characterized. Most importantly perhaps, the simultaneous activity of the various neurons involved in the generation of feeding behaviour has not been explored. The ability to characterize populations of neurons associated with the feeding CPG and the way these populations interact in the context of reward is a key reason for developing multi-unit recording methods that can be applied to the study of *Lymnaea*. As we saw in Section 1.1 much motor behaviour is generated by circuits that incorporate a large and variable number of pattern generating mechanisms and neurons. In the following Sections we saw that dopamine is often distributed widely within neural circuits, affecting many neurons simultaneously. Thus it is only by monitoring the simultaneous activity of many neurons associated with the acquisition of a reward that we can hope to fully understand the dynamic, distributed processes by which neural circuits generate adaptive behaviour. In the case of the *Lymnaea* feeding CPG, this means monitoring several neurons responsible for the core feeding motor pattern as well as a larger population of neurons whose activity guides and modulates the motor pattern and ensures its coordination with other behaviours and with the availability of nutritious food.

1.4 Multi-electrode array (MEA) technology

This thesis introduces a method for using a dish containing an array of up to 252 planar electrodes (Figure 1.7) to extracellularly monitor the electrical activity of many neurons in the intact brain of *Lymnaea* (and other preparations of a similar size). MEA dishes were first introduced as a tool for neuroscience research in the 1970s and 1980s (Gross, 1979; Pine, 1980; Thomas et al., 1972). Today they are commercially available and widely used to study neural and other electrogenic tissues, both in academia and industry. Multi Channel Systems (Germany) is the largest manufacturer of the type of MEAs used here; glass dishes with the electrode array located in the centre. Each electrode is up to 30 μm in diameter – larger than many neuronal cell bodies. This means that it is possible to record the voltage spikes of many neurons on each electrode, and a total of hundreds or thousands of neurons on a single MEA.

Separating the voltage spikes of individual neurons however is hard and is often

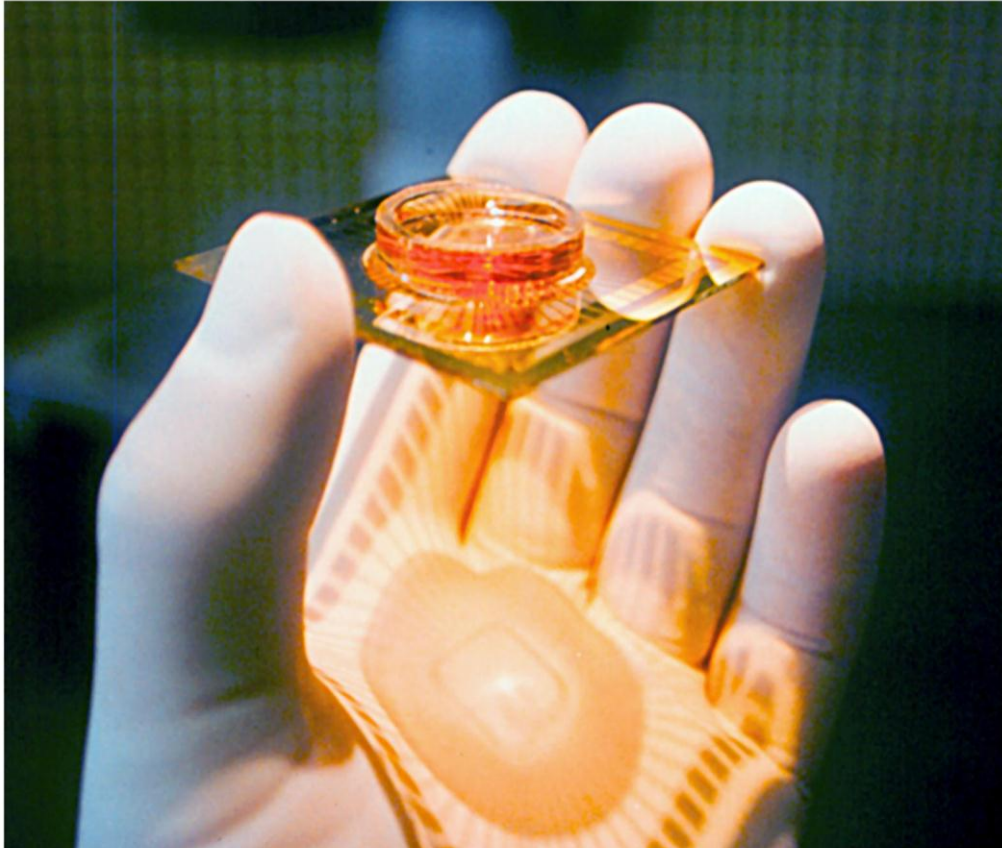


Figure 1.7. The MEA dish

Photo of the MEA dish. The dimensions of the dish are 49 mm x 49 mm x 1 mm.

Photo: Steve M. Potter.

not attempted. One approach to spike sorting is to assume that spikes generated by different neurons have distinct wave-forms and to use clustering algorithms to sort spikes by those distinguishing features (Quiroga et al., 2004). This approach assumes however that the detailed wave-forms specific to each neuron can be extracted from the data, whereas in practice it is frequently only the peak of a neuron's voltage spike that can be observed above the noise. This approach also assumes that the wave-form of a neuron does not change much over time, whereas the wave-forms of for example many bursting neurons in fact change dramatically during the course a burst (Pouzat et al., 2004; Stratton et al., 2012).

Another approach is to triangulate the location of spikes (Gross, 1979; Novak and Wheeler, 1986; Prentice et al., 2011). This approach assumes that the spikes of an individual neuron will always be generated and recorded in the same location in the brain. That can be a good assumption but problems emerge when the spikes of a neuron can be detected at similar amplitudes on multiple sites, e.g. along an axon, or when the time separating spikes from different neurons is less than the sampling rate of the MEA. The method also requires spikes to be detected on at least three neighbouring electrodes to allow triangulation and is thus poorly suited to small neurons (e.g. $<10\ \mu\text{m}$ soma) or sparse arrays with significant distances between electrodes (e.g. $>200\ \mu\text{m}$).

MEA dishes are typically used to study dissociated populations of neurons, frequently from the brain of the embryonic rat. Neurons are enzymatically dissociated, deposited on the surface of the MEA and cultured for days, weeks or months, allowing new synaptic connections to form. Such cultures develop complex patterns of activity and are important models of pattern generation (Wagenaar et al., 2006). Another type of MEA-based experiment involves tissue slices. Here entire slices of brain tissue are allowed to settle on the MEA, enabling the simultaneous recording of many neurons while preserving at least some organotypic synaptic connectivity. Such studies have advanced our understanding of the behaviour of neural circuits in various regions of the nervous system, including the region of the spinal cord that contains the locomotor CPG (see Section 1.1) (Streit et al., 2006).

Many invertebrate brains are small enough that the entire brain can be fitted

onto an MEA. However, only two published papers describe the use of MEAs to record from intact invertebrate ganglia (Gross, 1979; Novak and Wheeler, 1986). These involved custom-made arrays of 32 electrodes onto which the abdominal ganglion of *Aplysia* was pressed and held by attaching loose nerves to small pieces of iron and a flexible magnetic strip. Spikes of an estimated 15-20 unique neurons could be detected in such preparations, but only a few cells were characterized in terms of location, size and firing pattern. A range of questions regarding the use of MEAs to study intact invertebrate brains have therefore yet to be addressed. For example, how can entire brains, preferably with attached sensory organs, be positioned firmly on the MEA? How can such preparations be perfused without disrupting the recording? How can we combine MEA recording of intact brains with the use of intracellular electrodes or nerve stimulation? What is the best way of sorting the spikes that invertebrate brains generate on an MEA?

1.5 Aim and thesis structure

The main aim of this thesis is to show how MEAs can be used to characterize populations of neurons associated with adaptive foraging behaviour in *Lymnaea*. By studying many interacting neurons in the context of dopamine-mediated reward I aimed to uncover general principles of operation and adaptation that might apply to many different CPGs. This is in contrast to the identification of individual neurons by means of intracellular electrodes. The single-unit recording technique has provided critically important connectivity diagrams that guide research on CPGs, but in terms of understanding circuit function it tends to yield idiosyncratic results that apply only to a particular behaviour generated by a particular species (Selverston, 2010; Yuste, 2008). To overcome this limitation a considerable amount of time had to be devoted to the development and refinement of MEA recording and spike sorting techniques; as such methods had not previously been developed for intact brains or semi-intact invertebrate preparations. Chapter 2 describes how to monitor the intact brain of *Lymnaea* on an MEA. Practical aspects of the method are described, including the use of semi-intact preparations, the necessary modifications to the MEA system, and various perturbation techniques. The method is not limited to the study of *Lymnaea*

but could be applied to a range of invertebrate systems (for an example, see Section 2.9). Chapter 3 describes a new spike sorting procedure specifically developed for the data recorded on the MEA. In Chapter 4 these techniques are applied to the analysis of neuronal populations associated with the feeding CPG. The spatiotemporal structure of the data and the application of various sensory, pharmacological and electrical perturbations confirmed that the rhythmic feeding motor pattern of the CPG can be recorded on the MEA. In Chapter 5, evidence is presented for the existence of a previously uncharacterized neuronal population whose alternating pattern of activity and quiescence reflects a network refractory period that modulates the core feeding CPG and adapts its motor output to the availability of food reward. The central role of dopamine in this adaptive process is explored and characterized in some detail. The MEA recording method and the results of its application to the study of the *Lymnaea* feeding CPG are discussed in Chapter 6, which concludes that the newly identified neuronal population and network refractory period constitute an adaptive mechanism that may adapt the activity of a wide range of CPG circuits to reward.

I co-authored two journal articles while writing this thesis. The first paper describes the MEA recording method and the effects of a range of stimulation protocols (Harris et al., 2010). The second paper introduces the spike sorting method and its application to analysis of the feeding CPG (Harris et al., 2012). This second paper also describes the distinct neuronal populations associated with the feeding CPG and the reward-sensitive refractory period.

The Appendix, finally, introduces a web-based science communication project aimed at promoting public engagement with some of the themes of this thesis (Harris and Kilarski, 2009).

Chapter 2

Materials and methods

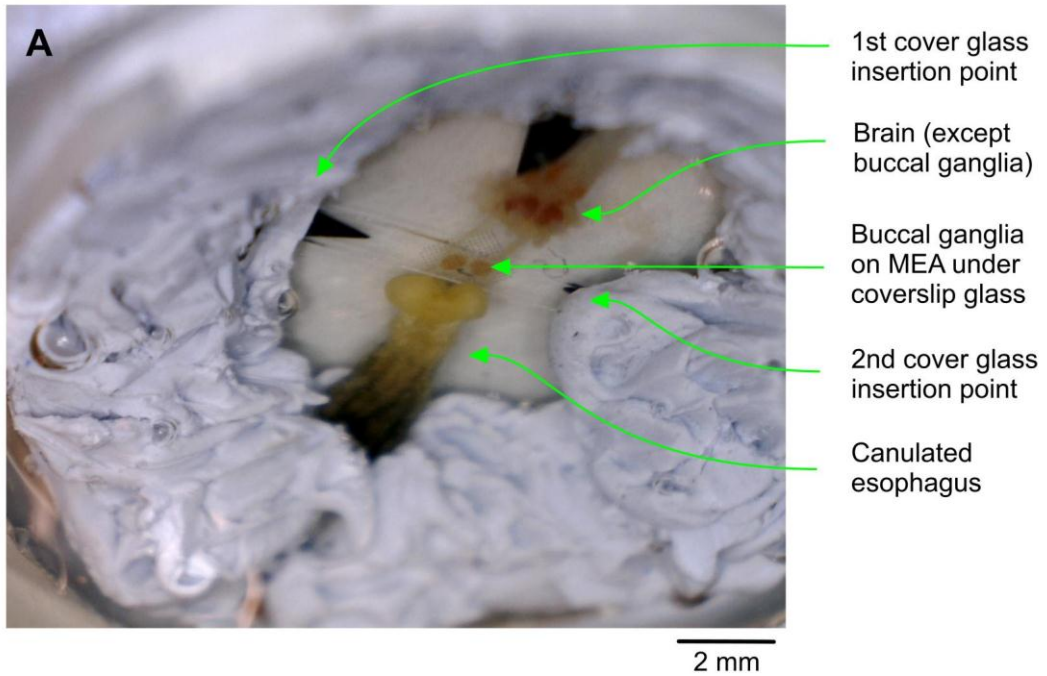
2.1 Animals

Snails (*Lymnaea stagnalis*) were raised in breeding facilities at the University of Sussex. The animals were fed lettuce three times per week and fish food once per week. They were kept at 20°C on a 12 h light-dark cycle. Before dissection the snails were taken from the breeding facilities and kept in copper-free, unheated water (approx. 17°C) without access to food for between one and five days. The snails were adult (approx. 5 months old) at the time of dissection.

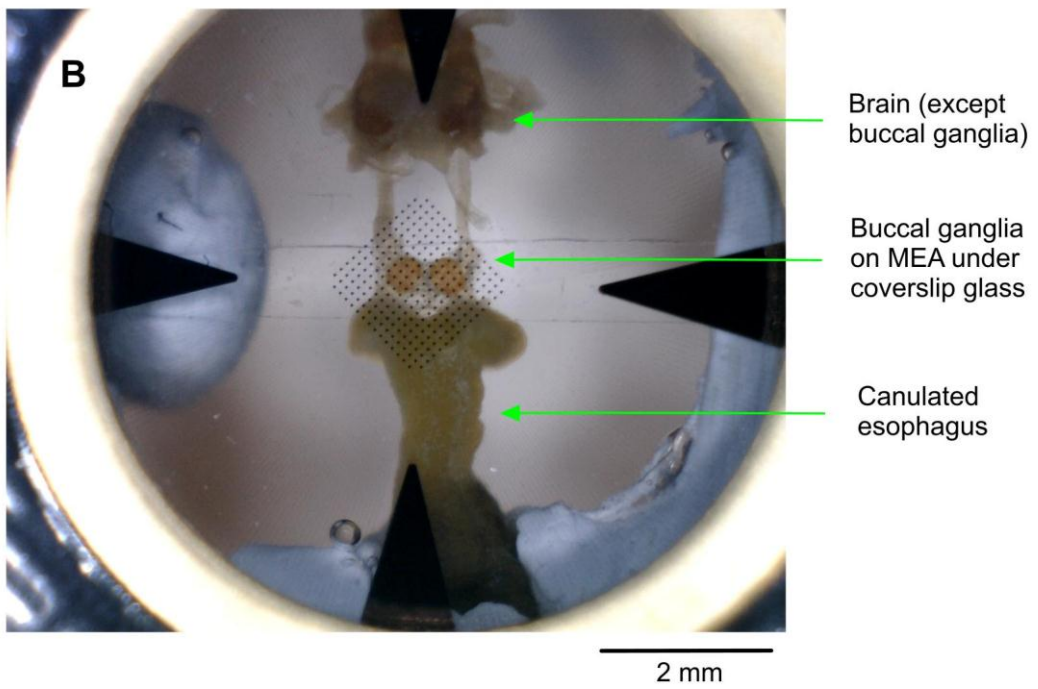
2.2 Semi-intact preparations

Three types of semi-intact preparation were used. The most frequently used preparation (the '*brain-esophagus preparation*') consists of the intact brain with a 2-3 mm segment of the esophagus attached by the dorsobuccal nerve to the buccal ganglia (Figure 2.1A-C). This preparation was typically used to record from the buccal ganglia while the esophagus was perfused with sucrose (in saline). This preparation was also used in experiments that did not involve any perfusion, as attaching the esophagus to the dish wall (see Section 2.4) is a convenient way of keeping preparations steady while positioning the brain on the MEA. In some preparations the cerebral commissure that connects the two cerebral ganglia was cut so that the brain could be flattened on the MEA, allowing simultaneous monitoring of all ganglia in the brain. Dissections were carried out in a Sylgard coated dish filled with saline [NaCl (50 mM), KCl (1.6 mM), MgCl₂ (3.5 mM), CaCl₂ (2.0 mM) and HEPES (10 mM) in culture grade water (pH 7.9)].

View from above



View from below



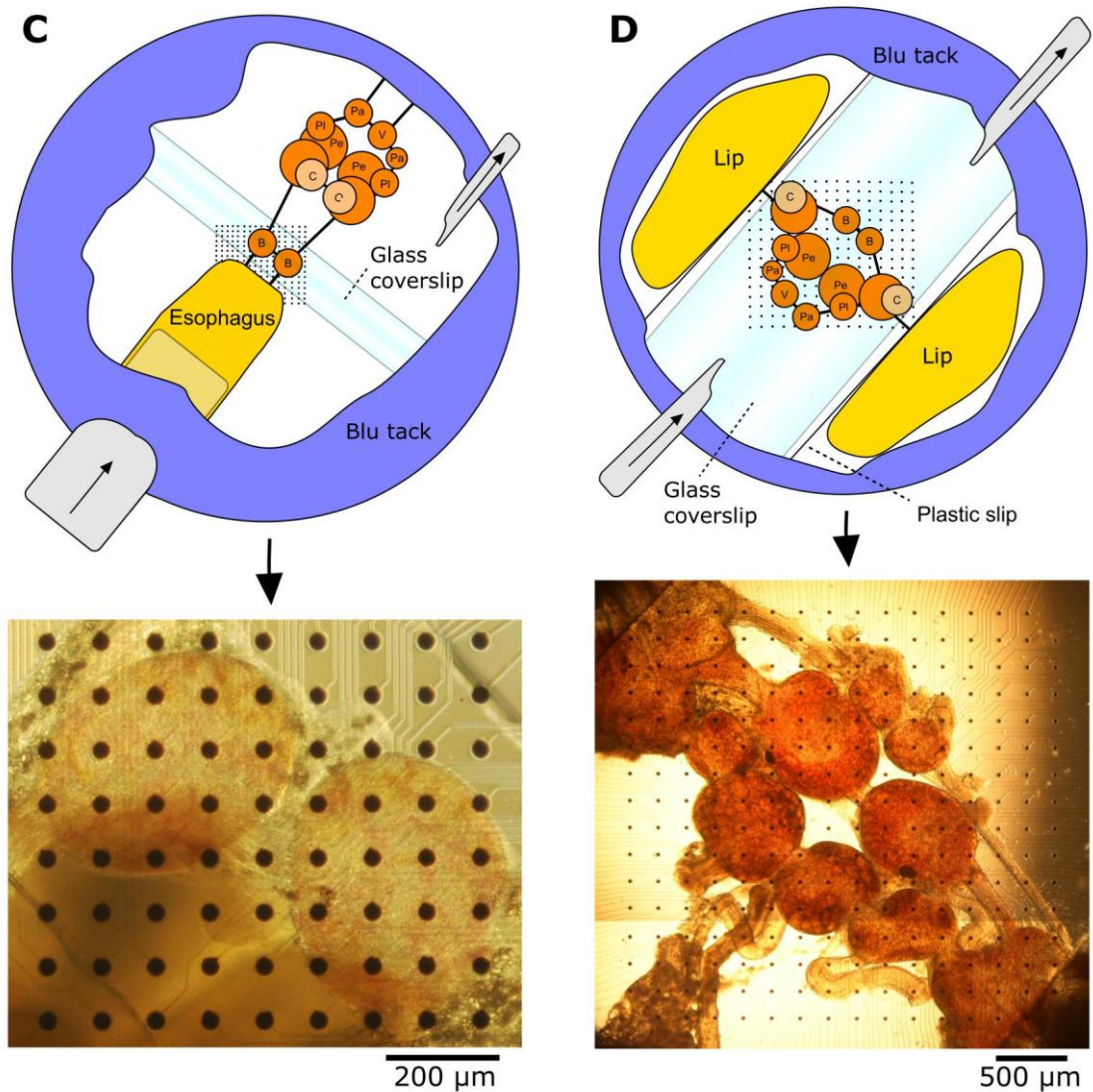


Figure 2.1. Semi-intact preparations of *Lymnaea* stabilized on the MEA

A-B: View of a brain-esophagus preparation stabilized in an MEA dish. The view is from above (**A**) or below (**B**). The pale purple substance is blu tack. The black arrowheads are ground electrodes integrated into the floor of the dish. **C:** Brain-esophagus preparation with the dorsal surfaces of the buccal ganglia on an MEA with 30 μm diameter electrodes spaced 100 μm apart. **D:** Split brain-bisected lip preparation on an MEA with 30 μm diameter electrodes spaced 200 μm apart (dorsal view).

A second, similar preparation (the '*lip-brain-esophagus preparation*') consists of the intact brain with both the esophagus and the intact lip attached to the brain by their respective nerves (Figure 1 in (Harris et al., 2010)). This preparation was used in experiments aimed at inducing classical reward conditioning (see Section 4.6).

A third preparation (the '*split-brain-bisected-lip preparation*') consisted of the brain with the bisected lip attached by the lip nerves to the cerebral ganglia (Figure 2.1D). In this preparation the cerebral commissure was cut, allowing us to record from the entire dorsal or ventral surface of the brain while perfusing the lip with chemosensory stimuli, including sucrose, amyl acetate (a neutral stimulus at low concentrations and an aversive stimulus at high concentrations) and lemongrass (an aversive stimulus). Such chemosensory stimulation was used to study population activity associated with feeding or withdrawal (see Chapters 4 and 5). It is helpful, when using this preparation, to leave the esophagus attached until the brain has been properly positioned in the dish (see Section 2.4).

To improve electrical contact between neurons and electrodes, individual ganglia were always de-sheathed before being positioned on the MEA. This involves removal of a thick outer sheath of connective tissue that covers most surfaces of the brain, while leaving a thin inner sheath intact. Removing the inner sheath did not improve signal-to-noise, probably because cells dispersed instead of being flattened against the MEA when pressure was applied (see Section 2.4). Treating the inner sheath with protease for 1-5 min before recording, a routine procedure in experiments involving intracellular electrodes, also did not appear to improve signal-to-noise. Moreover, one of the early studies involving MEA recordings from the abdominal ganglion of *Aplysia* found that treatment with protease caused a gradual reduction in the amplitude of extracellularly recorded spikes (Novak and Wheeler, 1986).

2.3 MEA recording equipment

Figures 2.2 and 2.3 show buccal ganglia and entire brains on MEAs with a range of different layouts. Most MEA dishes used here contain a square grid of 8x8 or 16x16 electrodes (minus one electrode for each corner). The electrodes have a diameter of

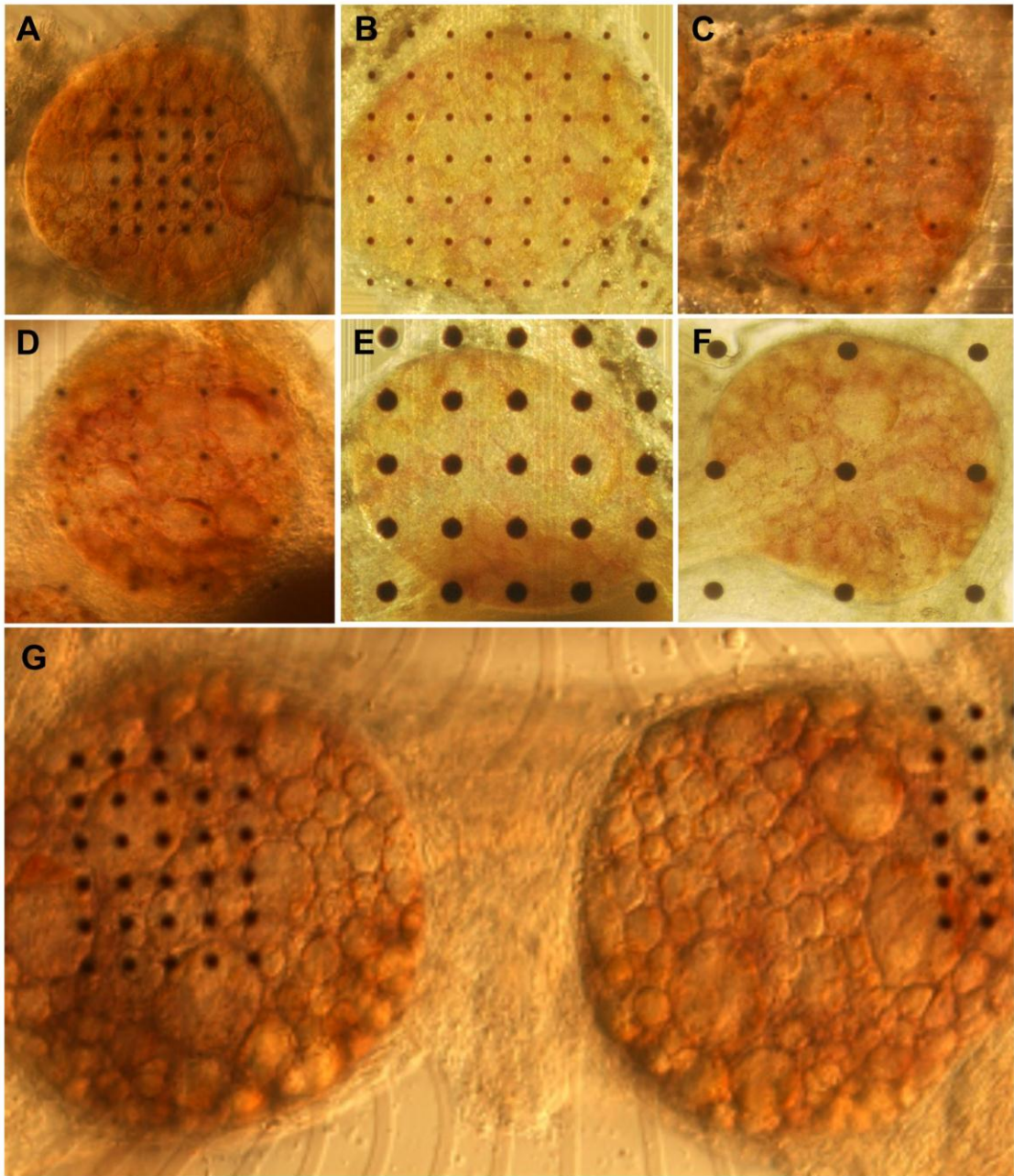


Figure 2.2. Buccal ganglia on the MEA

A-F: Buccal ganglia (dorsal surface, right ganglion) on different size MEAs. The following numbers indicate electrode diameter, inter-electrode spacing and total number of electrodes in the array: **A:** 10x30x60. **B:** 10x60x252. **C & D:** 10x100x60. **E:** 30x100x252. **F:** 30x200x252. **G:** Dorsal surfaces of both buccal ganglia on a 10x30x60 array. This is a particularly clear image showing the outline of nearly all cell bodies located on the surfaces.

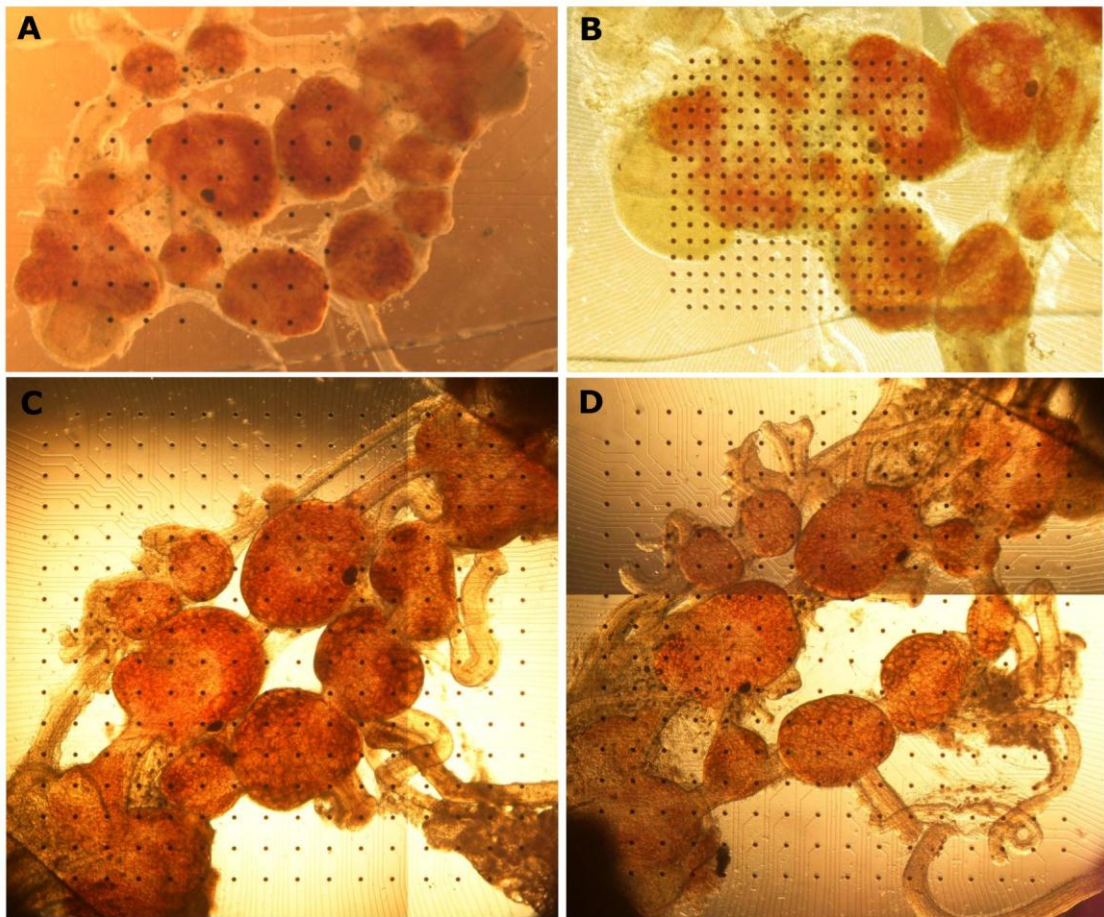


Figure 2.3. Entire brains on the MEA

Lymnaea brains (dorsal view) on different size MEAs. The following numbers indicate electrode diameter, inter-electrode spacing, and total number of electrodes: **A:** 30x200x60. **B:** 30x100x252. **C & D:** 30x200x252.

either 10 or 30 μm . 10 μm electrodes can be spaced as little as 30 μm apart (Figure 2.2A & G) whereas 30 μm electrodes are spaced at least 100 μm apart (Figure 2.2E). However, 10 μm electrodes have higher resistance and noise levels than 30 μm electrodes, and dense MEAs with small electrodes did not appear to record more neurons than the more sparsely spaced MEAs with large electrodes. I therefore primarily used the MEAs with 30 μm diameter electrodes spaced 100 μm apart to monitor the buccal ganglia, even though the buccal tissues covered at most 50 out of the 252 electrodes (Figure 2.1C). To record from the entire brain I used MEAs with 30 μm diameter electrodes spaced 200 μm apart (Figure 2.1D). Electrical activity was recorded using a USB-MEA256-System amplifier for the 16x16 arrays and an MEA1060 amplifier for the 8x8 arrays (Multi Channel Systems, Germany).

2.4 Stabilizing the brain on the array

A fundamental challenge when using an MEA dish to record from an intact brain is to ensure that the pressure keeping the ganglia on the MEA is stable, even and sufficient to achieve good electrical conductance between neurons and electrodes. Initial solutions explored here involved placing relatively large pieces of microscope coverslip glass on top of the ganglia before carefully moving the MEA dish to the recording rig. This allowed a small number of spatially distinct sources of spikes (putative neurons) to be simultaneously recorded, but signal-to-noise was low and the preparations dislocated easily, which made perfusion near-impossible. Coating the dish floor with polyethyleneimine in order to improve surface adhesion did not noticeably increase signal-to-noise.

The solution developed here is to hold the coverslip glass in place by means of a thick ring of pressure sensitive adhesive (blu tack) attached to the dish wall (Figure 2.1). The dish is modified as follows. A ring of blu tack (approx. 2 mm thick), is placed along the dish wall and repeatedly pressed against it with a blunt instrument. It is important that the blu tack attaches firmly to the base where the wall joins the floor of the dish. The dish must be completely dry for this to happen. Additional bits of blu tack are added to until the edge of the blu tack ring is approximately 2-3 mm from the MEA (see Figure 2.1). Recordings that involve perfusion of the esophagus require the

incorporation of a thin segment (5 – 7 cm) of silicone tubing into the blu tack ring (Figure 2.1C). The tube is bent 90°, wrapped in blu tack and inserted into a hollowed out cavity in the blu tack ring, leaving about 2 mm of tubing exposed. Both the blu tack and the tube can be left in the dish and used repeatedly as the blu tack does not soften. The dish is subsequently filled with saline and the semi-intact preparation placed in the dish. The esophagus is attached to the ring of blu tack or cannulated, i.e. threaded onto the exposed bit of silicone tubing. Cannulating the esophagus is best done by using two forceps to hold both sides of the cut esophagus opening and gently pulling the esophagus over the silicone tube. When intending to perfuse the esophagus it is important to fasten it with blu tack on all sides of the silicone tube and to leave only a short segment of esophagus between the tube and the brain. This is partly to ensure that all the fluid goes through the esophagus and partly because the esophageal opening closest to the brain is narrow, meaning that the esophagus inflates easily if the flow rate is too high. Inflation of the esophagus obscures visibility and might activate mechanoreceptors (Elliott and Benjamin, 1989). Conversely it is also important not to leave the esophagus completely taut, as this increases the likelihood that spontaneous muscle contractions will pull on and dislocate the brain on the MEA. Episodic movement of the esophagus can be observed during recordings but does not significantly impact signal-to-noise as long as the precautions outlined above are adhered to.

Having fastened the esophagus on one side of the dish, the brain's long posterior nerves are then attached to the blu tack on the opposite side of the dish, leaving the brain loosely stretched over the electrode array (Figure 2.1A-C). If a *split-brain-bisected-lip* preparation is used the bisected lip should at this point be stabilized and kept away from the MEA by means of thin slips of plastic attached to the blu tack (Figure 2.1D). The esophagus and posterior nerves can then be cut and removed from the dish, as the stabilized lips hold the brain steady.

Once the appropriate ganglia have been positioned over the MEA, a rectangular glass coverslip is inserted between the base of the blu tack ring and the dish floor and carefully lowered onto the ganglia, perpendicular to the nerves that hold the brain steady (Figure 2.1). The glass should be about 10x1 mm when used to cover the buccal

ganglia and about 10x4 mm when used to cover the whole brain. Leaving a thin sheath of blu tack under the glass coverslip where it is inserted under the ring of blu tack (see Figure 2.1A) helps ensure an equal pressure gradient on the ganglia. Blu tack is subsequently applied to the glass on the opposite side of the dish until the glass is roughly horizontal and appropriate pressure on the ganglia has been achieved. The level of pressure can be gauged kinetically but also visually through the dissection microscope as an increase in the diameter and transparency of ganglia. Excessive pressure can result in rupturing of the inner connective tissue, causing a sudden outburst of neurons at a point somewhere along the edge of a ganglion. The functional impairments caused by such damage are not known, and ruptured preparations should probably not be used for experiments. Additionally, the orange colour of the ganglia will sometimes spread to protruding nerves when pressure is applied. This probably represents destruction or dislocation of individual neurons and should be kept to a minimum. Examples of appropriately pressured ganglia are shown in Figures 2.1, 2.2 and 2.3. The entire process from dissection to stabilizing the brain on the array takes about 20-30 min depending on the complexity of the preparation.

2.5 Microscopy and perfusion

After the brain has been stabilized on the MEA the dish is placed in an amplifier. MEA amplifiers have a circular hole directly under the MEA, allowing a view from below. Here, the amplifier was mounted on an adjustable steel stand (Scientifica, UK) and positioned over the lens of an inverted microscope (Nikon, Japan) (Figure 2.4). Attached to the microscope is a custom made gravity-driven perfusion system as well as a suction system driven by a mechanical pump (Scientifica, UK) (Figure 2.4). The perfusion system consists of syringes and glass bottles connected by silicone tubes to plastic tips. The plastic tips were either attached to the movable microscope lamp head and lowered into in the dish (as in Figure 2.4) or mounted on an adjustable steel stand that allows the tips to be positioned anywhere in the MEA dish. Each silicone tube was fitted with a gauge to control flow rate. A separate set of syringes attached to plastic tubes were joined by a plastic connector with a pipette tip. This tip plugs into the silicone tube used to perfuse the esophagus (see Section 2.4). The plastic connector is

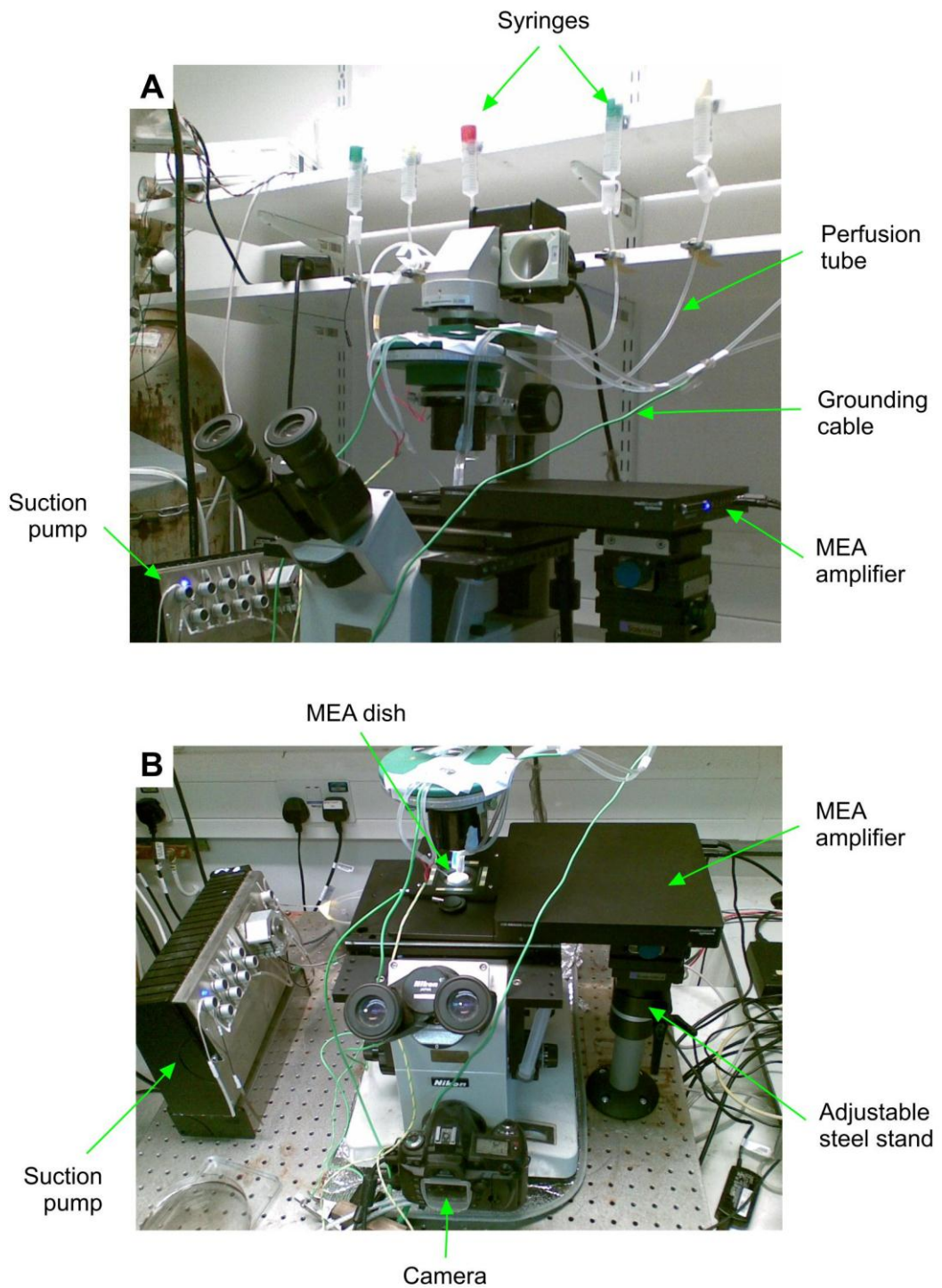


Figure 2.4. MEA recording rig

A & B: The MEA amplifier is positioned over the inverted microscope on an adjustable steel stand. Syringes are used to perfuse the dish. An automatic pump is used to transport liquid out of the dish.

required for rapid switching between saline and sucrose perfusion of the esophagus, whereas separate pipette tips can be used when perfusing the dish. Yet another silicone tube, connected to a mechanical pump, is attached to the microscope lamp head and used to suck liquid out of the dish. Mechanical noise generated by the suction of liquid out of the dish is a recurring problem and must be avoided. Currently the best solution is to diagonally cut the pipette tip at the end of the tube that transports liquid out of the dish. Noise can be reduced further by filling the cut tip with blu tack and using a thin needle to create a narrow passage through the blu tack. These measures allow a thin and even stream of fluid to be sucked out of the dish. Finally the entire perfusion system must be grounded by replacing a short portion of each silicone tube with a grounded steel pipe.

A camera directly attached to the microscope (Figure 2.4B) was used to take photographs of the preparations on the MEA at the beginning of each recording. Examples are shown in Figures 2.1, 2.2 and 2.3. The number of individual cell bodies that could be identified in these photographs varied greatly in different preparations.

2.6 Electrical stimulation techniques

Two procedures for simultaneous MEA recording and electrical stimulation were developed. The first procedure involved moving dish and amplifier to an intracellular recording rig and inserting electrodes into ganglia other than those being recorded on the MEA (see Section 4.1). MEA-recorded ganglia are of course covered by glass and thus not accessible to intracellular electrodes.

The second stimulation procedure involved a fire-polished glass suction electrode. Loose nerve endings were sucked into the saline-filled electrode tip, creating a reasonably tight seal. Current was then passed through the nerve, from a silver wire inside the electrode to a second wire on the outside. This method was primarily used to stimulate the dorsobuccal nerve, which carries information about food from the esophagus to the buccal ganglia (Section 1.3). A short 0.2 V pulse (1 s, 5 Hz, 5 ms pulse-width) to the dorsobuccal nerve reliably induced fictive feeding (Section 5.2).

2.7 Recording software and settings

Recordings were made in MC_Rack (Multi Channel Systems, Germany) at a sampling frequency of 5-10 kHz. Maximum sampling frequency is 40 kHz but produces enormous data files and is currently not required as our spike sorting technique (see Chapter 3) uses only spike amplitude and not detailed waveforms. Recording from 252 electrodes at a 10 kHz sampling rate produces 4.8 MB of voltage data per second. Recordings were saved as 120-second segments to prevent complete data loss in the event of a system crash. MC_DataTool (Multi Channel Systems, Germany) was used to merge the files at the end of each recording.

2.8 Protocols

Three protocols were used to generate most of the data presented in Chapters 4 and 5. Each recording lasted 1000 s. Preparations were perfused at a rate of about 3 ml/min. In the first protocol the esophagus was perfused with saline for 12 min, then with 20 mM sucrose in saline for 2 min, then again with saline. This is the most effective way of inducing fictive feeding *in vitro*.

The second protocol was identical to the first but in addition the dish was also, using a separate tube, perfused with saline for the first 10 min, then with the dopamine receptor antagonist methylergonovine in saline for 4 min, then again with saline. The aim of this protocol was to test whether the dopamine antagonist would interfere with sucrose-induced acceleration of the feeding CPG. The concentrations of methylergonovine used were between 1 and 1000 μM . Methylergonovine has been shown to act as a dopamine antagonist in mollusks (Ascher, 1972; Teyke et al., 1993) and is frequently used to study dopamine-mediated reward processes in molluscan systems, including classical reward conditioning in *Lymnaea* (Kemenes et al., 2011).

The third protocol was identical to the first except that 0.1 mM dopamine hydrochloride was used rather than sucrose. This concentration has previously been shown to induce high-frequency fictive feeding *in vitro* (Kyriakides and McCrohan, 1989) but this had not previously been demonstrated on an MEA.

2.9 Monitoring the stomatogastric ganglion on the MEA

After having developed the MEA method to enable us to record multi-neuronal activity in the *Lymnaea* brain, we investigated its suitability for use with another invertebrate preparation. To this end, a few initial pilot experiments were conducted with the aim of using the MEA to record activity in the stomatogastric ganglion (STG) of the crab *Cancer pagurus*. The STG contains two well-characterized CPGs associated with mastication (Marder and Bucher, 2007). Figure 2.5 shows an example of the STG on the MEA. The techniques used were almost identical to those used to monitor *Lymnaea* on the MEA except that in the case of the STG the ganglion was fully de-sheathed to improve signal-to-noise. Although multiple spike trains could be recorded on the MEA for at least two hours, all rhythmic bursting disappeared within minutes of the start of recording. This suggests that some aspect of stabilizing the STG on the MEA, such as the application of pressure, is detrimental to the CPGs, which normally produce rhythmic bursting continuously. More experiments are required and the results will not be discussed further.

2.10 Using laser to record neural activity on the MEA

A feasibility trial was conducted with the aim of using infrared laser to record neural activity in the buccal ganglia while these were monitored on the MEA. This involved construction of an optical recording rig in which the MEA dish and amplifier could be positioned such that a 200 μm diameter laser beam could be shone through the ganglia. Two collimators were used to polarize the laser beam at different angles on either side of the MEA. Cross-polarized light has previously been used to detect neural activity in the crustacean leg nerve (Carter et al., 2004; Schei et al., 2008; Yao et al., 2005). These studies found that neural activity induced a change in the birefringence of the nerve, and thus in the intensity of light passing through the polarisers on opposite sides of the nerve. However, in our system the method was not successful. Even the population-wide bursts of activity associated with activation of the feeding CPG produced no measurable change in birefringence. This may indicate a flaw in our implementation of the technique. However, the previous studies involving the crustacean leg nerve detected a change in birefringence only during electrical

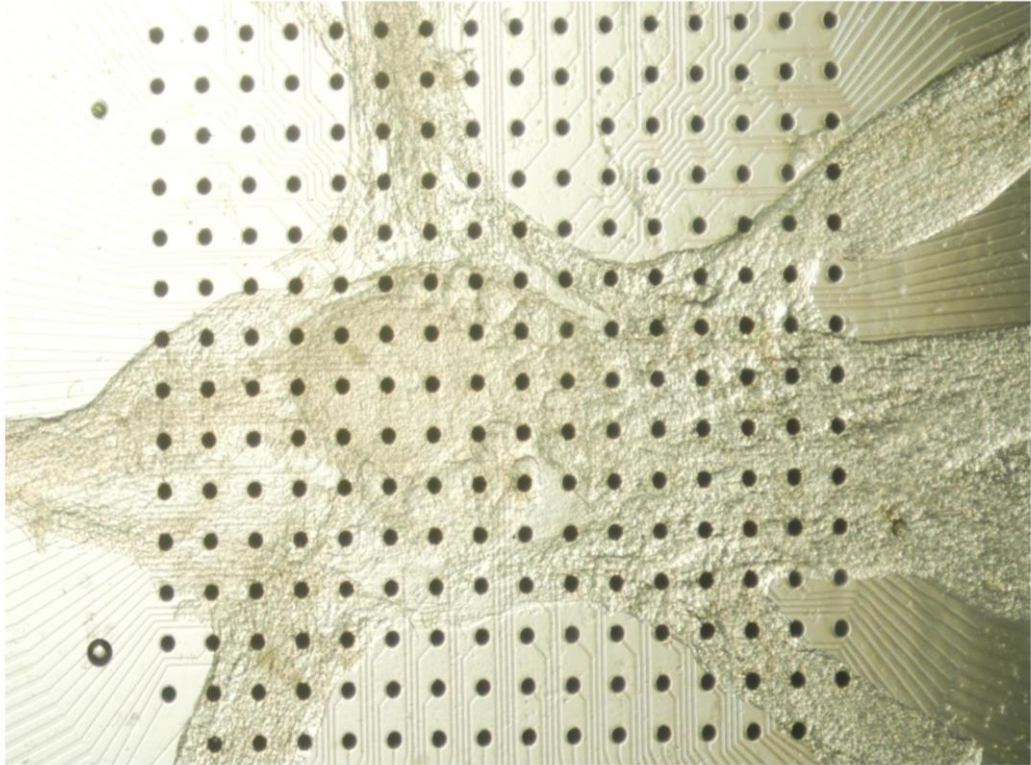


Figure 2.5. The stomatogastric ganglion on the MEA

Stomatogastric ganglion (dorsal view) on an MEA with 30 μm diameter electrodes spaced 100 μm apart.

activation of the nerve. The absence of birefringence changes in the buccal ganglia may therefore just as well indicate that the method is not effective for measuring biologically plausible patterns of neural activation. The laser-based recording method will not be discussed further.

Chapter 3

Results: Spike sorting

The MEA records voltage spikes on most electrodes that are in contact with ganglia. This does not necessarily mean that there are distinct spiking neurons at each such electrode, as individual spikes were often detected simultaneously on multiple neighbouring electrodes. On the other hand, spikes were not detected on electrodes located at a distance from or even adjacent to the brain. This is presumably because the pressure applied to the brain by the glass coverslip significantly increases conductance in the narrow space between the brain and the MEA, allowing charge to travel along the horizontal plane and be detected at a distance. In the absence of spikes the MEA recorded baseline noise levels of about $\pm 30 \mu\text{V}$ on $30 \mu\text{m}$ diameter electrodes and $\pm 40 \mu\text{V}$ on $10 \mu\text{m}$ diameter electrodes. The noise has a slow 2 Hz component and a fast 50 Hz component, both of which are significantly attenuated by removal of the perfusion system from the dish. Spikes ranged in amplitude from about -0.5 to +1 mV (Figure 3.1). The main up- or down-swing of spikes typically lasted 2-4 ms. Many high-amplitude spikes also featured an 'afterhyperpolarization' that lasted 4-6 ms (Figure 3.1A) and some spikes had complex shapes, such as double peaks (Figure 3.1C).

Many electrodes recorded two or more spike trains with clearly distinguishable amplitudes and firing patterns (Figure 3.2). These spike trains are presumably generated by different neurons. This conclusion is based on the observation that spikes belonging to distinct spike trains were consistently and simultaneously detected on specific combinations of electrodes, with high amplitudes at one or a few central electrodes and lower amplitudes on neighbouring electrodes, suggesting a unique

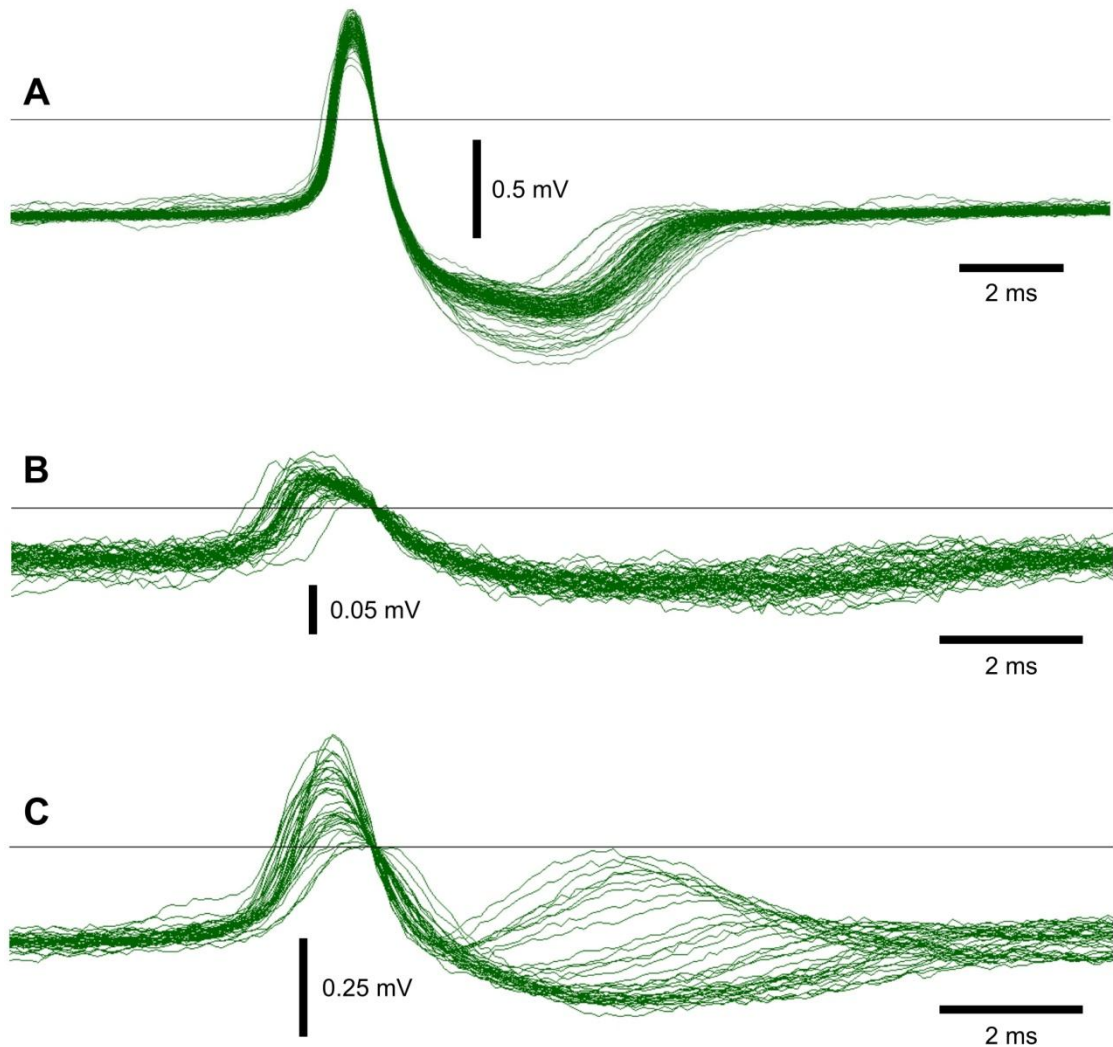
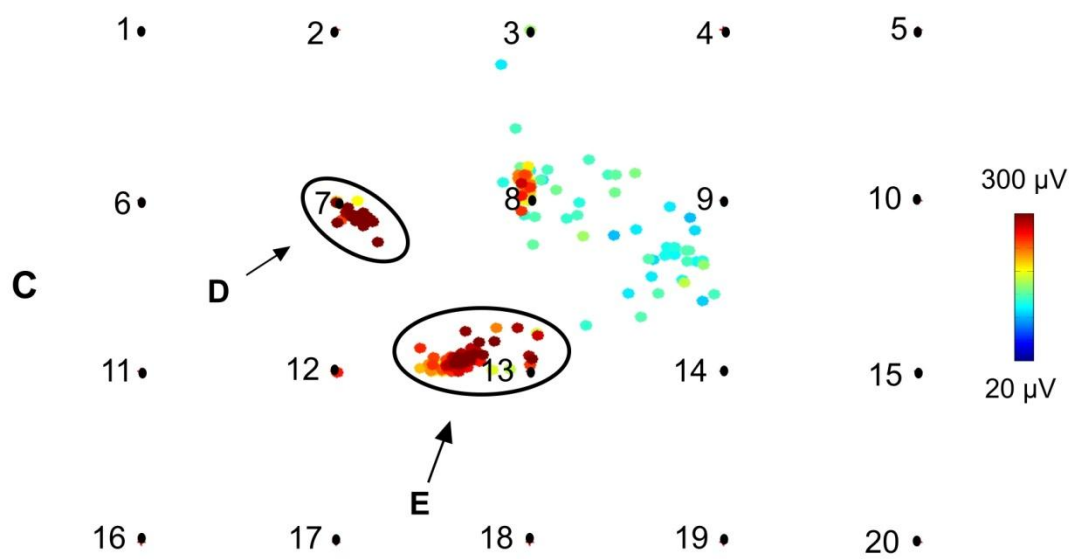
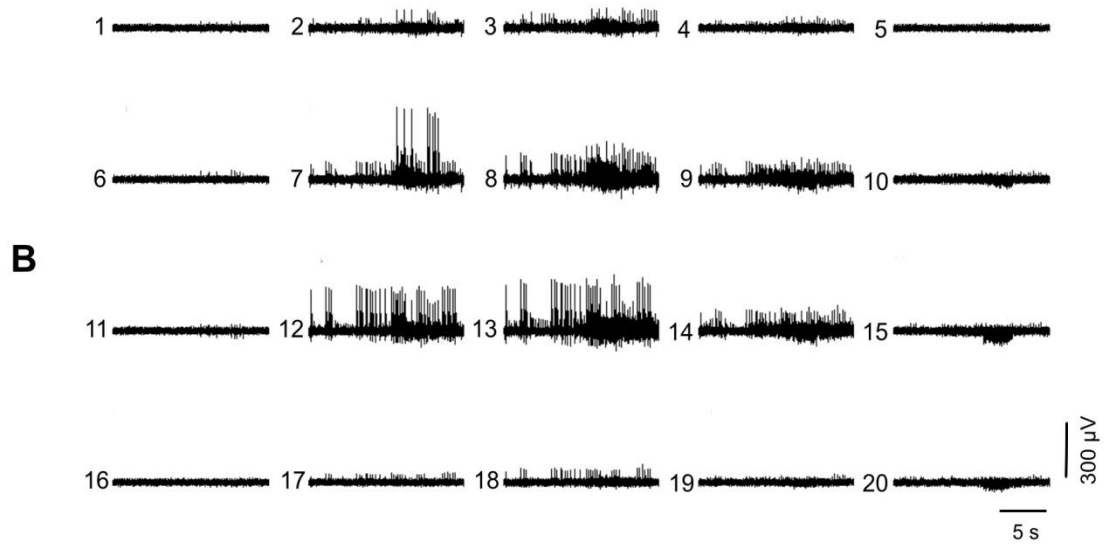
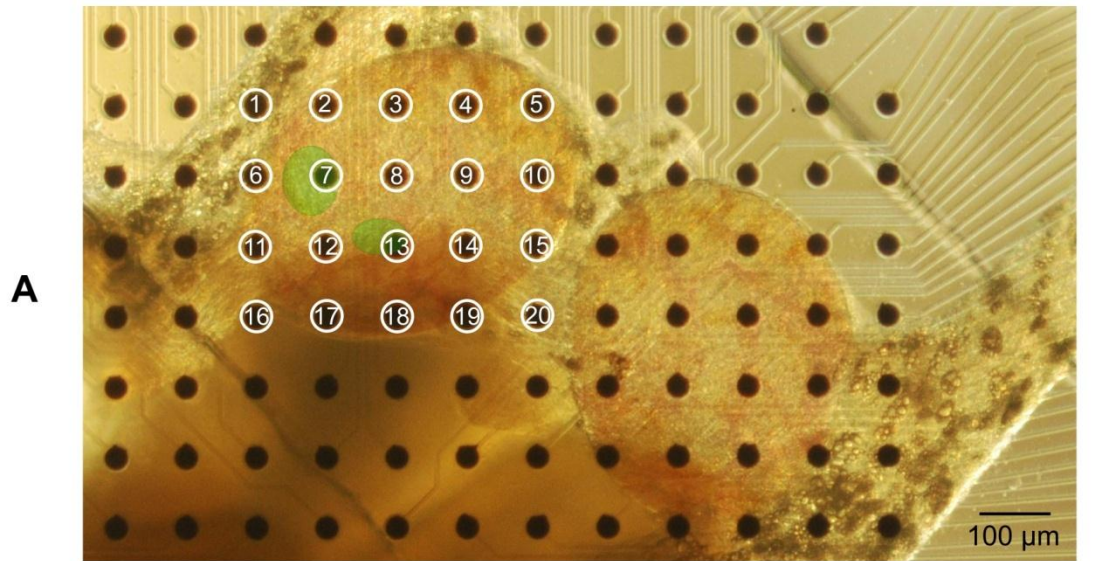


Figure 3.1. Voltage spikes recorded on the MEA

Spikes recorded sequentially on three different 30 μm diameter electrodes at a sampling frequency of 10 kHz. **A:** 100 high-amplitude spikes of a tonically firing neuron (inter-spike interval approx. 1 s). **B:** 50 medium-amplitude spikes of a tonically firing neuron (inter-spike interval approx. 1 s). **C:** 34 spikes of a bursting (protraction-phase) neuron during a single feeding cycle (inter-spike interval approx. 150 ms). Note the variable spike waveform. Early in the cycle the spikes had a high amplitude and a depolarized post-spike period, whereas later in the cycle they had a reduced amplitude and a hyperpolarized post-spike period. This in-burst waveform variability complicates the spike sorting process.



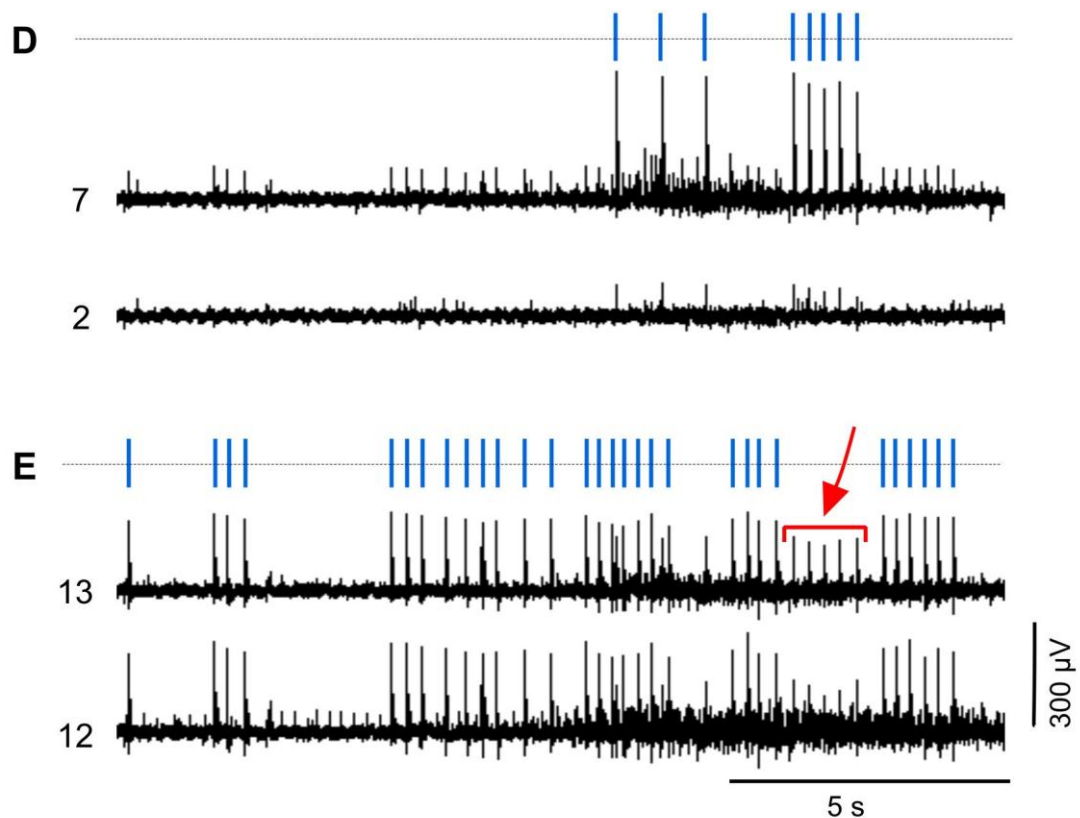


Figure 3.2. Summary of the spike sorting process

A: Photomicrograph of the buccal ganglia on the multi-electrode array. The black dots are electrodes. Two neuronal cell bodies are highlighted in green. **B:** Voltage data recorded on the numbered electrodes in A. **C:** Spike sorting was performed using triangulation (see text, a 50 μV spike detection threshold was used). The coloured dots represent the amplitude (colour bar 20 – 300 μV) and estimated spatial origin of spikes detected on the numbered electrodes in A. Two spike clusters are indicated by ellipses. Note that their location corresponds to the two neurons highlighted in A. Their spike-sorted rasters are shown in **D** and **E**. **D & E:** Spikes in the two clusters highlighted in **C** correspond to identically timed spike patterns recorded on multiple electrodes, which are presumed to originate in individual neurons. The sorting process distinguishes spikes generated by different neurons that are recorded on the same electrode. For example, the spikes in the voltage data recorded on electrode 13 indicated by a red arrow and bracket in fact originate at electrode 7, as evidenced by their higher amplitude there. Adapted from Harris et al., 2012.

spatial origin for each spike train (Figure 3.2, 3.3). Spike trains with similar amplitude, location and firing pattern were moreover observed across different preparations and presumably reflect the activity of some of the large identified buccal motoneurons (see Section 4.4).

A process was developed for assigning spikes with distinct spatial origins to different putative neurons. This chapter describes that process, which is summarized in Figure 3.2. Although the process should be applicable to MEA data generally, it was used here to sort spikes recorded in the buccal ganglia at a sampling frequency of 10 kHz on an array of 30 μm diameter electrodes spaced 100 μm apart. About 40 electrodes were in contact with the buccal ganglia in each recording. All results of spike sorting discussed below refer to data generated by this particular combination of tissue and array.

The MC_Rack software offers basic spike detection and sorting functionality based on manually adjustable thresholds. Sorting spikes in MC_Rack is very time consuming however and did not allow us to confidently isolate more than about 5 unique spike trains per recording. This was due to the detection of multiple spike trains on individual electrodes, individual spikes being detected on multiple neighbouring electrodes, and spike amplitudes varying during bursts, all of which complicate the separation of distinct spike trains by manual thresholding.

3.1 Pre-processing

A Butterworth 2nd order high-pass filter with a 100 Hz cut-off frequency was applied to the MEA data using the MC_Rack filtering function in order to reduce baseline noise and remove local field potentials and occasional noise emanating from the perfusion system or from spontaneous contractions of the esophagus. The filter reduced baseline noise to less than $\pm 20 \mu\text{V}$, without visibly attenuating absolute (peak-to-trough) spike amplitude. Higher cut-off frequencies resulted in only marginal additional noise reduction while significantly reducing total spike amplitudes. Although the 100 Hz filter did not change absolute spike amplitudes it invariably made spikes symmetric in the positive and negative direction. This is an unexpected result of filtering that warrants further investigation.

The MC_Rack data format is only readable by MC_Rack itself and a few

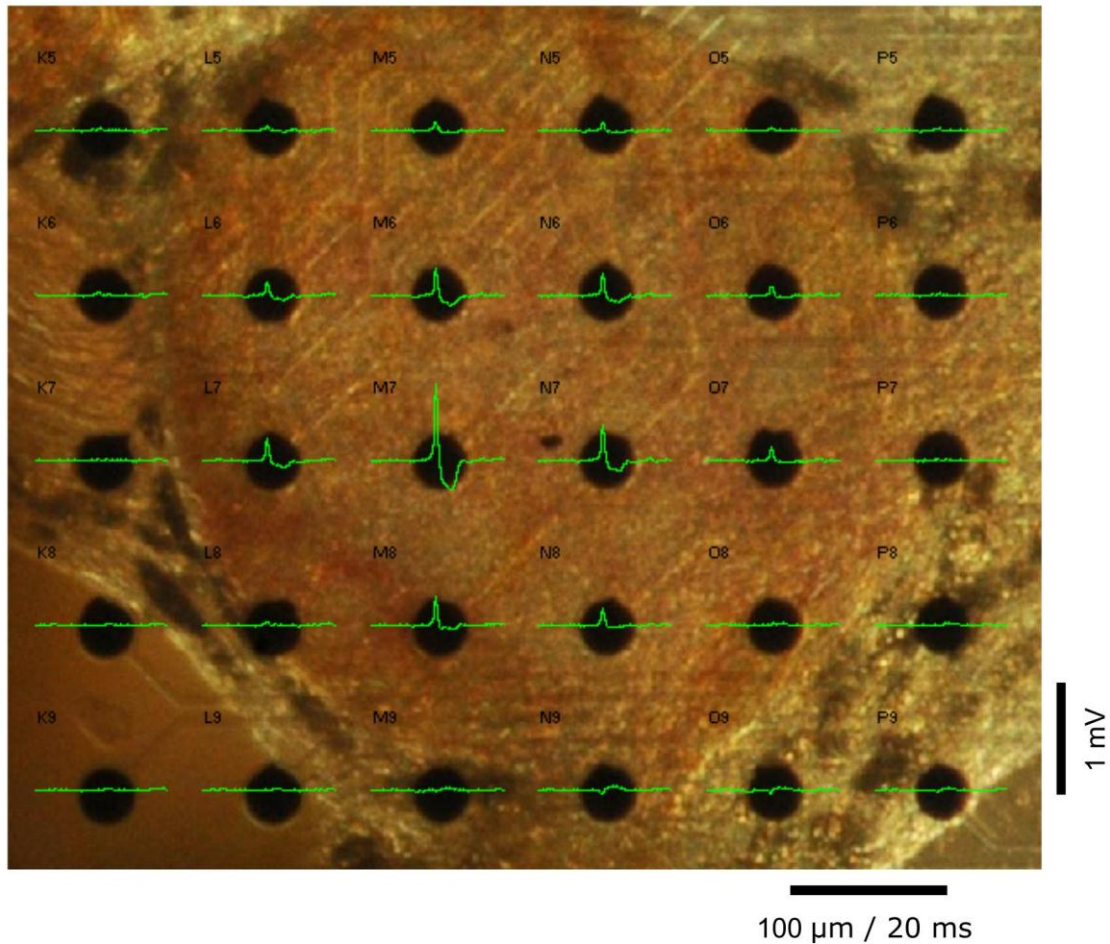


Figure 3.3. Spike amplitude at different electrodes indicate neuronal location

Buccal ganglion (dorsal surface) on an MEA with 30 μm diameter electrodes spaced 100 μm apart. A single high amplitude spike (green traces) is simultaneously detected on multiple neighbouring electrodes. Amplitude is highest at a central electrode (M7) and lower on surrounding electrodes, indicating that the neuron which produced the spike is located close to electrode M7. Note the particularly low amplitude at the neighbouring electrode L8. This reflects lower conductance at the edge of ganglia.

proprietary software packages, such as NeuroExplorer. The filtered MEA data was therefore converted to ASCII. All subsequent analysis was conducted in MATLAB (MathWorks, US).

3.2 Estimating the spatial origin of spikes

A threshold of 20 μV was used to detect spikes in the filtered MEA data. A maximum detection rate of 200 spikes per electrode per second was used to avoid multiple detection of the same spike on a single electrode. Spikes that were detected within 1 ms of each other on *different* electrodes were treated as originating from a single neuron (Figure 3.3). This is an oversimplification, since spikes from distinct neurons occasionally occur near-simultaneously. Such coincidences appear however to be rare in small regions of tissue, such as a few ganglia monitored on the MEA, but may be a problem when the entire dorsal or ventral surface of the brain is monitored.

Each set of spikes detected the within the 1 ms window is here called a ‘spike event’ and is defined by a time, a peak amplitude (equal to the maximum spike amplitude recorded on any electrode during the 1 ms time window) and a location or ‘center-of-mass’ (Gross, 1979; Novak and Wheeler, 1986), which is defined as:

$$x = \frac{\sum_i (x_i)(s_i)^2}{\sum_i s_i^2}, \quad y = \frac{\sum_i (y_i)(s_i)^2}{\sum_i s_i^2}$$

where x and y represent the spatial origin of the spike event; x_i and y_i are the coordinates of the i th recording electrode and s_i is the amplitude of the i th recorded spike. All amplitudes were squared to improve clustering. The average spike event was detected by about 7 electrodes. Only the electrode that registered the peak amplitude of the spike event, and its 8 neighbouring electrodes, were used in each centre-of-mass calculation. Coincident spikes detected further away from the peak of the spike event were discarded. Spike events with less than three detecting electrodes were also discarded. A typical recording from the buccal ganglia contained 16.9 ± 13.5 spike events per second (mean \pm standard deviation, $n = 37$ preparations). Spike amplitude

was 43.5 μV (median, $n = 581712$ spike events, inter-quartile range = 28 μV , skewness = 5.9). This median value is low relative to the example spikes in Figure 3.1 because it includes all spike events recorded on the MEA, about half of which were not assigned to neurons due to low amplitude and poor clustering (see Section 3.3).

3.3 Distinguishing spikes by location and amplitude

Figures 3.2C and 3.4A show spike events plotted according to their estimated location on the MEA. The spikes form clusters which are manually assigned to distinct neurons in two steps. First a circle is manually drawn around a spike cluster. Many clusters have clear boundaries and can be confidently circled, others are less obvious. Clear boundaries mean that spike density drops off sharply at the edge of a cluster (red arrow in Figure 3.4A) or that there is a distinct difference in amplitude between spikes in a cluster and the surrounding low-amplitude spikes (black arrow in Figure 3.4A).

After a cluster of spikes has been circled a histogram is drawn showing the amplitudes of all spikes located within the circle (Figure 3.4B). This allows clusters of high-amplitude spikes to be separated from the low-amplitude spikes that often surround them (dashed red line in Figure 3.4B). Close to the centre of ganglia especially there is typically a large number of low-amplitude spikes with no clear boundaries (e.g. middle of Figure 3.4B). These spikes were generally not assigned to neurons. Presumably they reflect the activity of small or poorly de-sheathed neurons. The poor clustering might be due to the large number of small neurons relative to bigger cells, and to the fact that the localization of low amplitude spikes is particularly sensitive to distortion by noise voltage fluctuations.

About half of all spike events were assigned to neurons during spike sorting. The process returned 15.2 ± 3.6 neurons per paired buccal ganglia (mean \pm standard deviation, $n = 37$ preparations), or about one neuron per three electrodes in contact with the brain. (There are about 100 neurons on the surface of each buccal ganglion (e.g. Figure 2.2G).) The typical amplitude of spikes that were assigned to neurons was 69.6 μV (median of the neuronal means, $n = 565$ neurons, inter-quartile range = 81 μV , skewness = 1.5). The amount of manual work required by the spike sorting method is similar to other location based semi-manual methods, which also require neuron-by-neuron sorting, e.g. (Prentice et al., 2011).

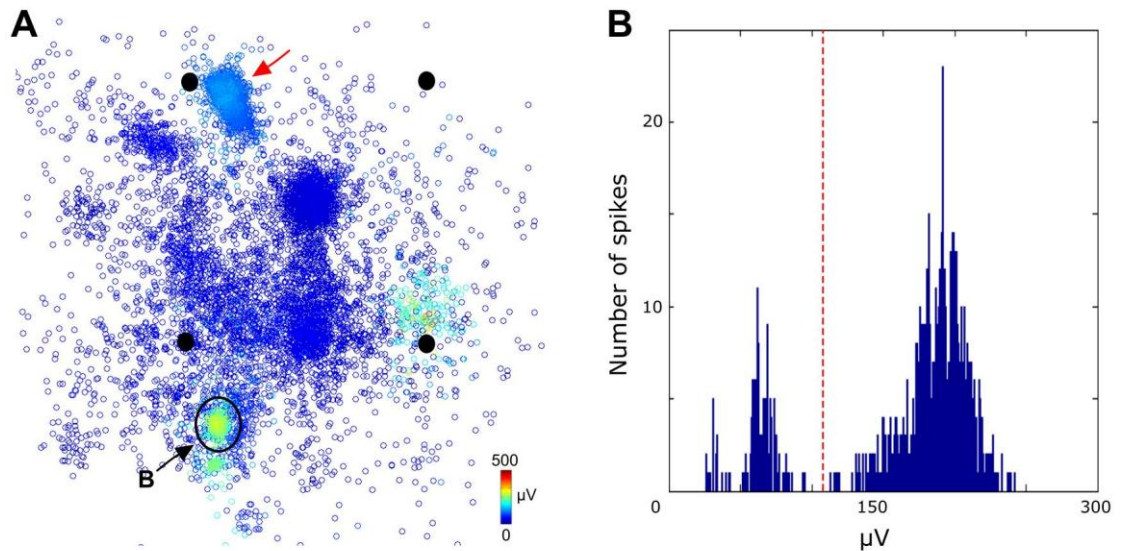


Figure 3.4. Delimiting spike clusters

A: Amplitude and estimated spatial origin of spikes recorded on one buccal ganglion in the vicinity of four neighbouring electrodes (black dots). 1000 s of data were processed. The red arrow indicates a spatially well-defined spike cluster. The black arrow and circle indicate a cluster of high-amplitude spikes surrounded by low-amplitude spikes. **B:** Amplitudes of all spikes circled and indicated by the black arrow in A. The dashed red line shows the threshold that was applied to separate high-amplitude spikes from the surrounding low-amplitude spikes.

3.4 Quality control

The spike sorting process was validated by plotting sorted spikes on or next to the raw voltage data (Figure 3.2D & E, 3.5). Sorted spikes appear to correspond to distinct spike trains, many of which could not have been distinguished using a simple threshold (e.g. electrode 12 in Figure 3.2D, electrode 3 in Figure 3.5).

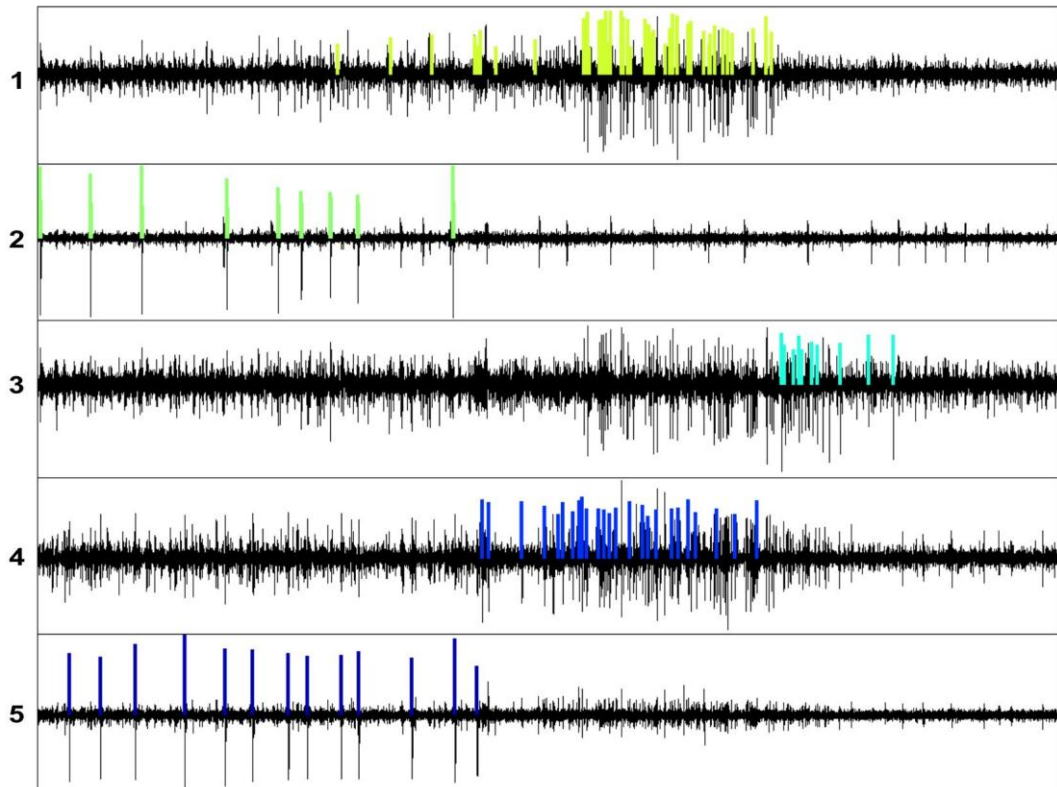


Figure 3.5. Validating the spike sorting process

Spikes from five spike clusters (putative neurons) are superimposed on MEA data from the electrode closest to the estimated spatial origin of the spikes. All data was simultaneously recorded and reflects a single cycle of fictive feeding. Although the sorting is not perfect, it appears to capture five spatiotemporally distinct spike trains, some of which (e.g. electrode 3), could not have been isolated by means of a simple threshold.

Chapter 4

Results: Fictive feeding and experimental perturbations

The previous two chapters show how to position semi-intact preparations of *Lymnaea* in the MEA dish and how to record the activity of multiple neurons while subjecting the brain to sensory, chemical or electrical perturbations. The aim of developing this method was to allow the characterization of populations of neurons associated with adaptive feeding behaviour. By analysing dopamine-mediated adaptation of CPG output at the level of neuronal populations my collaborators and I hoped to uncover general mechanisms of adaptive pattern generation and intelligent behaviour.

4.1 Fictive feeding induced by depolarization of a cerebral neuron

To confirm that the rhythmic activity of the feeding CPG could be recorded on the MEA we first used an intracellular electrode to depolarize the cerebral interneuron CV1a (Figure 4.1). Depolarization of this neuron is a well-established method for driving rhythmic activity in the feeding CPG (Kemenes et al., 2001). The firing of the neuron is also known to be phase locked with the feeding motor pattern during fictive feeding due to phasic input from the feeding CPG (McCrohan, 1984). Figure 4.1 shows the *Lymnaea* CNS with the buccal ganglia on the MEA and an intracellular electrode in the cerebral interneuron. This preparation was quiescent prior to stimulation, meaning that only sporadic single-unit activity was recorded on the MEA. Depolarization induced a burst in the CV1a neuron which was almost immediately followed by a multi-phasic pattern of rhythmic bursting in the buccal ganglia. Importantly, the firing of the CV1a neuron phase-locked with the oscillations recorded in the buccal ganglia.

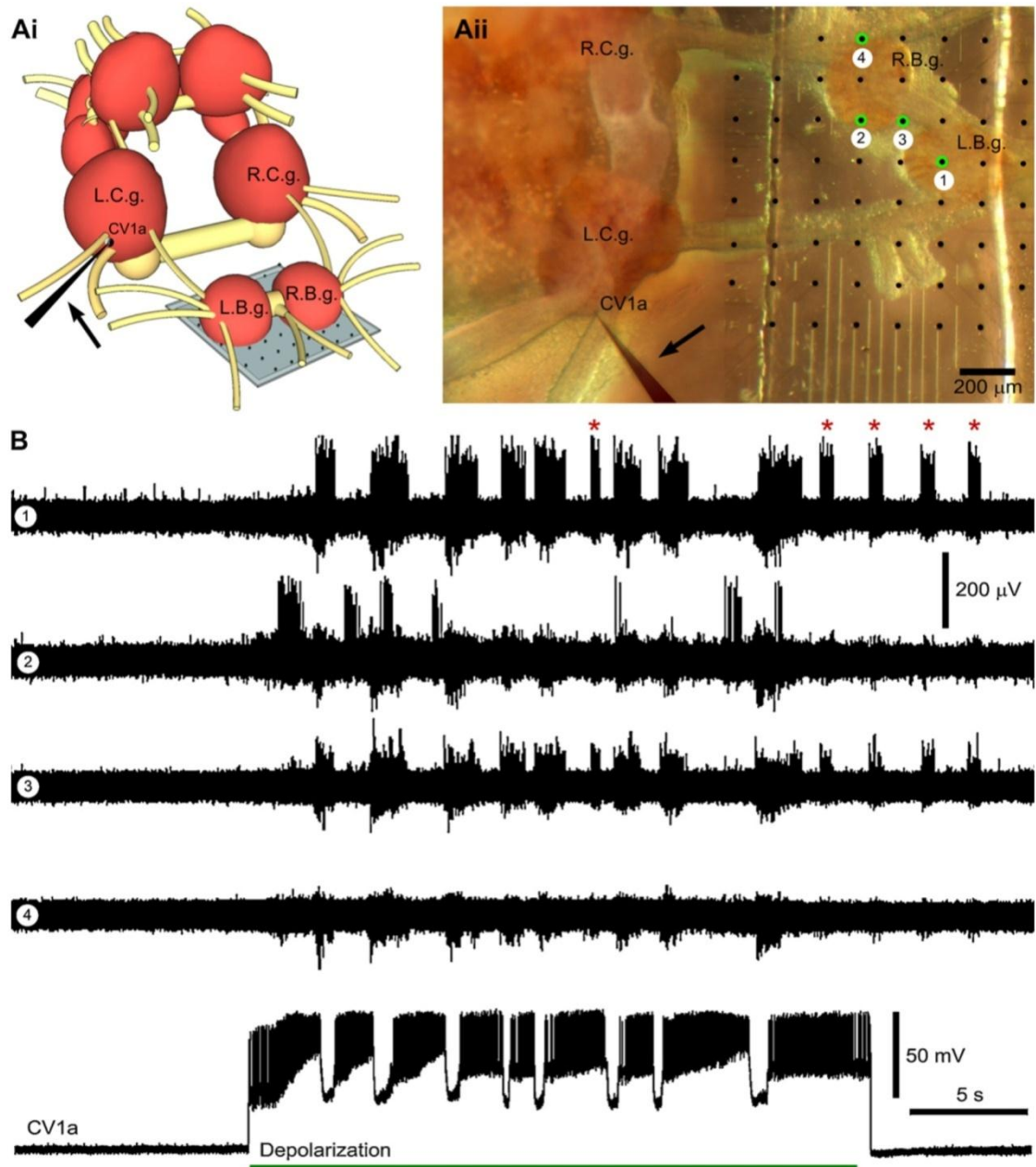




Figure 4.1. Fictive feeding induced by depolarisation of a cerebral interneuron

MEA recording of rhythmic feeding motor output triggered by the activation of a single command-like neuron of the *Lymnaea* feeding circuitry. **Ai:** A 3-D schematic of the preparation and the recording and stimulation arrangements. An intracellular microelectrode (arrowed) was inserted into the CV1a neuron in the left cerebral ganglion (L.C.g.). The paired (left and right) buccal ganglia (L.B.g. and R.B.g.) were positioned with the dorsal surfaces on the MEA. **Aii:** A photomicrograph of the preparation from which the intra- and extracellular traces shown in B were recorded simultaneously. The left half of the image was photographed from above and the other half from below. The black dots represent individual electrodes of the MEA. The microelectrode used to record and stimulate the CV1a neuron is indicated by an arrow. **B:** Activation of CV1a by steady depolarization through the bridge-balanced recording microelectrode (lowest trace) activates fictive feeding. CV1a monosynaptically activates interneurons of the feeding CPG, whose reciprocal monosynaptic connections with CV1a phase-lock its activity to the rhythmic fictive feeding pattern (McCrohan, 1984). The CPG neurons directly drive the motoneuronal burst activity recorded here with the MEA and shown in the example traces recorded on the electrodes circled in green and labelled 1–4 on the photomicrograph in Aii. Notice that in the recording from electrode 1 the longer bursts of activity are phase locked to periods of inhibition of the CV1a neuron (lower trace) but that briefer bursts at this electrode (marked by asterisks) are not associated with the inhibition of CV1a. Adapted from Harris et al., 2010.

Whereas the bursts recorded on electrode 1 were consistent, occurring in every cycle, the spikes recorded on electrode 2 varied greatly in number in each feeding cycle. This highlights the variable spatiotemporal structure of feeding cycles, a feature also observed in experiments involving traditional single-unit methods. The depolarising stimulus moreover triggered a distinct pattern of bursting (asterisks in Figure 4.1) that was not phase-locked with the main feeding rhythm and which outlasted the end of the current injection. This shows that the MEA can detect neural activity that is associated with feeding but not reflective of a previously identified neuron of the CPG.

These observations show that the rhythmic activity of the feeding CPG can be induced and recorded on the MEA. This particular experiment was considered proof-of-principle and was only repeated once, with similar results (data not shown).

4.2 Fictive feeding induced by a chemosensory sucrose stimulus

Having confirmed that rhythmic activation of the feeding CPG can be recorded on the MEA we proceeded to investigate whether the CPG could also be activated on the MEA by a sensory food stimulus. Previous experiments have shown that perfusing the esophagus or lip of a semi-intact preparation with sucrose [20 mM] accelerates fictive feeding *in vitro* (Kemenes et al., 1986). Figure 4.2 shows the buccal ganglia attached to the cannulated esophagus. The ganglia remain attached to the rest of the brain during the experiment (not shown). Application of the sucrose stimulus induced a repeating pattern of activity characteristic of fictive feeding in nearly all preparations (see below). In the preparation shown in Figure 4.2, protraction-phase activity was recorded in both ganglia on two cell bodies located in the region of the ganglia where the protraction-phase B1 motorneuron is typically found. Rasp-phase activity was recorded in the posterior region of both ganglia, where the rasp-phase B4CL motorneurons are found. Finally swallow-phase activity was recorded on one centrally located electrode. As Figure 4.2Bi indicates, these multi-phasic bursts of activity were also generated in the absence of the sucrose stimulus, albeit at a much reduced rate. Moreover, the MEA again recorded patterns of activity that were simultaneous but not phase-locked with feeding (e.g. Figure 4.2Bii, electrode 6).

The spatiotemporal structure of the motor pattern varied from preparation to preparation. Although the 3-phase pattern was unmistakable in some preparations

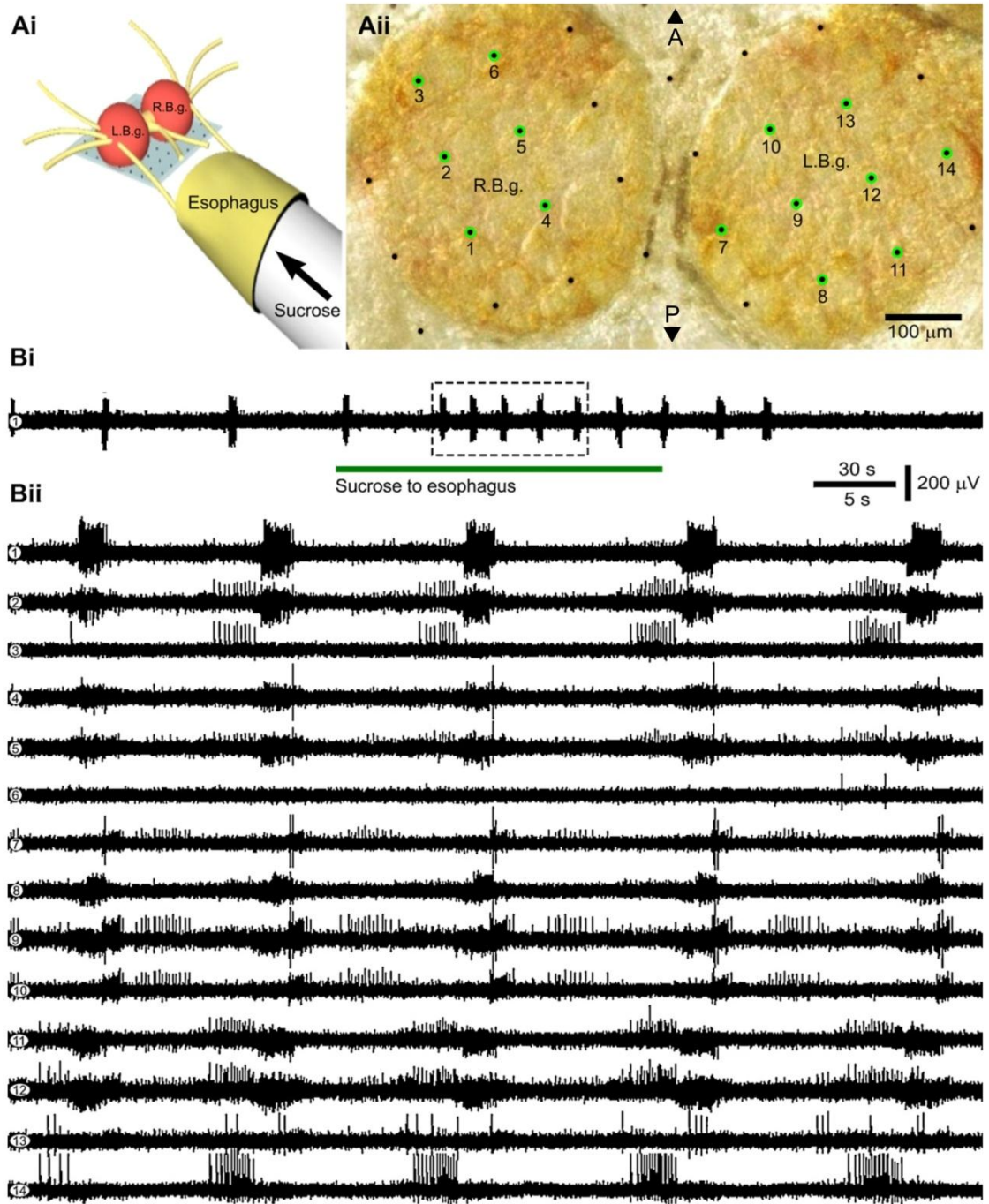




Figure 4.2. Fictive feeding induced by a sensory sucrose stimulus

MEA recording from the buccal ganglia during rhythmic feeding motor output triggered by perfusion of the esophagus with sucrose. **Ai**: A 3-D schematic showing the paired (left and right) buccal ganglia (L.B.g. and R.B.g) on the MEA with a cannulated esophagus attached. **Aii**: A photomicrograph of the dorsal surfaces of the buccal ganglia from which the extracellular traces shown in **B** were recorded simultaneously. **Bi**: A bout of several fictive feeding bursts in rapid succession is induced by perfusion of the esophagus with sucrose. The recording is from electrode 1 shown in **Aii**. The duration of the sucrose stimulus is indicated by the horizontal bar under the recording trace. The window defined by the dashed line shows the region of the recording expanded in **Bii**. **Bii**: 14 extracellular traces recorded on the electrodes circled in green in photomicrograph **Aii**. The traces show activity recorded during the dashed window in **Bi**. Each feeding cycle lasts about 8 s and consists of a sequential pattern of spikes and bursts that is synchronized across both buccal ganglia (see electrodes 3 and 14; 1 and 8; 4 and 7). Adapted from Harris et al., 2010.

(summarized in Figure 4.3) it was less obvious in others. Figure 4.4 shows examples of sucrose-induced feeding motor patterns recorded in different preparations. Sometimes only two of the three phases were observed, at other times there were more than three distinct phases. However, as Figure 4.4 shows the population bursts had a spatiotemporal structure that was distinctive to each preparation and varied only moderately from burst-to-burst. Such stereotypy indicates that cycles of the feeding CPG were recorded on a somewhat random sample of CPG neurons in each preparation. The fact that sucrose-induced population bursts generally appeared to have the same spatiotemporal structure as spontaneously generated population bursts (see Figures 4.3 and 4.6), though they occurred at a significantly higher rate, reinforces this interpretation. Although most sharp increases in the total rate of spiking recorded in the buccal ganglia correspond to these stereotyped, multi-phasic population bursts, some such increases reflected the synchronized bursting of only a few neurons and lacked the distinctive multi-phasic structure. This type of population burst is not characteristic of fictive feeding and such bursts were discarded during the identification of feeding cycles in the raw or spike sorted data.

In one group of preparations the application of sucrose to the esophagus increased the rate of fictive feeding from 0.5 ± 0.2 to 2.9 ± 0.5 cycles per min (all results represent mean \pm standard deviation unless otherwise indicated, $p < 0.001$, $n = 13$ preparations, Wilcoxon rank sum test). Here feeding cycles were detected in the raw voltage data. In another group of preparations the sucrose stimulus increased the rate of fictive feeding from 0.4 ± 0.2 to 2.3 ± 1.0 cycles per min ($p < 0.001$, $n = 17$ preparations, Wilcoxon rank sum test). Here feeding cycles were detected in spike sorted data. In most preparations the rate of fictive feeding returned to pre-stimulus levels within a minute of the end of the stimulus (data not shown). Sucrose-induced feeding cycles sometimes appeared to involve more neurons and a higher rate of firing than spontaneously generated feeding cycles, but these differences were not consistent across preparations (Figure 4.3). Most feeding cycles had a duration of approximately 10 s - the expected duration of feeding cycles recorded *in vitro* (Tuersley and McCrohan, 1987).

To summarize, sensory-induced acceleration of the feeding CPG was readily observed in semi-intact preparations whose buccal ganglia were monitored on the

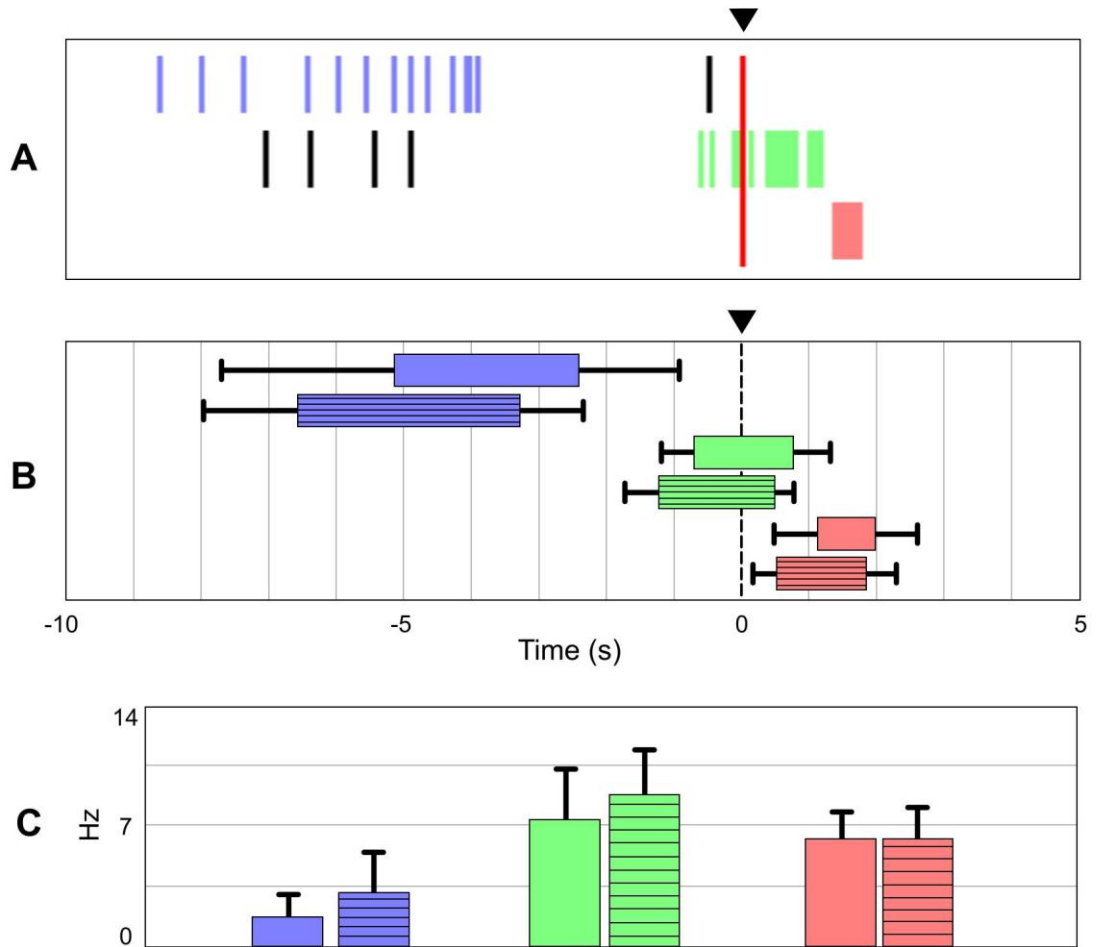
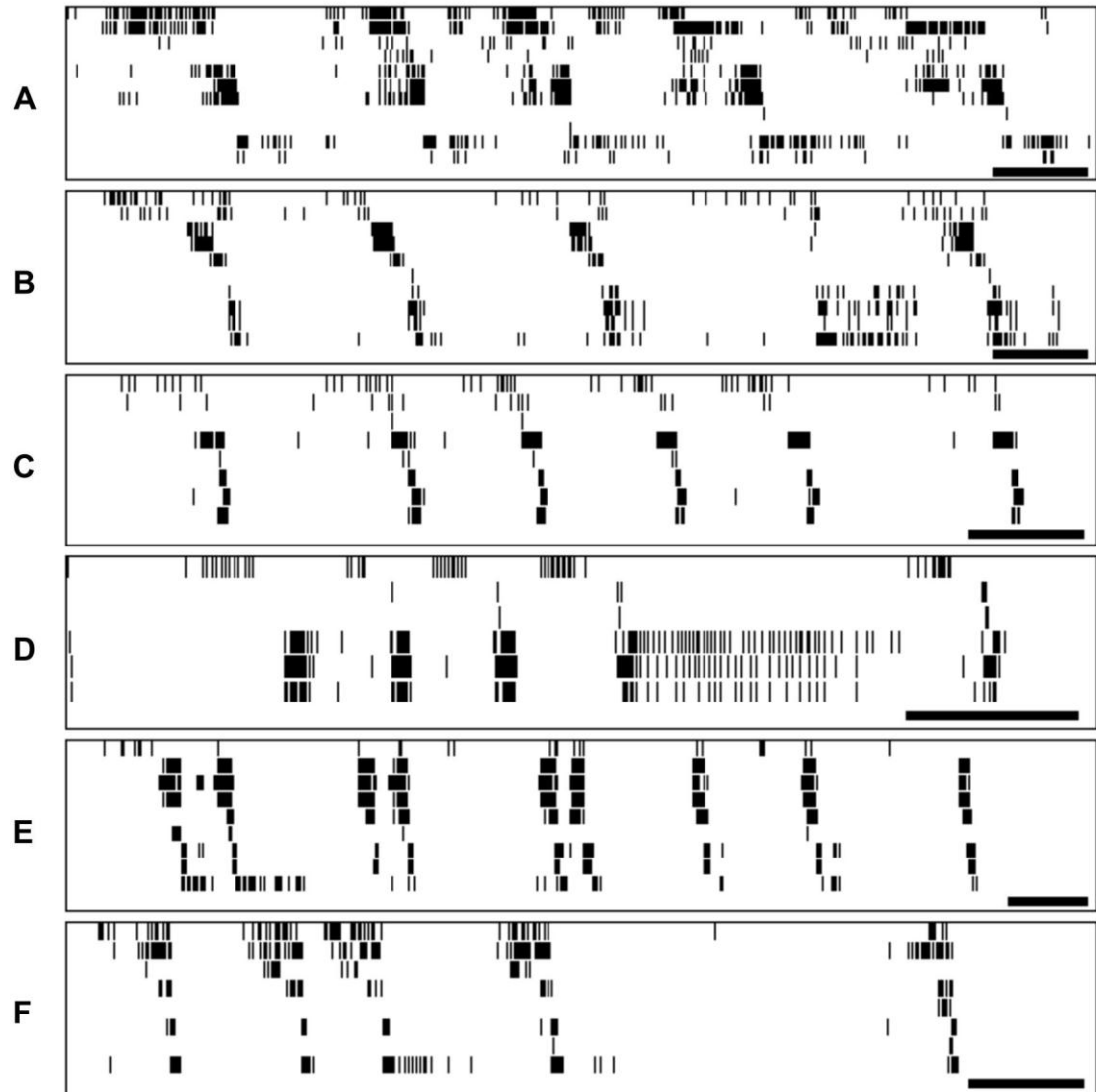


Figure 4.3. Phase structure of 3-phase feeding cycles

Feeding cycles with clearly identifiable protraction (blue), rasp (green) and swallow (beige) phase bursts were selected for analysis of burst onset, offset and peak firing rate. 23 neurons (6 protraction-, 7 rasp-, and 10 swallow-phase) recorded in 5 preparations were analysed during 29 cycles (12 spontaneous and 17 sucrose-induced). **A:** An example feeding cycle. Bursts were identified manually. Sparse or out-of phase spiking was excluded (black spikes). **B:** Burst onset and offset (mean \pm SD) for each neuron type during spontaneous (clear bars) and sucrose-induced (striped bars) feeding cycles. Values are relative to the time of the peak firing rate of the phasic population, which occurs at the beginning of the rasp phase (black arrow-head). **C:** Peak in-burst firing rate for each neuron type during spontaneous (clear bars) and sucrose-induced (striped bars) feeding cycles. This statistic was calculated using a spike density function with a 3 s kernel width.



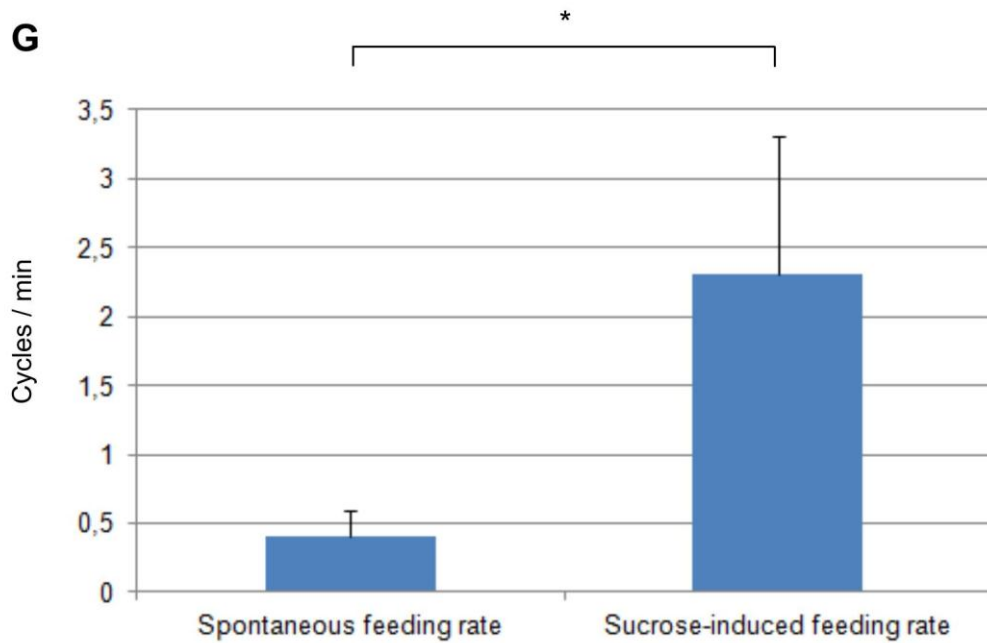


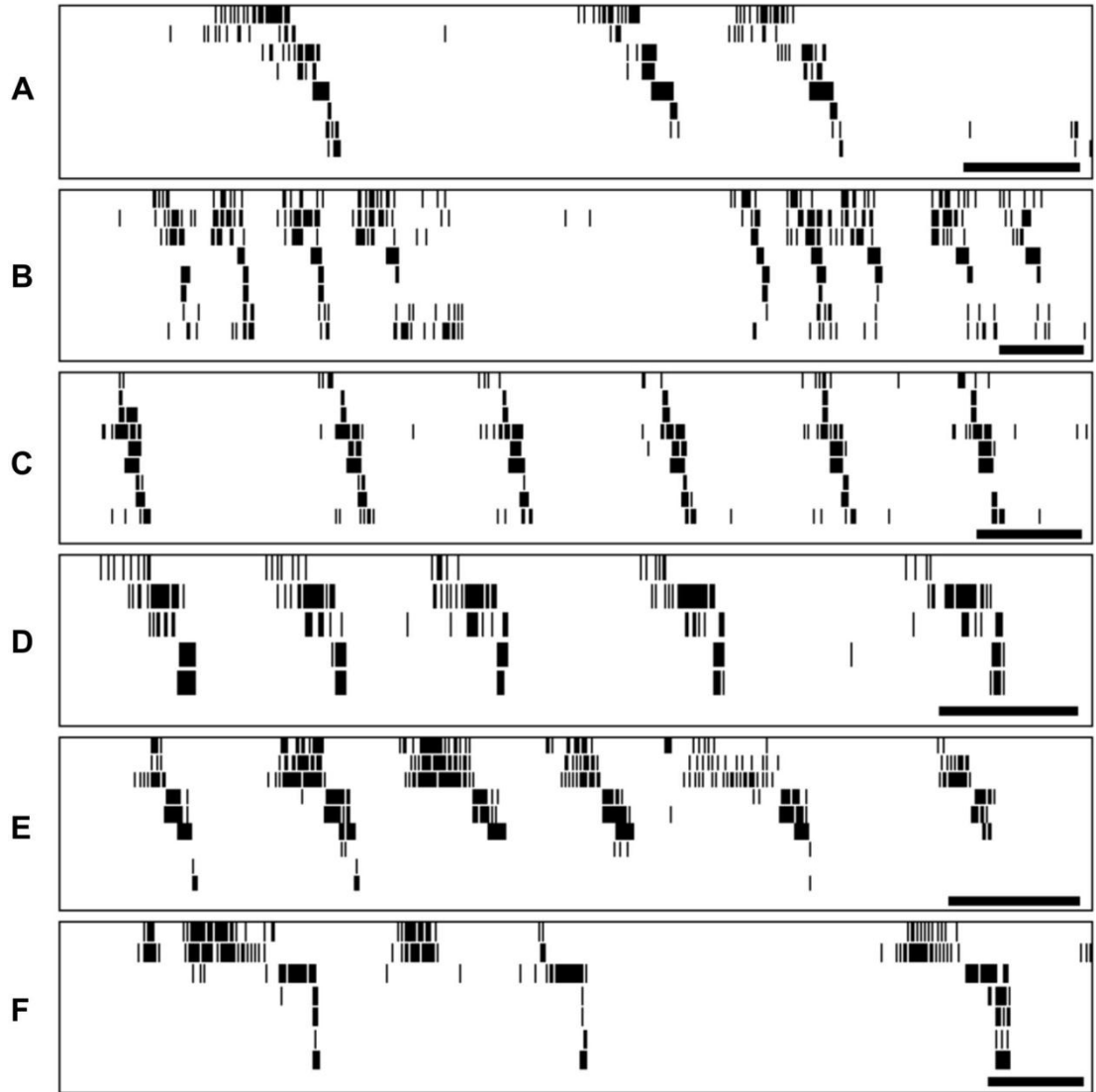
Figure 4.4. Sensory sucrose stimulus induces fictive feeding

A-F: Neurons that reflect the motor pattern of the feeding CPG were selected in six preparations. Rhythmic cycles of fictive feeding were induced by application of sucrose to the esophagus. Preparations were perfused with sucrose throughout the recordings shown. Note the ‘failed’ fourth cycle in **B**. Also note the how the first three cycles in **E** are duplicated; such cycles were generally counted as a single cycle. Black bars represent 10 s. **G:** Spontaneous vs. sucrose-induced feeding rate (mean \pm SD). * $p < 0.001$, $n = 17$ brains (Wilcoxon rank sum test).

MEA. Feeding cycles could be detected both in the raw and spike sorted voltage data. In several cases the pattern included the individual protraction, rasp and swallow phases of the fictive behaviour. However, most preparations did not feature clearly 3-phasic feeding cycles, but rather a spatiotemporal sequence of bursting that was characteristic to each preparation and changed relatively little from cycle-to-cycle. This indicates that a random set of buccal motoneurons is being recorded on the MEA in each preparation.

4.3 Dopamine is necessary and sufficient for rapid fictive feeding

A central aim of the research presented in this thesis was to investigate the role of dopamine in adapting the activity of neuronal populations associated with the feeding CPG to the availability of food. Previous studies have shown that application of dopamine [10 μ M] to the isolated brain of *Lymnaea* induces high-frequency fictive feeding comparable to that induced by a sensory sucrose stimulus (Kyriakides and McCrohan, 1989). We attempted to replicate this finding by perfusing the brain with dopamine while monitoring the buccal ganglia on the MEA. In our case, dopamine accelerated the rate of fictive feeding from 0.5 ± 0.2 to 3.1 ± 1.3 cycles per min ($p < 0.001$, $n = 13$ preparations, Wilcoxon rank sum test). Here too we observed the characteristic 3-phase spatiotemporal structure in some preparations and a more random sample of feeding motor neurons in others (Figure 4.5). In a few preparations we applied a sensory sucrose stimulus, washed out for 10 min, then applied the dopamine stimulus, washed out for 10 min and then applied the sucrose stimulus again. Each stimulus accelerated the rate of fictive feeding, and visual inspection of these recordings suggest that almost all aspects of the spatiotemporal structure of dopamine-induced feeding cycles are very similar to those of both spontaneous and sucrose-induced feeding cycles (Figure 4.6). This again indicates that the same circuit is activated by the different stimuli, but that different neurons are recorded in different preparations. No consistent differences were found between spontaneously generated feeding cycles and those induced by dopamine (data not shown). However, complete cessation of activity in a tonically active neuron was observed in a few preparations, presumably reflecting dopamine-induced inhibition of the large B2 type neuron which has previously been reported (Kyriakides and McCrohan, 1989).



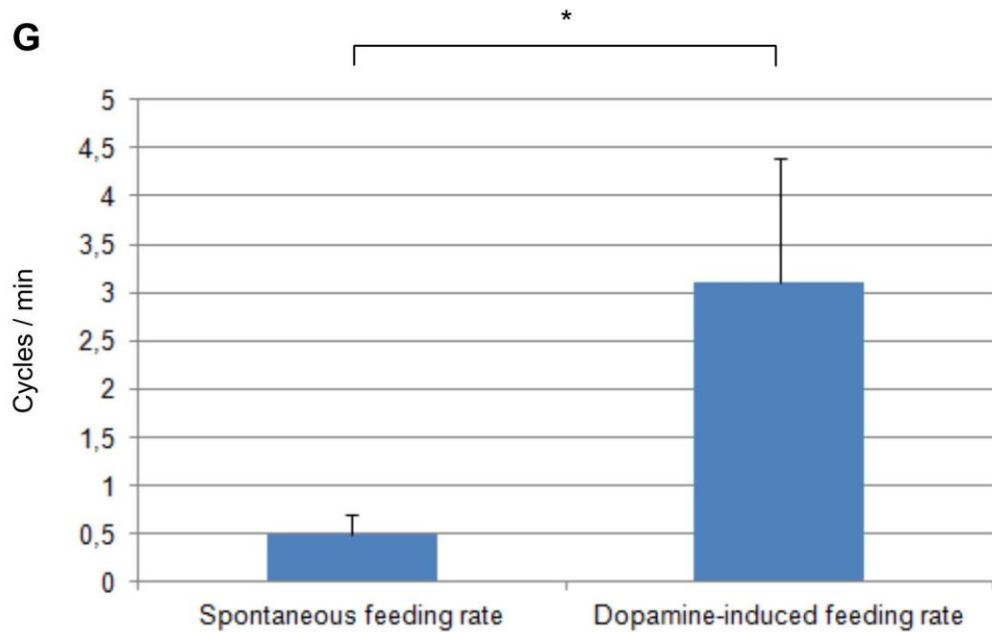


Figure 4.5. Dopamine induces fictive feeding

A-F: Neurons that reflect the motor pattern of the feeding CPG were selected in six preparations. Rhythmic cycles of fictive feeding were induced by application of dopamine to the brain. Preparations were perfused with dopamine throughout recordings shown. Black bars represent 10 s. **G:** Spontaneous vs. dopamine-induced feeding rate (mean \pm SD). * $p < 0.001$, $n = 13$ brains (Wilcoxon rank sum test).

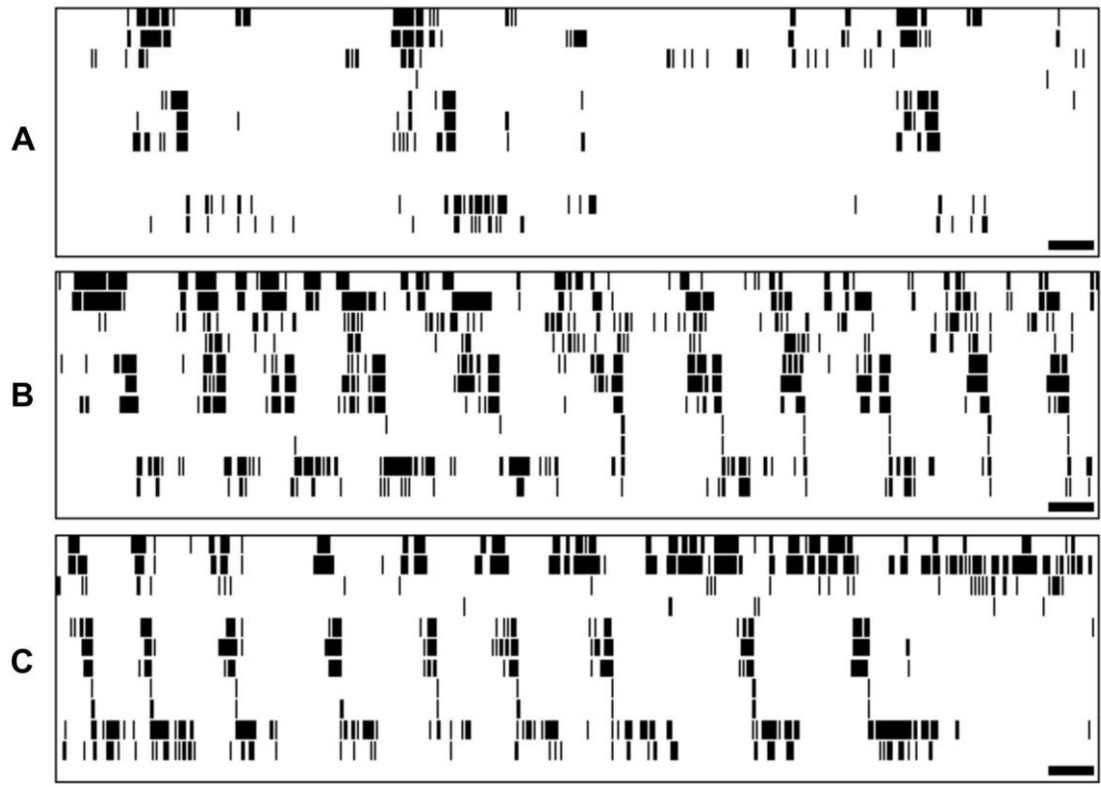


Figure 4.6. Spontaneous and stimulus-driven feeding cycles are similar in a preparation

Spontaneous, sucrose-induced and dopamine-induced feeding cycles recorded in a single preparation (A-C). A 10 min washout period separates B and C. Preparations were perfused with sucrose (B) and dopamine (C) throughout the recordings shown. The spatiotemporal structure of the cycles appears similar across all three conditions, with the exception of two neurons (numbers 3 and 4 from the bottom) which were silent in all spontaneous cycles but fired consistently at the beginning of the swallow phase in most stimulus-induced cycles. Black bars represent 10 s.

High concentrations of dopamine [0.5 mM] (applied only to a few preparations) induced feeding cycles that were initially similar to spontaneously generated cycles but in which the firing rate and duration of firing of some neurons increased markedly with each cycle (Figure 4.7). At very high concentrations of dopamine this expansion of activity resulted, within a few cycles, in near-constant bursting across the buccal ganglia (data not shown).

To further investigate the role of dopamine in the acceleration of the feeding CPG we applied the dopamine antagonist methylergonovine [10 μ M] to the dish two minutes prior to and during the application of the esophageal sucrose stimulus. This experiment had not previously been conducted, but methylergonovine has been used to inhibit classical reward conditioning in *Lymnaea* (Kemenes et al., 2011) and is known to act as a dopamine antagonist in molluskan neurons (Ascher, 1972; Teyke et al., 1993). We found that the dopamine antagonist eliminated the sucrose-induced acceleration of the feeding CPG, i.e. there was no rate-difference between spontaneous and sucrose-induced fictive feeding in the presence of the antagonist ($p = 0.45$, $n = 7$ preparations, Wilcoxon rank sum test) (Figure 4.8). At the concentrations of the antagonist used in these experiments [10 μ M] population activity in the buccal ganglia remained otherwise relatively normal, although some feeding cycles that occurred in the presence of the antagonist had an atypical temporal structure including fewer bursting neurons (data not shown). Lower concentrations [1-5 μ M] of the antagonist failed to eliminate sucrose-induced acceleration of the feeding CPG. Higher concentrations [250-1000 μ M] abolished all fictive feeding and induced highly atypical activity, including persistent tonic firing in several neurons that had previously been silent or only firing sparsely (data not shown).

Taken together these results show that perfusion with dopamine on the MEA is an effective method for inducing fictive feeding at a high frequency. They also show that unimpaired dopamine signalling is required for sensory-induced acceleration of the feeding CPG. The experiments involving sequential perfusion using different stimuli also show that long experiments (>30 min) involving multiple stimuli can be performed on the MEA.



Figure 4.7. Excessive concentrations of dopamine induce expanding bursts

Simultaneous recordings from both buccal ganglia in one brain. Application of high concentrations of dopamine [0.5 mM] to the brain induces rhythmic activity. The first population bursts are characteristic of fictive feeding but the number of spikes per bursts increases rapidly with each cycle. Dopamine was applied throughout the shown recording.

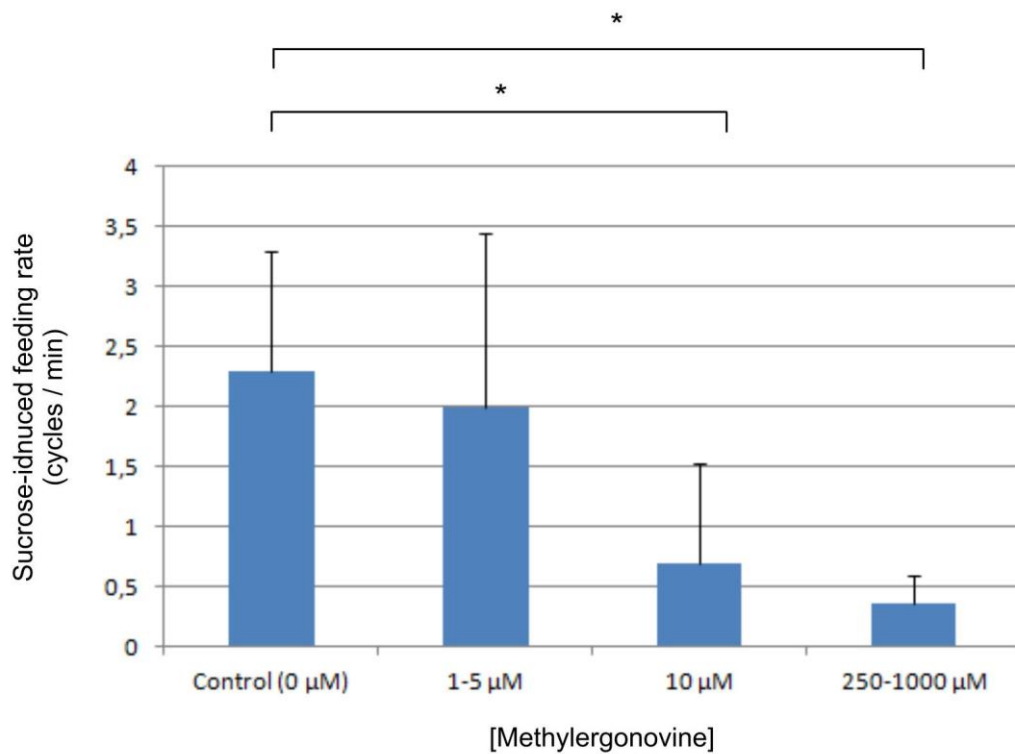


Figure 4.8. Dopamine antagonist prevents sucrose-induced CPG acceleration

Different concentrations of the dopamine antagonist methylergonovine (1-5 μM, n = 8; 10 μM, n = 7; 250-1000 μM, n = 7; control, n = 17) were applied to preparations prior to and during sensory sucrose stimulation. A significant reduction of the sucrose-induced feeding rate was seen at 10 μM of the antagonist and higher. Graph shows mean ± SD. *p<0.001 (Wilcoxon rank sum test).

4.4 Locating identified motorneurons in the buccal ganglia

The previous sections show that fictive feeding can be recorded on the MEA. Feeding cycles appear as characteristically patterned bursts of activity involving multiple neurons. A limitation with any extracellular recording technique is that neurons cannot be identified with the confidence conferred by an intracellular recording. However, the spike localization and sorting technique presented in the previous chapter makes it possible to assay the probable identity of individual neurons in preparations where feeding cycles featured clear protraction, rasp and swallow phases. Four types of motorneuron in particular could be identified in multiple preparations on the basis of their consistent location in the buccal ganglia and their firing pattern within fictive feeding cycles (Figure 4.9). The first neuron type, probably the protraction-phase B1 neuron, fired high-amplitude spikes at a modest rate during the first phase of feeding cycles. This neuron was consistently found at the edge of the buccal ganglia close to the dorsobuccal nerve, where the cell body of the B1 neuron is often visible (e.g. Figure 4.2, electrodes 3 & 14).

The second type of neuron, probably the rasp-phase B4CL and/or B10 types, fired high-amplitude spikes at a high rate during the second phase of feeding cycles. This type of neuron was found in the posterior part of the buccal ganglia where the B4CL neurons and B10 neurons are located (e.g. Figure 4.2, electrode 1). Firing in this neuron type also appeared spatially and temporally correlated with local field potentials (LFPs) observed in the raw voltage data. LFPs manifest as a negative-going followed by a positive-going fluctuation of a few hundred μV and last around one second (Figure 4.10). These large, slow voltage fluctuations indicate the simultaneous activation of multiple neurons; presumably the large, numerous and tightly packed B4CL neurons. Rasp-phase activity was also observed in the anterior part of the buccal ganglia where the rasp-phase B3 neuron is located.

The third type of neuron, probably the early swallow-phase B4 neuron, fired one or a few very high amplitude spikes with high temporal precision, marking the end of the LFP and the transition from the second to the third phase of feeding. This neuron was found in the medial to posterior region of the buccal ganglia, where the B4 cell is located (e.g. Figure 4.2, electrode 4 & 7).

The fourth type of neuron, probably the swallow-phase B8 or B4CL type, fired a

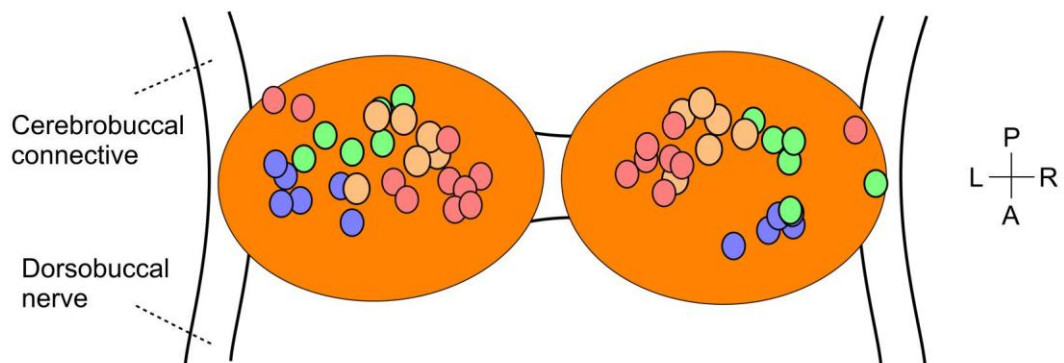


Figure 4.9. Putatively identified neurons

Schematic of the buccal ganglia with the estimated location of four neuron types recorded in 10 preparations. The neuron types had protraction (blue), rasp (green), rasp/swallow (beige), or swallow (red) phase firing characteristics (see text). The location of the different neuron types was relatively consistent across preparations, indicating putative neuronal identity. Note that the spike sorting technique often estimates neuronal location to be closer to the centre of ganglia than it actually is. This is due to the difference in conductance at the centre and at the edge of ganglia (see Figure 3.3).

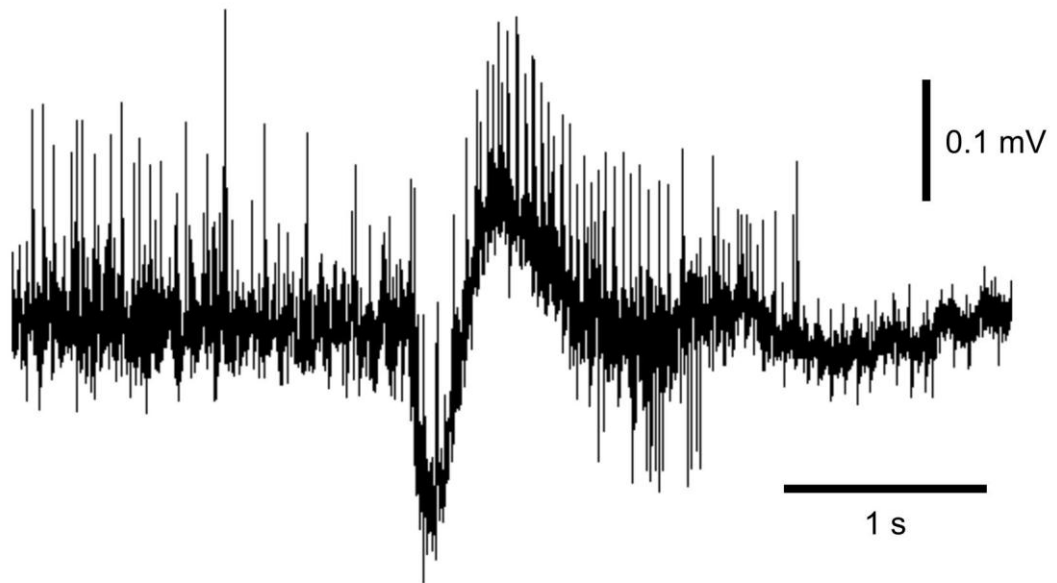


Figure 4.10. Local field potentials

Local field potential (LFP) recorded on a 30 μm diameter electrode. LFPs occurred during the rasp phase of fictive feeding. They consist of a negative-going followed by a positive going voltage fluctuation and last about 1 s. LFPs varied in amplitude but never exceeded ± 0.2 mV. They were consistently recorded in the posterior region of the buccal ganglia where the rasp-phase B4CL neurons are located and probably represent simultaneous bursting in these large, tightly packed neurons during the rasp phase of feeding.

characteristic burst of spikes with progressively increasing spike amplitude and interspike interval, beginning immediately after the brief firing of the B4 neuron and marking the end of the feeding cycle. This neuron was recorded in several locations although mainly in the posterior region of the ganglia, where the swallow-phase B8 neuron as well as the B4CL neurons, some of which fire during the swallow phase, are located (e.g. Figure 4.2, electrode 9).

Figure 4.9 shows that neurons active in different phases of the feeding cycle were consistently found in particular regions of the buccal ganglia. This analysis shows that it is possible to associate characteristic firing patterns with neurons in specific locations on the ganglia; that such associations can be constant across preparations and that these consistent properties suggest probable neuronal identities.

4.5 Cerebral and pedal activity associated with feeding

In addition to the neurons of the buccal ganglia, such as those identified in the previous section, fictive feeding also involves phasically active neurons in the cerebral ganglia (Benjamin, 2012). Moreover, the feeding motor output of the buccal ganglia must be coordinated with behaviours controlled by circuits located elsewhere in the brain, such as the locomotor CPG output of the pedal ganglia, which receive inhibitory input from the feeding CPG and is inhibited during the generation of feeding cycles (Kyriakides and McCrohan, 1988). A main advantage of the MEA over traditional single-unit methods is that it allows us to sample a wide range of neurons in any region of the CNS during the activation of the feeding CPG. This may ultimately allow us to identify new neurons and neuronal populations whose activity is associated with feeding. As a first step we should expect to see the known patterns of cerebral and pedal feeding-associated activity in the MEA-recorded data. Figure 4.10 shows a split-brain preparation recorded on the MEA. Application of sucrose to the esophagus affected activity not only in the buccal ganglia but also in the cerebral and pedal ganglia. In the cerebral ganglia bursts were recorded that were phase locked with buccal feeding cycles. These bursts originated in the anterior region of the cerebral ganglia, which is known to contain phasically active neurons associated with feeding (Benjamin, 2012). In the pedal ganglia on the other hand there was a transient cessation of tonic activity during each buccal feeding cycle. This experiment was a proof-of-principle and was

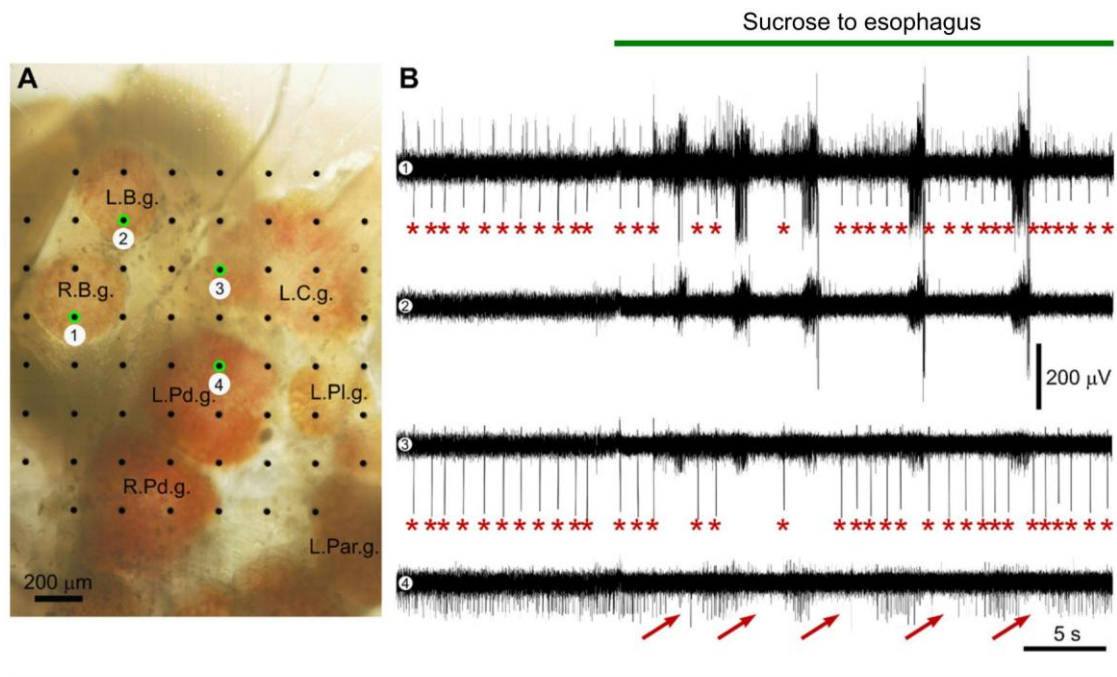


Figure 4.11. Cerebral and pedal activity associated with fictive feeding

MEA recording of synchronized activity in the buccal, cerebral and pedal ganglia during sucrose-induced feeding motor output. **A:** A photomicrograph showing a *Lymnaea* CNS on an MEA. The cerebral commissure has been cut to allow access to the dorsal surfaces of the left and right pedal ganglia (L.Pd.g and R.Pd.g.). Also shown are the dorsal surfaces of the left and right buccal ganglia (L.B.g. and R.B.g.), the ventral surface of the left cerebral ganglion and the dorsal surface of the left pleural and parietal ganglia (L.C.g., L.Pl.g. and L.Par.g.). Extracellular electrodes from which the traces shown in B were recorded are circled in green. **B:** Perfusion of sucrose through the esophagus triggered rhythmic feeding bursts in the buccal ganglia (electrodes 1 and 2). These bursts were accompanied by bursts in the cerebral ganglion (electrode 3). Tonic activity was phasically inhibited in the pedal ganglia (arrows) during each feeding burst. Asterisks indicate the spiking of the soma or axon of the left cerebral giant cell interneuron, which also was inhibited phasically during the first few feeding bursts. Adapted from Harris et al., 2010.

only repeated a few times, with similar results (data not shown).

Application of an aversive chemosensory stimulus known to induce defensive withdrawal [0.1% amyl acetate] to the lip resulted in a very different pattern of activity throughout the brain (Figure 4.11). This pattern was more widespread and involved constant rather than rhythmic activity changes. This experiment was repeated several times with similar results (data not shown).

These initial experiments involving whole-brain preparations demonstrate that the MEA can record activity associated with feeding behaviour throughout the brain as well as activity associated with aversive chemosensory stimuli. This will hopefully allow us to identify new neurons and patterns of interaction between different CPGs.

4.6 Classical reward conditioning on the MEA

Given the successful use of stimuli known to activate the feeding CPG we attempted a more complex experiment aimed at inducing classical reward conditioning on the MEA. By pairing amyl acetate (a neutral chemosensory stimulus at low concentrations) with a sucrose reward it is possible to induce long-term conditioning in *Lymnaea* such that a subsequent encounter with amyl acetate elicits a significant feeding response (Figure 4.12). Such conditioning has been observed both *in vivo* and *in vitro* (Alexander et al., 1984; Marra et al., 2010). Here we used *lip-brain-esophagus* preparations in which the buccal ganglia were monitored on the MEA. The CS [0.54 μ M amyl acetate] was applied to the lip two minutes prior to and during the application of sucrose to the esophagus and lip. After a 10 min washout the CS was again applied to the lip. The CS-induced rate of fictive feeding was significantly higher on the second presentation; 0.8 ± 0.2 cycles per min, compared with 0.2 ± 0.3 cycles per min on the first presentation ($p < 0.001$, $n = 11$ preparations, paired t-test, $df = 10$, $t = 5.6$). Preparations that did not respond to an application of sucrose to the lip 10 min after the CS-application were considered non-responsive and were discarded. This experiment shows that long-term memory can be manipulated on the MEA, and that extended experiments (>30 min) involving different chemosensory stimuli are possible.

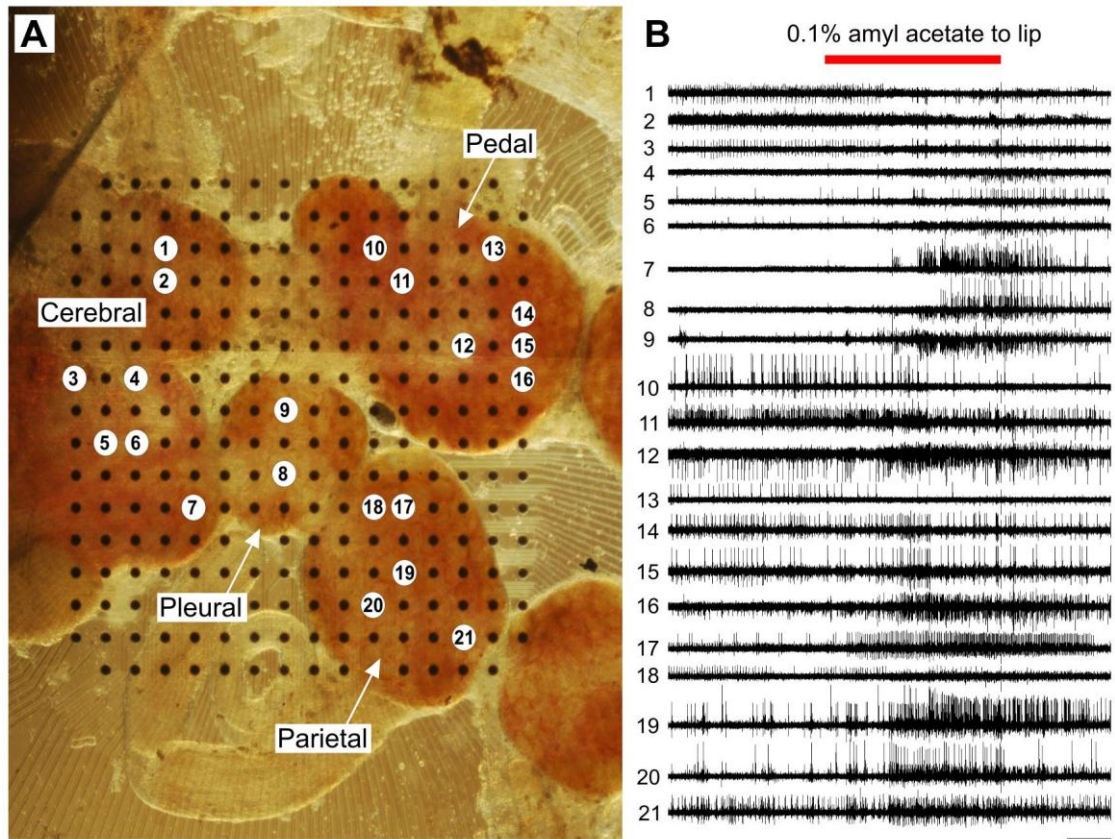


Figure 4.12. Withdrawal-associated activity recorded throughout the brain

A: *Lymnaea* brain (dorsal view, left side) on an MEA with 30 μm diameter electrodes spaced 200 μm apart. Text labels indicate the names of different ganglia. Numbers indicate the electrodes on which the traces in B were recorded. **B:** Extracellular recordings shows diverse patterns of tonic spiking activity. Stimulating the lips with 0.1% amyl acetate, a chemosensory stimulus known to induce withdrawal, resulted in significant changes in recorded activity throughout the brain. Black bar represents 30 s.

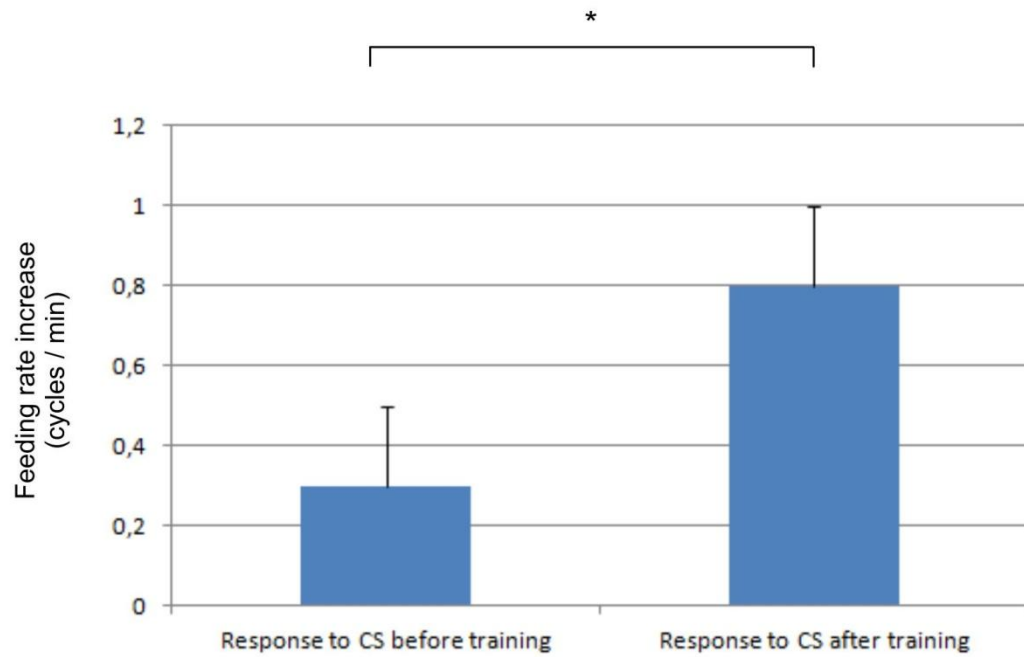


Figure 4.13. *In vitro* classical reward conditioning on the MEA

Application of amyl acetate (CS) prior to and during sensory sucrose stimulation induces classical conditioning. Application of amyl acetate thus increased the rate of feeding by 0.2 ± 0.3 bursts/min before training and by 0.8 ± 0.2 bursts/min 10 min after training ($n = 11$ preparations, paired t-test, $df = 10$, $t = 5.6$, $p < 0.001$).

Chapter 5

Results: A reward-sensitive network refractory period

The previous chapter showed that the feeding CPG generates fictive feeding spontaneously on the MEA, and that the rate of fictive feeding can be accelerated by a variety of sensory, pharmacological and electrical stimulation techniques. Importantly, it showed that dopamine appears to mediate the acceleration of fictive feeding that is associated with food reward, and that direct application of dopamine to the brain is sufficient to drive an accelerated rate of fictive feeding on the MEA. The aim of developing these techniques was to analyse dopamine-mediated adaptation of CPG activity at the level of neuronal populations. This chapter shows that the techniques made possible the identification of two distinct populations of neurons associated with the CPG. Analysis of the interaction between these two populations in the context of dopamine-mediated food reward suggests a new and potentially general modulatory circuit mechanism which here adapts the rate of feeding to the availability of food.

5.1 Feeding cycles are followed by a period of quiescence

The ability of the MEA to monitor a somewhat random sample of many neurons in the buccal ganglia allows us to analyse a range of different patterns of activity. The previous chapter characterized a population of neurons whose bursting activity is reflective of the cycles of the feeding CPG. However, these neurons typically represent less than half of all buccal neurons recorded on the MEA. Figure 5.1 shows a second population of neurons (indicated by a blue bar) that was primarily active between feeding cycles. This is in stark contrast to neurons of the first population (indicated by a

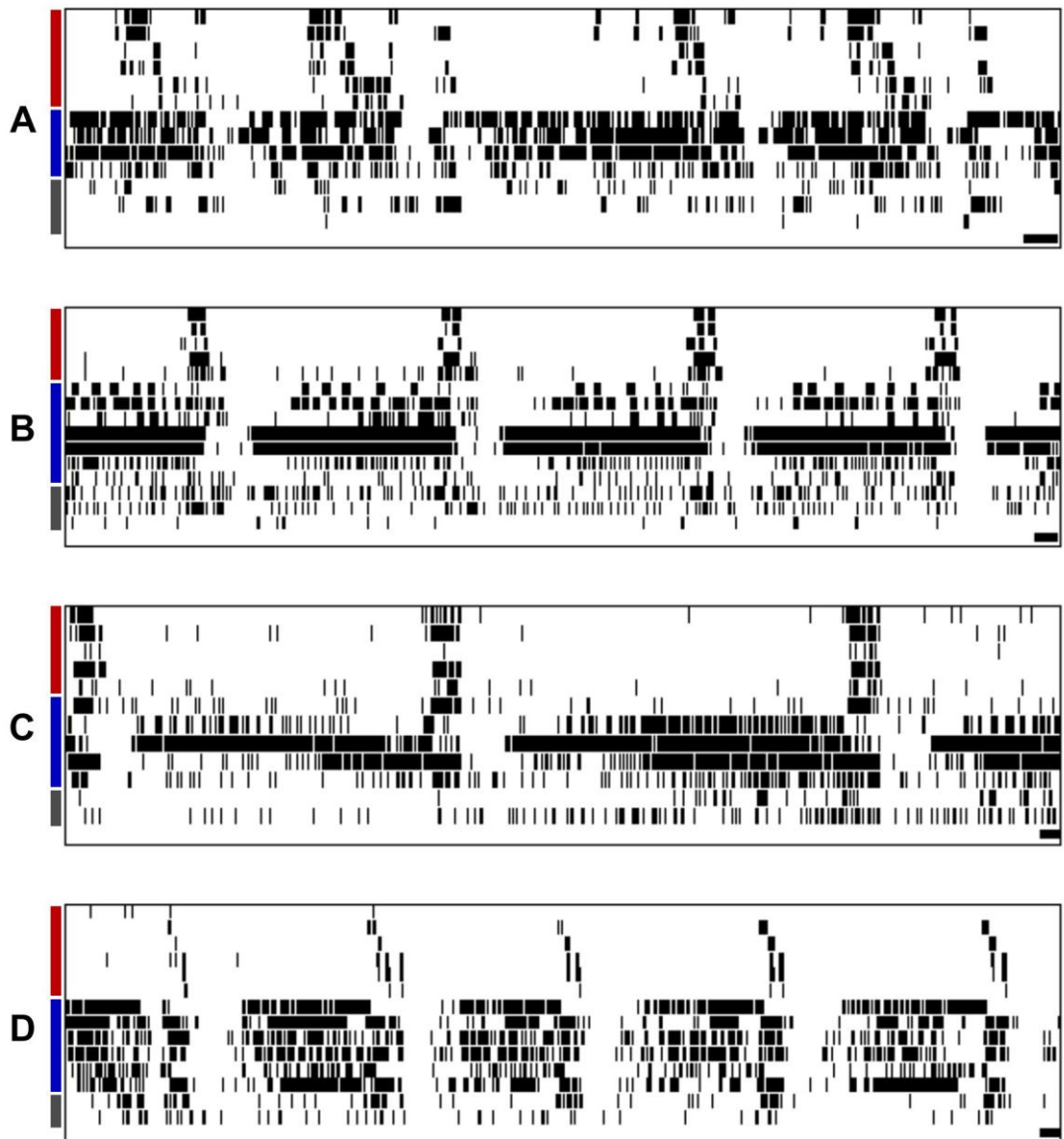


Figure 5.1. Feeding cycles are followed by a period of quiescence

Four raster plots show the spiking activity of all neurons recorded in the buccal ganglia in four separate preparations (A-D). Physically bursting neurons whose activity reflects the motor output of the feeding CPG are indicated by red bars. A second population of tonically active neurons are indicated by blue bars. Grey bars indicate neurons that could not be unambiguously assigned to either population. Note how the tonically active population becomes transiently quiescent following each feeding cycle. Black bars indicate 10 s.

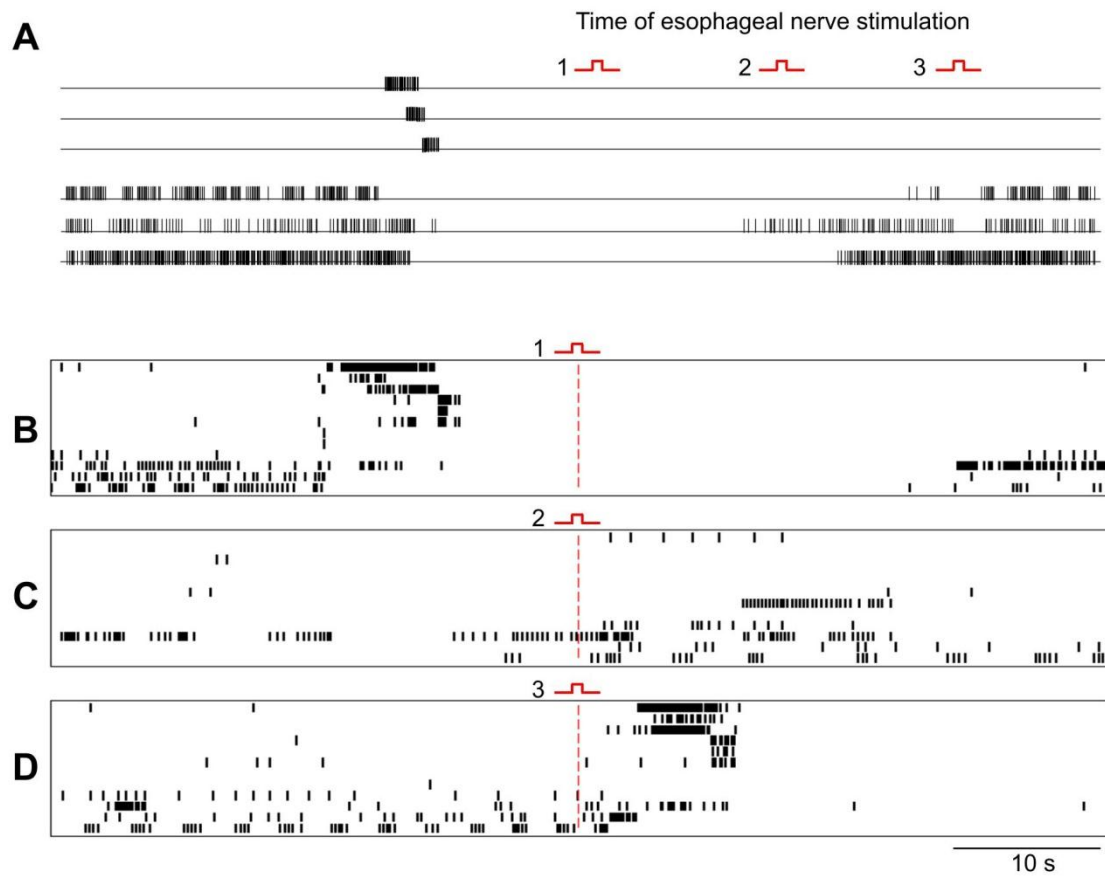
red bar) which fired almost exclusively during their particular phase of the feeding cycle. We can therefore refer to the first population as *phasic* and the second population as *tonic*. Neurons of the tonic population had diverse firing patterns ranging from continuous activity to intermittent bursting. All however showed a full or partial suppression of firing during or immediately following the feeding cycles of the phasic population and remained quiescent for a variable period of time (see Section 5.3). Firing tended to resume in a fixed sequence, with some tonic neurons recovering relatively quickly and others consistently lagging behind. Tonic neurons with a high and constant baseline firing rate tended to resume firing sooner than those with an intermittent pattern of firing.

To analyse the relationship between the two populations in more detail we identified neurons whose pattern of activity placed them definitively in the phasic or tonic population. About 31% of all neurons recorded in each preparation were clearly members of the phasic population ($n = 145$ neurons in 31 preparations). These neurons were mostly silent in-between feeding cycles: in total they had an above zero firing rate during only 5 ± 5 % of the seconds they were recorded (all results represent mean \pm standard deviation unless otherwise indicated; zero vs. above zero firing rate was calculated by counting the number of spikes in successive 1-s bins, a spike density function was used for all other calculations of firing rate). Conversely, about 26 % of all neurons recorded in each preparation were considered part of the tonic population. These neurons fired in the near-continuous mode at a mean rate of 1.1 ± 0.7 Hz ($n = 123$ neurons in 31 preparations). They had an above zero firing rate during 43 ± 20 % of the seconds they were recorded. The remaining 41 % of recorded neurons often expressed firing patterns similar to those in the tonically or phasically active populations, but also out-of phase burst firing or long periods of quiescence that made them unsuitable for quantitative analysis of the two populations. Analysis of the quiescent period showed that the total firing rate of neurons in the tonic population dropped from 6.5 ± 3.5 Hz in the 10 s period prior to the onset of feeding to a much reduced rate of 0.3 ± 0.7 Hz at the time of minimal activity during the subsequent quiescent period associated with the cycle ($n = 74$ spontaneously generated feeding cycles). Further feeding cycles did not occur during the quiescent period.

Interestingly, a similar pattern of neuronal activity has previously been observed in populations of neurons associated with the locomotor CPG of the rat, which were also monitored on MEAs (see Figure 1.2) (Darbon et al., 2002; Darbon et al., 2003; Streit et al., 2006). In this locomotor CPG, intrinsically spiking neurons recruit other neurons through recurrent excitation. This eventually leads to population-wide bursts that drive contraction of the leg muscles during locomotion. The authors found that upregulation of the Na/K-pump during population bursts facilitates burst-termination by hyperpolarizing neurons, resulting in a transient cessation of intrinsic spiking activity following each burst (Figure 1.2). During this quiescent period the pattern-generating network was refractory to further bursting, even when an electrical stimulus was applied. The authors therefore termed the quiescent period a ‘network refractory period’ (NRP) (Darbon et al., 2003; Streit et al., 2006). That a similar pattern of activity and quiescence is present also in the *Lymnaea* feeding CPG has not previously been recognized. Tonic firing between feeding cycles *can* be observed in intracellular recordings from the buccal motorneuron types B2, B5 and B7, e.g. (Benjamin and Rose, 1979), but the coordinated cessation of the firing of many neurons associated with each feeding cycle could not have been observed using single-unit recording techniques.

5.2 The quiescent period is a network refractory period (NRP)

The previous section showed that two populations of buccal neurons are recorded on the MEA, and that the tonically active population becomes quiescent for a variable period following each feeding cycle. This period of quiescence is reminiscent of an NRP, previously shown to regulate the frequency of phasic population bursts in a locomotor CPG (Darbon et al., 2002; Darbon et al., 2003; Streit et al., 2006). To determine whether the quiescent period recorded in the buccal ganglia reflects an NRP we stimulated one of the pair of dorsobuccal nerves during or following the quiescent period, in order to test for refractoriness of the CPG (Figure 5.2). Stimulation of this nerve had not previously been carried out in *Lymnaea*, but stimulation of an ostensibly homologous nerve in *Aplysia* is known to induce individual cycles of fictive feeding (Horn et al., 2004). If the quiescent period reflected an NRP we expected the stimulus



E

		Effect	
		Feeding cycle	No feeding cycle
Time of stimulation	During the quiescent period	19	7
	Following the quiescent period	1	15

Figure 5.2. Stimulation of a nerve that mediates food stimuli fails to activate the feeding CPG during the quiescent period

A: Schematic showing the spiking activity of neurons before during and after the generation of a feeding cycle. Electrical stimulation of the esophageal nerve was applied randomly at one of three time points (1-3) during spontaneously generated activity recorded in 5 preparations. The preparations were allowed to recover for 1-2 minutes between each stimulus. The effects of stimulation at the different time points are shown in a representative recording from one preparation (**B-D**). **B:** Electrical stimulation during the quiescent period associated with a feeding cycle had no effect on population activity. **C:** When tonic activity had only partially resumed following a feeding cycle, electrical stimulation elicits some additional tonic activity but fails to activate the CPG. **D:** When all tonically active neurons have resumed spiking electrical stimulation triggers a full feeding cycle. Adapted from Harris et al., 2012. **E:** Summary table showing the difference in effect of electrical stimulation applied during and after the quiescent period ($p < 0.001$, $n = 42$ nerve stimulations in a total of 5 preparations, $\chi^2 [1,42] = 20.2$).

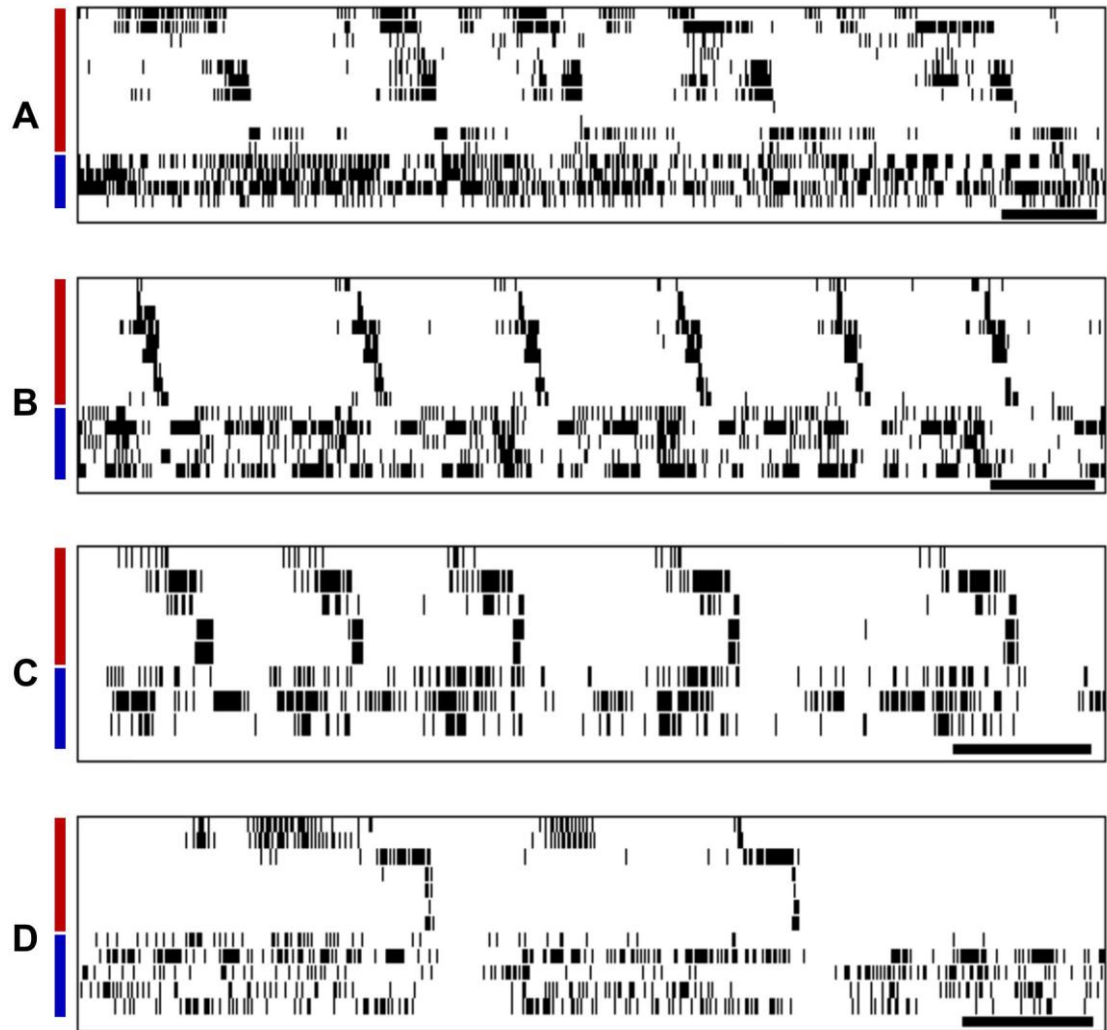
to be ineffective during but not following the quiescent period, as previously observed in the rat locomotor CPG (Darbon et al., 2002; Streit et al., 2006).

Electrical stimulation triggered a feeding cycle 19 times out of 26 if the stimulus was delivered after the quiescent period had ended but only one time out of 16 if the stimulus was delivered during the quiescent period ($p < 0.001$, $n = 42$ nerve stimulations in a total of 5 preparations, $\chi^2 [1,42] = 20.2$). Stimulation delivered late in the quiescent period tended to induce some additional tonic activity (Figure 5.2C) but failed to trigger full feeding cycles. Thus the cessation of tonic activity following feeding cycles reflects a period of refractoriness, during which the feeding CPG is not responsive to input from the esophageal food chemosensory pathway. This period will be referred to from now on as the NRP.

5.3 Sensory sucrose and dopamine shorten the NRP

The previous sections show that feeding cycles are followed by a previously unidentified NRP. To analyse whether the NRP might also be sensitive to changes in dopamine and food stimuli we selected pairs of consecutively generated feeding cycles ($n = 138$) for further analysis. Of these, 76 pairs were spontaneously generated in 18 preparations, 26 pairs were generated in 7 preparations following application of the sucrose stimulus and 36 pairs were generated in 7 preparations following application of dopamine. The criterion of selection was that both the feeding motor output of the phasic population and the inter-cycle activity of the tonic population could be readily identified in the recorded activity patterns (e.g. Figures 5.1, 5.2).

Formally the NRP can be defined as the interval from the beginning of a feeding cycle to the time when activity in the tonically active population returns to its average firing rate following the period of quiescence. Using this definition, spontaneously generated feeding cycles were calculated to have an NRP of 37.2 ± 13.9 s ($n = 76$ feeding cycles). Sucrose and dopamine dramatically attenuated the NRP (Figure 5.3). Some neurons in the tonically active population continued to fire continuously during stimulus-induced fictive feeding (e.g. 5.3A); other tonically active neurons became briefly quiescent after each cycle but resumed firing much sooner than during



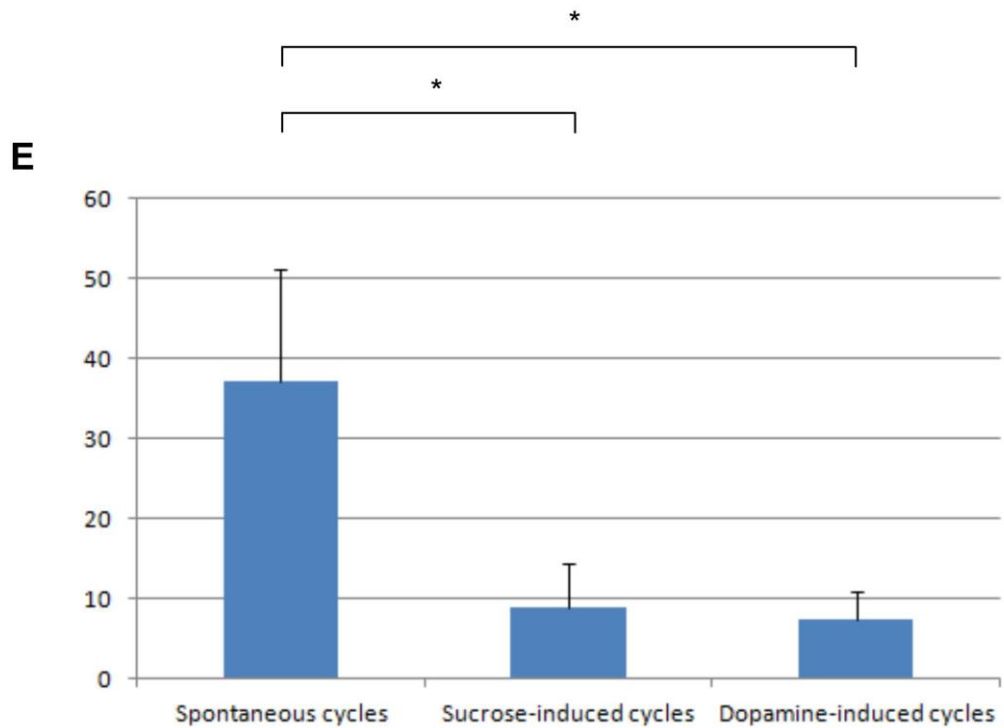


Figure 5.3. Sucrose and dopamine stimuli shorten the NRP

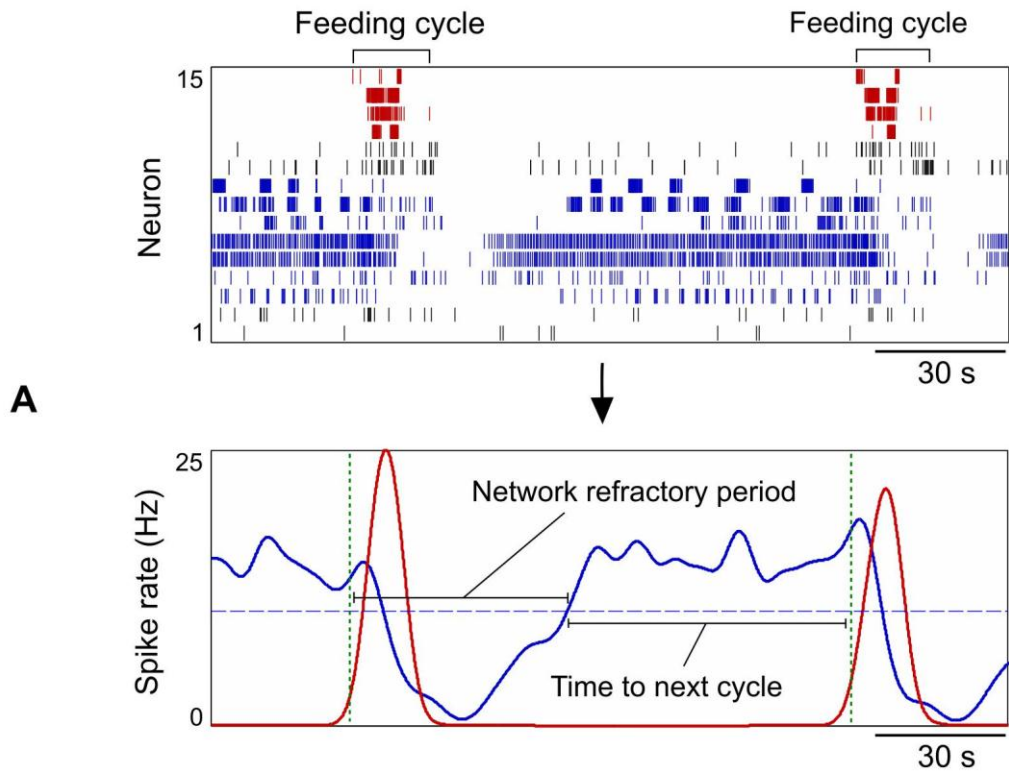
A-D: Accelerated fictive feeding induced by sucrose (**A**) and dopamine (**B-D**) in four separate preparations. Phasic and tonic populations are indicated by red and blue bars respectively. Preparations were perfused with sucrose (**A**) or dopamine (**B-D**) throughout the recordings shown. Note that the cessation of tonic activity following stimulus-induced feeding cycles is much briefer than following spontaneously generated feeding cycles (Figure 5.1). Black bars indicate 10 s. **E:** The duration of the quiescent period was much shorter following sucrose- ($n = 26$) or dopamine-induced ($n = 36$) feeding cycles than following spontaneously generated cycles ($n = 76$). $*p < 0.001$ (Wilcoxon rank sum test).

spontaneously generated fictive feeding (e.g. 5.3B-D). The mean NRP recorded in the presence of the sucrose stimulus lasted 8.8 ± 5.6 s ($n = 26$ feeding cycles). The mean NRP recorded in the presence of dopamine lasted 7.3 ± 3.6 s ($n = 36$ feeding cycles). Many tonic neurons appeared to fire at a higher baseline firing rate in the presence of the sucrose stimulus, though this was difficult to quantify given that several tonic neurons express a transient burst of activity during the initial phase of feeding, which increases their overall firing rate proportionally to the rate of feeding (data not shown). However, in the few preparations that did not generate feeding cycles in response to sucrose, the stimulus did induce a constant increase in the firing rate of the tonic population (data not shown).

These findings show that the NRP is dramatically shortened by both the sensory sucrose stimulus and the dopamine stimulus. It is not yet clear whether these reward-associated stimuli act directly on neurons in the tonically active population to reduce the NRP or on a third, afferent population or mechanism common to both the tonic and phasic populations. This important issue is discussed further in the next chapter.

5.4 The NRP predicts future activation of the feeding CPG

The NRP in the activity of the feeding circuitry suggests that a process of recurrent excitation may contribute to the generation of feeding cycles (Streit et al., 2006) (see Section 1.1). This in turn suggests that the variable inter-cycle interval (ICI) observed during spontaneously generated fictive feeding may be correlated with the speed with which intrinsically spiking neurons resume firing following feeding cycles. To test this we correlated the duration of the NRP with the time from the end of the NRP to the next feeding cycle. Here we found a small but significant correlation ($r^2 = 0.15$, $p < 0.001$, $n = 76$ pairs of spontaneously generated feeding cycles, all correlations represent Pearson's linear correlation coefficient). The correlation was stronger when only pairs of feeding cycles with an inter-cycle interval of 2 min or less were considered ($r^2 = 0.32$, $p < 0.001$, $n = 37$). This correlation is shown in Figure 5.4. The NRPs and inter-cycle intervals of feeding cycles induced by sucrose and dopamine were brief and invariant, and the correlation was not significant when cycles from either of these two conditions were considered ($p = 0.1$ and $p = 0.29$, respectively). The distributions of ICIs



B

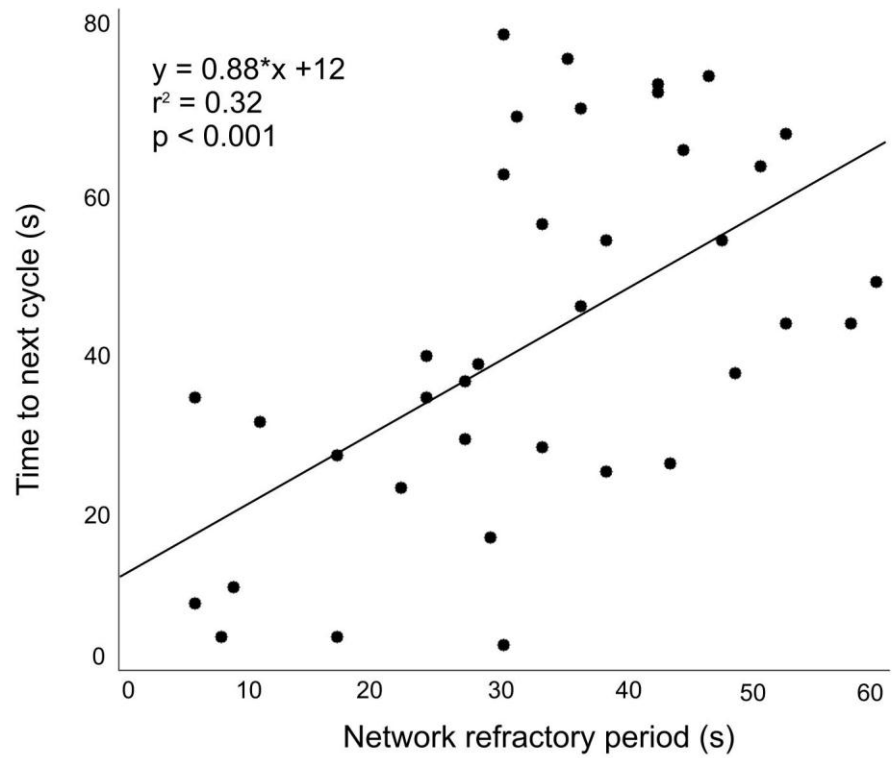




Figure 5.4. The duration of the NRP predicts the interval to next feeding cycle

A: The continuous activity of the tonically active population (blue spikes) is transiently suppressed following a feeding cycle (red spikes). The network refractory period (NRP) is defined as the duration from the beginning of a feeding cycle, through the subsequent reduction of spiking in the tonic population, to the time when the tonic population returns to its average firing rate (indicated here with a dashed blue line). **B:** Plotting the duration of the NRP against the remaining inter-cycle interval shows that the timing of the next feeding cycle is significantly correlated with the duration of the NRP preceding it ($r^2 = 0.32$, $p < 0.001$, $n = 37$ pairs of feeding cycles, Pearson's linear correlation coefficient). The solid line represents best-fit linear regression. Adapted from Harris et al., 2012.

in the three different conditions are shown in Figure 5.5.

The correlation between the duration of the NRP and the remaining inter-cycle interval imply that spontaneously generated cycles of the feeding CPG can be loosely predicted more than a minute into the future. This unusual observation underscores the possible importance of the NRP in determining the cycling frequency of the feeding CPG, and is discussed further in the next chapter.

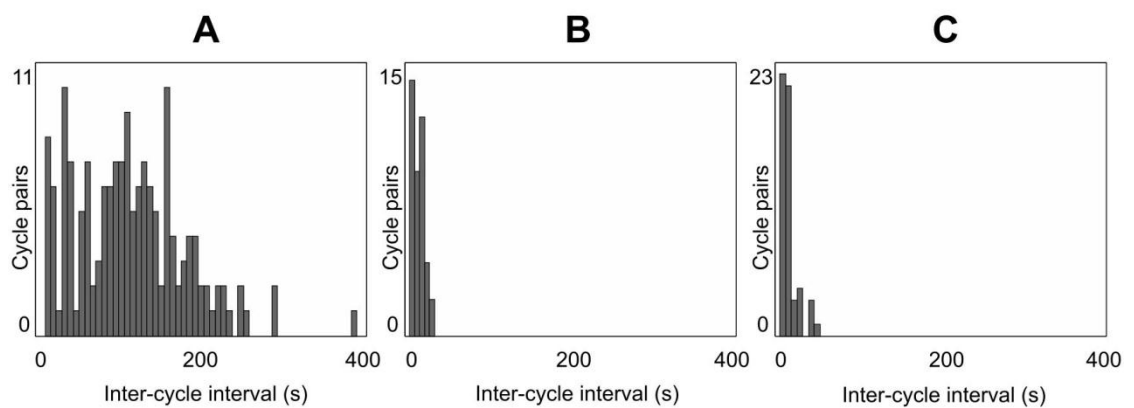


Figure 5.5. Inter-cycle interval (ICI) distributions

A: ICI distribution for 159 spontaneously generated pairs of feeding cycles recorded in 37 preparations. **B:** ICIs of 41 food-induced feeding cycle pairs recorded in 8 preparations. **C:** ICIs of 54 dopamine-induced feeding cycle pairs recorded in 8 preparations. Adapted from Harris et al., 2012.

Chapter 6

Discussion

I began this thesis by arguing that to understand the neural basis of intelligent behaviour we need to uncover general mechanisms that govern the generation of adaptive patterns of activity in neural circuits. I showed that mechanisms of pattern generation have been characterized at the level of neurons and networks in a range of invertebrate and vertebrate systems, and noted that similar mechanisms appear also to govern the operation of more complex circuits in the mammalian brain (Section 1.1). I argued that circuits that control goal-oriented behaviours, such as foraging and mating, deserve special attention because of their ability to adapt output, on short and long time scales, in ways that optimise performance and fitness in changing and unpredictable environments; arguably a fundamental feature of intelligent behaviour. I emphasised that such adaptation typically depends on dopamine signalling (Section 1.2). I then introduced the molluskan feeding CPG as a canonical example of a goal-oriented pattern generating circuit that is adaptively modulated by dopamine-mediated sensory reward (Section 1.3). Specifically, dopamine has been shown to facilitate classical conditioning, operant conditioning and cycle rate control in the molluskan feeding system (Brembs et al., 2002; Kemenes et al., 2011; Kyriakides and McCrohan, 1989). Since the subject of this thesis is the mollusk *Lymnaea*, for which techniques for operant conditioning of feeding behaviour have not yet been developed, I did not find opportunity to discuss the very important observation that spontaneous variability in the output of the feeding CPG of at least one mollusk (*Aplysia*), in combination with dopamine-mediated reward, appears to give rise to learning by trial-and-error and a proto form of free will (Brembs, 2011; Horn et al.,

2004; Nargeot et al., 1997). I also did not discuss the argument that the molluscan feeding CPG displays “higher” cognitive functions, including intentionality and expectations (Proekt et al., 2004). These observations support the argument that similar mechanisms underlie the generation of intelligent behaviour in both simple and complex brains (Grillner, 2006; Yuste et al., 2005).

My definition of the term reward does not require that rewards be the outcome of decision making. This seems appropriate, for the reasons given in Section 1.2, but nevertheless constitutes a partial deviation from the way the term reward is used in everyday language. For example, an unexpected tax-return is a reward according to my definition. One might therefore argue that the term 'positive stimulus' should be used instead. However, this term has the serious disadvantage of not being a verbal noun. That is, whereas there is general understanding of the noun 'reward' and the associated verb 'rewarding', there is no established meaning of the compound verb 'positively stimulating' associated with the compound noun 'positive stimulus'. If anything, 'positive' has optimistic or ethical connotations that would jar with the amoral and downright destructive topics often discussed in relation to reward, such as addiction and overeating. The term 'appetitive stimulus' (and 'appetitively stimulating') avoids this problem but implies a focus on satisfying bodily needs, particularly hunger, whereas the key property of reward is that it applies to any desired state or goal. Until a better term is developed (perhaps one that denotes activation of key populations of dopaminergic neurons) I suggest we stick with reward, using the definition in Section 1.2, accepting it as a slight neologism. The lack of requirement that rewards necessarily be the consequence of decision making should be appropriately tempered by the understanding that most rewards in fact *do* occur as consequences of decision making – specifically, as the result of exploration, trial-and-error, or more complex goal-oriented behaviours.

In the first chapter I showed that the pattern generating mechanisms of the *Lymnaea* feeding CPG are well-characterized, but I also argued that the way the animal adapts its rate of feeding to the availability of nutritious food remains poorly understood. This is debatable; intracellular recordings *have* revealed several neurons that modulate the rate of feeding, both within (e.g. the SO cell) and external to (e.g.

the CBI cells) the buccal ganglia. These neurons are activated by food reward and their depolarization drives fictive feeding at a high rate (Benjamin, 2012). However, since neuronal homologues are rare, even within closely related species such as mollusks, the characterization of individual identified modulatory neurons associated with a CPG does not necessarily yield general mechanisms of adaptation that apply broadly across a range of CPGs (Selverston, 2010; Yuste, 2008). Such mechanisms may be better sought at the network or population level (Yuste, 2008).

To facilitate the simultaneous recording of multiple neurons in semi-intact preparations of *Lymnaea* I developed a new technique involving planar MEA technology (introduced in Section 1.4). Whether this approach is ultimately preferable to optical recording techniques is not clear. Both methods have limited signal-to-noise profiles. The MEA has vastly superior *temporal* resolution but I have yet to find a good use for a sampling rate of 40 kHz, the current maximum the USB-MEA256-System. Such use may include spike time onset-based spike sorting or analysis of spike time dependent plasticity. In contrast, optical recording techniques have vastly superior *spatial* resolution. The limited spatial resolution of the MEA meant that about half of all triangulated spikes could not be separated into spatial clusters, imposing a fundamental limit on the number of neurons that can be confidently distinguished and recorded (see Section 6.2). Optical recording methods also enable imaging along the z-plane. This ability would allow the core interneurons of the feeding CPG and several other important neurons to be monitored simultaneously with the many neurons located on the surface of the *Lymnaea* brain. However, although optical recording of firing patterns in the buccal ganglia of *Lymnaea* has been demonstrated (Kojima et al., 2001) I have yet to see convincing spike sorting performed on the resulting data. Attempts at optical recording in our laboratory have so far been unsuccessful due to very limited signal-to-noise. It is possible that the strong pigmentation of the *Lymnaea* CNS makes it inappropriate for optical recording.

It should also be noted that the MEA technique has other advantages over optical recording techniques. It is fast; 20-30 min from dissection to recording. It does not necessitate the use of voltage sensitive dyes, at least one of which (RH155) both hyperpolarized the interneurons of the buccal feeding CPG and attenuated their

sucrose-induced rhythmic response (Kojima et al., 2001). The MEA technique is moreover straightforward and could easily be taught to undergraduates or technicians. This latter point suggests that the MEA technique could be used as an additional high-throughput assay in drug development. The pharmaceutical industry is currently the principal user of planar MEAs and might benefit from the ability to monitor the effects of different drugs on the complex operations of intact brains and semi-intact preparations prior to more expensive animal trials.

6.1 The MEA recording method

There are numerous minor improvements to the MEA recording technique that may improve the quality of data. The effect of keeping animals in unheated water for days prior to dissection should be investigated and perhaps avoided. De-sheathing and microscopy techniques need to be re-examined to account for the extreme variability in the number of cells that are visible in photographs of the ganglia on the array (compare Figures 2.2B and 2.2G). The possibility of introducing a delay between dissection and recording, and between the stabilization of preparations in the dish and recording, should be explored, since both treatments may significantly affect neural activity and responsiveness to stimuli. A delay might ameliorate such effects. Further attempts to use high density arrays (10 μm electrode diameter, 60 μm spacing, e.g. Figure 2.2B) to record from the buccal ganglia need to be made. These arrays did not appear to record more neurons than the MEA with 30 μm diameter electrodes spaced 100 μm apart (Figure 2.2E) which was used to collect most of the data discussed in this thesis, but only a couple of attempts with the high density arrays were ever made.

The effects on neural activity of the materials and methods used to stabilize the semi-intact preparations in the MEA dish need to be explored. Intracellular recordings of key neurons associated with the feeding CPG should be conducted in the presence of blu-tack and compared with controls, to test for possible effects of the adhesive on neural tissue. The effects of the significant pressure applied to ganglia prior to and during recording also need to be investigated. Here the design of an appropriate experiment is challenging, since the glass coverslip used to apply pressure on the ganglia prevents intracellular recording of neurons monitored on the array. One

solution would be to use laser to drill small holes (approx. 50 μm diameter) in the glass coverslip to permit simultaneous intracellular and MEA recording from the same ganglion. My initial enquiries with a UK-based laser micromachining company indicate that 10 such coverslips can be produced at a cost of about £650. The simultaneous access by intracellular and MEA electrodes that such perforated coverslips would enable could of course also be used to manipulate the membrane potential of key neurons in the feeding CPG while monitoring the effect on multiple neurons recorded on the MEA – potentially a very fruitful line of research.

Although the MEA system allows stimulation through the MEA electrodes, this feature was not systematically used. In the few attempts I did make I was sometimes able to induce transient bursting in a small number of neurons by stimulating ganglia or associated nerves, but the effect was not consistent. Presumably the inner connective tissue separating neurons from electrodes significantly impairs electrical contact. This is unfortunate given that the ability to stimulate as well as record is one of the advantages of MEA technology. If attempts to stimulate through the MEA are completely abandoned then the use of CMOS arrays should be considered for future experiments. CMOS arrays contain several thousand sensors (e.g. 128 x 128) and have sampling frequencies in the kHz range. They cannot deliver current but record extracellular neural activity perfectly well and are now commercially available, for example from Aptina Imaging, US.

6.2 Spike sorting

The semi-manual spike sorting technique presented in Chapter 3 was developed following extensive attempts at unsupervised spike sorting (Passaro et al., 2008). Although unsupervised approaches based on waveform analysis have been successfully applied to MEA data from the mammalian brain (Quiroga et al., 2004) they were less effective on MEA data from *Lymnaea*. It has previously been pointed out that unsupervised sorting techniques struggle with phasically active neurons, which often change waveform dramatically during the course of a burst (e.g. Figure 3.1C) (Pouzat et al., 2004; Stratton et al., 2012). Unlike most algorithms, human observers can draw on contextual information that distinguish different neurons, such as the expected firing

pattern of a putative cell, and make individual decisions with varying degrees of confidence in each case. Incidentally, phasic neural activity also complicate functional connectivity analyses using Granger causality (Kispersky et al., 2011).

The semi-manual method presented here has several shortcomings. First, it is by no means except from the challenge posed by bursting neurons. Specifically, some neurons did not consistently fire at sufficient amplitude to be distinguished from the surrounding low-amplitude spikes (see Section 3.3). The amplitudes of spikes within such clusters produced characteristic histograms containing two overlapping Gaussians: one reflecting the bursting neuron and one the surrounding low-amplitude spikes. When this happened I chose to error largely on the side of caution by only including spikes with amplitude higher than the amplitude demarcating the two Gaussians. Quality control (Section 3.4) applied to spikes sorted in this way almost invariably showed that low-amplitude spikes produced during the latter portion of bursts were systematically excluded (example in Figure 6.1). About a quarter of all sorted neurons produced this problem, although the varying degree of overlap between Gaussians makes the frequency difficult to quantify. An alternative approach would have been simply to increase the threshold for spike detection, but this would have excluded low-amplitude clusters that were *not* surrounded by numerous low-amplitude spikes. A step-wise approach in which spikes at different amplitudes or with different degrees of clustering are captured sequentially may be helpful here, perhaps in combination with automated clustering techniques.

Although the exclusion of spikes during bursts is a problem, it is less important for tasks such as the identification of feeding cycles, where observing part of a burst is often sufficient to classify an event as multi-phasic. It may however have contributed to our inability to find systematic differences in the spatiotemporal structure of feeding cycles induced spontaneously and by different stimuli (e.g. Figure 4.3). For example, the protraction-phase activity shown in Figure 6.1 was partially excluded in *most* sucrose-induced feeding cycles recorded in that preparation but was not excluded during spontaneous feeding, when the firing rate of the neuron was lower and its spike amplitudes relatively constant. This led to the erroneous conclusion that protraction-phase activity in the preparation was higher during spontaneously generated cycles.



Figure 6.1 Partial spike sorting failure during certain bursts

Voltage data recorded from a protraction-phase neuron during sucrose-induced fictive feeding. Spikes detected during spike sorting are shown in green. The firing rate of the neuron increases with each burst. This apparently results in significantly reduced spike amplitude during the latter part of bursts (also see Figure 3.1C). These low-amplitude spikes are missed by the spike sorting process (red arrows).

6.3 Feeding cycles

The identification of feeding cycles is another potentially confounding variable. Feeding cycles are generally identified manually even when data is recorded intracellularly, and spontaneously generated cycles in particular are sometimes hard to classify unambiguously (P. Benjamin, *personal communication*). Many preparations recorded on the MEA expressed feeding cycles with an unmistakable triphasic spatiotemporal structure that made their identification in the raw or spike sorted data straightforward (e.g. Figures 4.2Bii, 4.4A & B, 4.5A & B & D, 4.6). In other preparations feeding cycles had a different spatiotemporal structure, which was nevertheless stereotyped, varying little from cycle-to-cycle (e.g. Figure 4.4E, 5.1B-D). This simply suggests that a relatively random set of feeding CPG neurons are recorded in each preparation. Indeed, preparations that include atypical neurons (e.g. neurons that fire two bursts in each cycle, as the second neuron from the top in Figure 5.1B) are important, because localizing and subsequently recording from such neurons intracellularly may lead to the identification of new or overlooked components of the feeding CPG. In yet other preparations however some phasic population bursts were too variable or involved too few neurons to be confidently identified as feeding cycles. In some of these preparations it was possible to identify one or two 'canonical' feeding cycles (usually induced by sucrose or dopamine) and then check whether other phasic population bursts had a sufficiently similar spatiotemporal structure to also be considered feeding cycles. Preparations where no such canonical burst could be identified were typically excluded.

The ideal solution would be a method for quantitatively identifying feeding cycles in a way that satisfies subsequent visual analysis by persons familiar with the CPG and the MEA recording method. A simple threshold applied to the total raw or spike sorted firing rate captures a majority of visually identified feeding cycles but struggles with out-of-phase bursting, 'failed' feeding cycles (e.g. Figure 4.4B), and multiple detection of individual cycles. Applying such a threshold to the first principal component of spike sorted data improves performance only marginally. One approach that should be explored is to take the multi-neuronal spike rate structure of a canonical burst in a recording and use that template to identify how closely the activity of all neurons resemble that template at other points in the recording. Presumably a sliding

window of 10 s (the approximate duration of a feeding cycle) would be used and the auto-correlation of each neuron within that window combined to give a single value for each time point. However, as recordings from different molluskan systems show, there is considerable and probably instrumental cycle-to-cycle variability in the buccal feeding circuit (Elliott and Andrew, 1991; Horn et al., 2004). Attempting to identify a 'canonical' template cycle may therefore be to fundamentally misunderstand the function of such systems (Brembs, 2011; Brezina et al., 2006; Horn et al., 2004).

6.4 The NRP

A main finding of the work presented in this thesis is that the cycles of the feeding CPG are almost invariably followed by a transient cessation of all spiking recorded on the MEA. This phenomenon can be observed in individual intracellular recordings from identified motoneurons including the B2, B5 and B7 types (Benjamin and Rose, 1979) but appears to have been overlooked, presumably because it had not previously been observed in the simultaneous activity of many neurons.

Periods of quiescence following activation of a CPG have previously been observed in the spinal locomotor CPGs of the rat, chick and frog tadpole (Darbon et al., 2002; Darbon et al., 2003; Fedirchuk et al., 1999; Streit et al., 2006; Tabak et al., 2001; Zhang and Sillar, 2012) (see Figure 1.2). In these systems the sodium influx associated with population bursts triggers upregulation of the Na/K-pump. The hyperpolarizing effect of the pump is reason for the NRP: the effect outlasts the end of the population bursts, produces a transient cessation of spiking activity in affected neurons, and makes the CPG refractory to activation by electrical stimulation (Streit et al., 2006). Attempts to activate the feeding CPG by stimulating the dopamine-containing dorsobuccal nerve demonstrated that the feeding CPG too is refractory during the quiescent period (see Section 5.2).

In the locomotor CPG of the rat the post-burst hyperpolarization appears to be limited to intrinsically spiking neurons (Streit et al., 2006). Since intrinsic spiking and recurrent excitation are the pattern generating mechanisms of the CPG, this explains why the NRP limits the frequency of rhythmic activity and makes the circuit refractory to activation. This mechanism may also regulate the rate of feeding in *Lymnaea*. The population of tonically active neurons in the buccal ganglia likely includes B2 and B7

type neurons. B7 neurons are numerous in the buccal ganglia and many of them are electrically connected to the pattern initiating N1M type interneurons (Staras et al., 1998). Hyperpolarization of such B7 neurons prevents cycling of the feeding CPG (Staras et al., 1998). B2 type neurons on the other hand use nitric oxide as a transmitter, the only transmitter other than dopamine known to be necessary and sufficient for acceleration of the feeding CPG (Elphick et al., 1995). Thus both neuron types directly promote generation of the feeding motor pattern. Both neuron types also accelerate their firing rate during fictive feeding (Benjamin and Rose, 1979). It is therefore plausible that a Na/K-pump-dependent hyperpolarization of these two neuron types might induce a transient cessation of their intrinsic activity following feeding cycles and thus an inhibition of further feeding cycles. A test of this hypothesis would be to record from these neurons (intracellularly, so that neuronal identity can be established on the basis of synaptic inputs) during application of an inhibitor of the Na/K-pump such as strophanthidin. This treatment should attenuate the NRP and also accelerate the rate of fictive feeding.

A Na/K-pump-dependent mechanism that modulates tonically active, feeding pattern initiating neurons is also compatible with the stimulating effects of food and dopamine on the cycling rate of the feeding circuit. Dopamine is known to exert an inhibitory effect on the Na/K-pump in neurons (Bertorello et al., 1990) and inhibition of the pump depolarises neurons (Darbon et al., 2003). Increased concentrations of dopamine in the buccal ganglia might therefore reduce the NRP of tonically active, pattern initiating neurons, such as the B7 and B2 types, and consequently increase the probability that N1M interneurons overcome inhibitory input from the N3t interneurons and initiate a cycle of feeding. During spontaneous exploratory feeding, dopaminergic input to the feeding circuit would be low and the NRP and ICI would be substantial. When the sampling of the environment results in ingestion of nutritious food into the esophagus, dopamine levels would rise, inhibiting the Na/K-pump-mediated NRP in pattern-initiating neurons and enabling a faster rate of feeding. This mechanism of Na/K-pump-based adaptation to reward is summarized in Figure 6.2. Given the ubiquity of the Na/K-pump protein in the nervous system this may be a very general mechanism by which dopamine-modulated CPGs adapt their rate of cycling to the level of sensory reward.

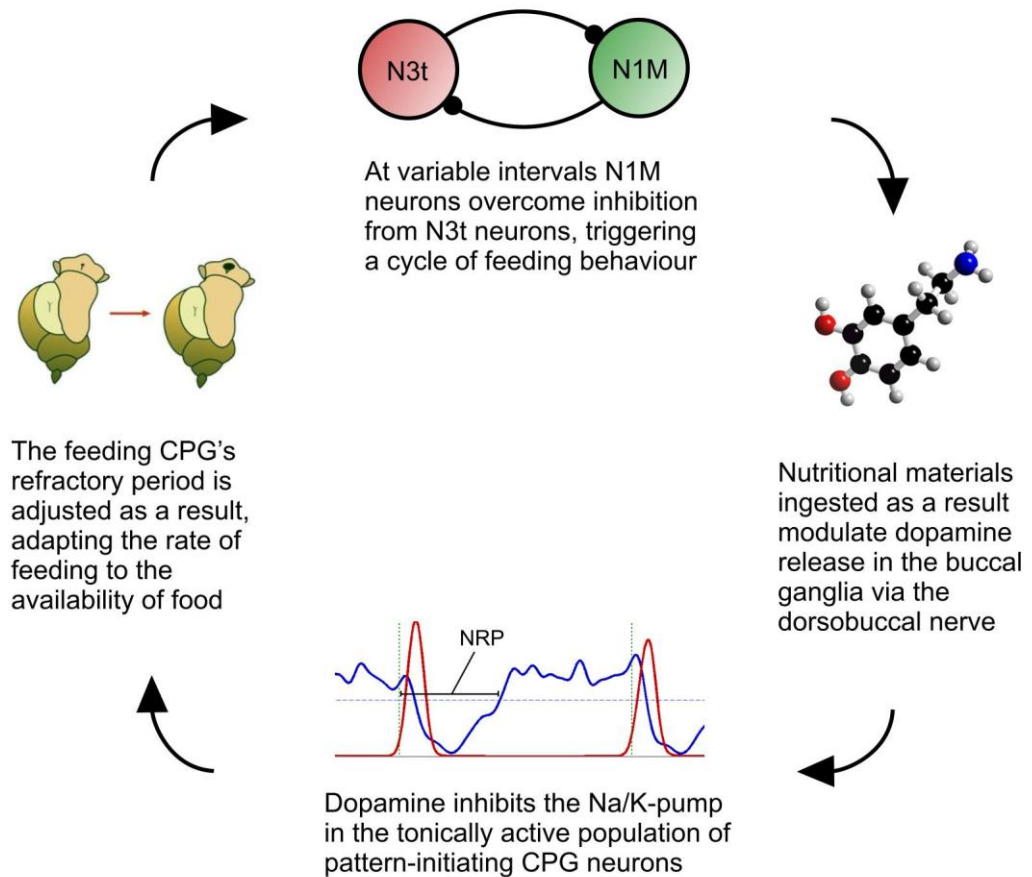


Figure 6.2 NRP-based mechanism for adapting CPG output to reward

This figure summarizes the proposed mechanism for how dopamine-mediated food reward modulates the activity of the feeding CPG. The drawing of *Lymnaea* is adapted from Benjamin, 2008.

It is not entirely clear what to make of the predictive properties of the NRP, the duration of which was significantly correlated with the subsequent amount of time required by the CPG to generate another feeding cycle. On the one hand it fits well with the idea that the resumption of activity in pattern-initiating neurons, such as the B7 and B2 types, promotes or even triggers subsequent cycles of feeding. The process might even include gradual recruitment of tonically active neurons by recurrent excitation, as in locomotor CPGs. On the other hand, such a predictive, straightforwardly deterministic mechanism has not to my knowledge been proposed in any spontaneously active neural system (with the possible exception of the 'readiness potential' (Libet, 1985; Soon et al., 2008)). Then again, this may be explained by the fact that the neuronal populations in which the NRP has previously been observed do not express the kind of variable ICI that characterizes the molluskan feeding CPG. Figure 5.5 shows the ICI distributions for the different conditions and highlights the considerable spread of the spontaneously generated ICIs. Even within individual preparations the standard deviation of the spontaneously generated ICIs was quite substantial; 53 ± 31 s (mean \pm standard deviation, $n = 151$ pairs of spontaneously generated feeding cycles recorded in 31 preparations). Spread of the data is of course required for effective prediction. It should also be pointed out that the word 'prediction' may be misinterpreted: the ability to predict a later event from an earlier event does not *necessarily* imply a causal relationship between the two, but may be due to a third mechanism common to both. The argument presented in this thesis is that the NRP indeed causally determines the duration of the ICI, but this conclusion remains hypothetical and further research is required, as outlined above.

Figure 6.3 is a summary diagram showing the correlation between the NRP and the time to the next feeding cycle for all ICI durations and all conditions. Within the different conditions the correlation was strongest for spontaneously generated feeding cycles with an ICI of 2 min or less ($r^2 = 0.32$, $p < 0.001$, $n = 37$, Pearson's linear correlation coefficient). A significant correlation was not observed when only sucrose- or dopamine-induced cycles were considered, which is not surprising, given that the spread of the ICIs was so small in these conditions (Figure 5.5). More variable stimulus-induced ICIs might be achieved by using lower concentrations of sucrose or dopamine. A significant correlation *was* observed when spontaneously generated ICIs (of all

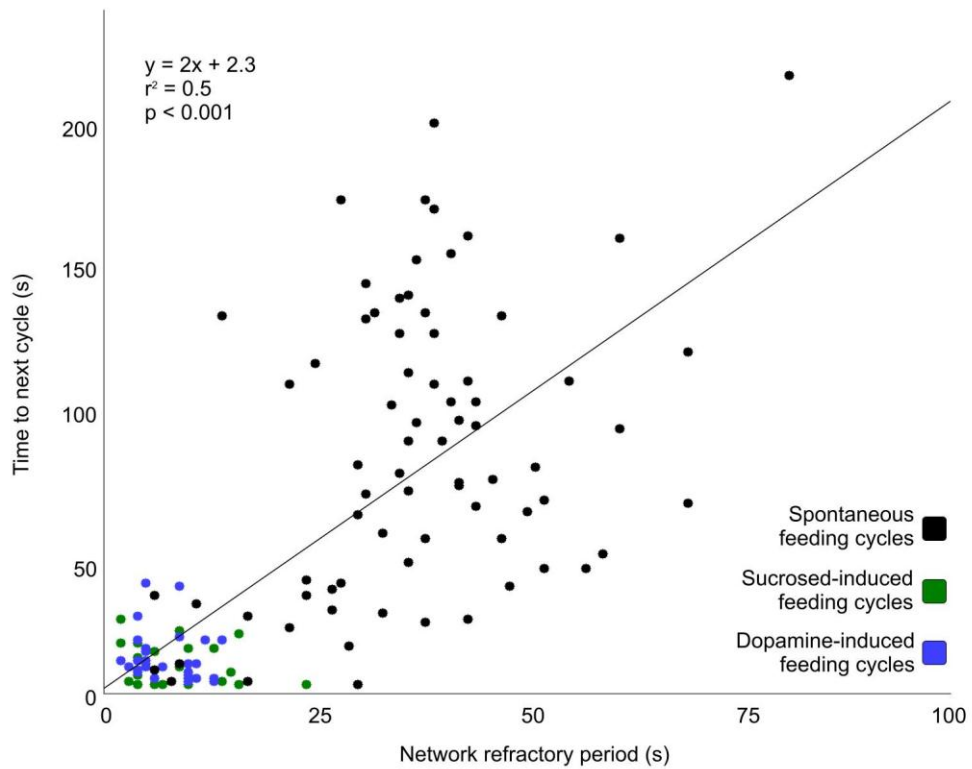


Figure 6.3 NRP vs. remaining ICIs, all durations and conditions

NRP plotted against the remaining ICI (all durations and conditions) shows a significant correlation ($r^2 = 0.5$, $p < 0.001$, $n = 138$, Pearson's linear correlation coefficient). The solid line represents best-fit linear regression.

durations) were considered but it was weak ($r^2 = 0.15$, $p < 0.001$, $n = 76$ pairs of feeding cycles, Pearson's linear correlation coefficient). The reason for the weakness of the correlation appears to be that beyond the 2 min period activity in the tonically active population often 'faltered' and dropped below the population average for extended periods before 'resurfacing' prior to the subsequent feeding cycle. This produced a number of what might be called 'false starts', where a build-up of tonic activity was not followed by the expected feeding cycle on the first 'attempt'. At other times tonically active neurons resumed firing following a feeding cycle and remained active but were simply not followed by another cycle until much later. These patterns of activity resulted in long ICIs relative to NRP and reduced the strength of the predictive correlation for ICIs exceeding 2 min. These observations serve as an important reminder that mechanisms other than the NRP contribute to the generation of feeding cycles. They indicate that the NRP may act as a gating mechanism.

One experiment that may shed some light on the function and predictive property of the NRP is to conduct extended (1-2 hr) recordings of individual preparations. Although the NRP was predictive of subsequent cycles in 3 or 4 individual preparations the majority of preparations did not have enough time to generate a sufficient number of feeding cycles in the period of spontaneously generated activity for such prediction to be possible. Long recordings would also allow other analyses. For example, the duration of the NRP of the frog tadpole locomotor CPG is proportional to the size of the previous population burst (Zhang and Sillar, 2012). Such a relationship was not observed in the data discussed here, but given the random sampling of phasically active neurons on the MEA there was no reasonable way of comparing the 'size' of feeding cycles generated in different preparations. Longer recordings would allow proper statistical analysis of burst size within individual preparations.

6.5 Conclusion

The aim of this thesis was to study population-level mechanisms that might explain how CPGs adapt to dopamine-mediated sensory reward. The MEA method that was developed is a relatively quick and easy way of recording the spiking patterns of multiple neurons on the surface of the intact brain of *Lymnaea*. Use of semi-intact preparations with active sensory receptors allowed the effects of chemosensory stimuli

to be monitored on the MEA. The acceleration of the feeding CPG that follows application of a sensory sucrose reward was shown to depend on dopamine signalling, and similar acceleration could be induced by direct application of dopamine to the brain. Fictive feeding could also be induced by a variety of other methods including intracellular depolarisation of a cerebral interneuron, stimulation of a dopaminergic nerve, and (following *in vitro* conditioning) by a conditioned taste stimulus.

Importantly, the MEA revealed that fictive feeding cycles are followed by a transient but very wide-spread cessation of spiking activity in the buccal ganglia. The duration of this quiescent period often predicted the timing of subsequent spontaneously generated cycles of feeding. Stimulation of a nerve that mediates food stimuli failed to activate the CPG during the quiescent period, indicating that the period is an NRP, a population-level mechanism previously shown to control cycling frequency in locomotor CPGs. Critically, both the sensory sucrose stimulus and the dopamine stimulus significantly shortened the NRP. The processes thought to underlie the NRP are ubiquitous in neural systems, suggesting that the reward-sensitive NRP observed here may be a general mechanism by which goal-oriented CPGs adapt their rate of cycling to maximise adaptive fitness.

References

Ahrens, M.B., Li, J.M., Orger, M.B., Robson, D.N., Schier, A.F., Engert, F., and Portugues, R. (2012). Brain-wide neuronal dynamics during motor adaptation in zebrafish. *Nature* 485, 471-477.

Alexander, J., Jr., Audesirk, T.E., and Audesirk, G.J. (1984). One-trial reward learning in the snail *Lymnaea stagnalis*. *J Neurobiol* 15, 67-72.

Ascher, P. (1972). Inhibitory and excitatory effects of dopamine on *Aplysia* neurones. *J Physiol* 225, 173-209.

Barron, A.B., Sovik, E., and Cornish, J.L. (2010). The roles of dopamine and related compounds in reward-seeking behavior across animal phyla. *Front Behav Neurosci* 4, 163.

Bayer, H.M., and Glimcher, P.W. (2005). Midbrain dopamine neurons encode a quantitative reward prediction error signal. *Neuron* 47, 129-141.

Benjamin, P.R. (2008). *Lymnaea stagnalis*, pp. 4124.

Benjamin, P.R. (2012). Distributed network organization underlying feeding behavior in the mollusk *Lymnaea*. *Neural systems & circuits* 2, 4.

Benjamin, P.R., and Rose, R.M. (1979). Central generation of bursting in the feeding system of the snail, *Lymnaea stagnalis*. *J Exp Biol* 80, 93-118.

Benjamin, P.R., Staras, K., and Kemenes, G. (2010). What roles do tonic inhibition and disinhibition play in the control of motor programs? *Front Behav Neurosci* 4, 30.

Bertorello, A.M., Hopfield, J.F., Aperia, A., and Greengard, P. (1990). Inhibition by dopamine of (Na⁺)+K⁺ATPase activity in neostriatal neurons through D1 and D2 dopamine receptor synergism. *Nature* 347, 386-388.

Bhatt, D.H., McLean, D.L., Hale, M.E., and Fetcho, J.R. (2007). Grading movement strength by changes in firing intensity versus recruitment of spinal interneurons. *Neuron* 53, 91-102.

Bishop, M.P., Elder, S.T., and Heath, R.G. (1963). Intracranial self-stimulation in man. *Science* *140*, 394-396.

Bizzi, E., D'Avella, A., Saltiel, P., and Tresch, M. (2002). Modular organization of spinal motor systems. *Neuroscientist* *8*, 437-442.

Bizzi, E., Tresch, M.C., Saltiel, P., and d'Avella, A. (2000). New perspectives on spinal motor systems. *Nature Reviews Neuroscience* *1*, 101-108.

Bovbjerg, R.V. (1968). Responses to Food in Lymnaeid Snails. *Physiological Zoology* *41*, 412-&.

Brembs, B. (2011). Towards a scientific concept of free will as a biological trait: spontaneous actions and decision-making in invertebrates. *Proceedings Biological sciences / The Royal Society* *278*, 930-939.

Brembs, B., Lorenzetti, F.D., Reyes, F.D., Baxter, D.A., and Byrne, J.H. (2002). Operant reward learning in *Aplysia*: Neuronal correlates and mechanisms. *Science* *296*, 1706-1709.

Brezina, V., Proekt, A., and Weiss, K.R. (2006). Cycle-to-cycle variability as an optimal behavioral strategy. *Neurocomputing* *69*, 1120-1124.

Briggman, K.L., and Kristan, W.B. (2008). Multifunctional pattern-generating circuits. *Annual review of neuroscience* *31*, 271-294.

Briggman, K.L., and Kristan, W.B., Jr. (2006). Imaging dedicated and multifunctional neural circuits generating distinct behaviors. *The Journal of neuroscience : the official journal of the Society for Neuroscience* *26*, 10925-10933.

Carter, K.M., George, J.S., and Rector, D.M. (2004). Simultaneous birefringence and scattered light measurements reveal anatomical features in isolated crustacean nerve. *J Neurosci Methods* *135*, 9-16.

Cools, R., and Robbins, T.W. (2004). Chemistry of the adaptive mind. *Philosophical transactions Series A, Mathematical, physical, and engineering sciences* *362*, 2871-2888.

Crofts, H.S., Dalley, J.W., Collins, P., Van Denderen, J.C., Everitt, B.J., Robbins, T.W., and Roberts, A.C. (2001). Differential effects of 6-OHDA lesions of the frontal cortex and caudate nucleus on the ability to acquire an attentional set. *Cerebral cortex* *11*, 1015-1026.

Darbon, P., Scicluna, L., Tschertter, A., and Streit, J. (2002). Mechanisms controlling

bursting activity induced by disinhibition in spinal cord networks. *The European journal of neuroscience* *15*, 671-683.

Darbon, P., Tschertter, A., Yvon, C., and Streit, J. (2003). Role of the electrogenic Na/K pump in disinhibition-induced bursting in cultured spinal networks. *Journal of neurophysiology* *90*, 3119-3129.

Djurfeldt, M., Ekeberg, O., and Graybiel, A.M. (2001). Cortex-basal ganglia interaction and attractor states. *Neurocomputing* *38*, 573-579.

Dudman, J.T., Eaton, M.E., Rajadhyaksha, A., Macias, W., Taher, M., Barczak, A., Kameyama, K., Huganir, R., and Konradi, C. (2003). Dopamine D1 receptors mediate CREB phosphorylation via phosphorylation of the NMDA receptor at Ser897-NR1. *Journal of Neurochemistry* *87*, 922-934.

Edelman, G.M. (1993). Neural Darwinism: selection and reentrant signaling in higher brain function. *Neuron* *10*, 115-125.

Elekes, K., Kemenes, G., Hiripi, L., Geffard, M., and Benjamin, P.R. (1991). Dopamine-immunoreactive neurones in the central nervous system of the pond snail *Lymnaea stagnalis*. *The Journal of comparative neurology* *307*, 214-224.

Elliott, C.J., and Benjamin, P.R. (1989). Esophageal mechanoreceptors in the feeding system of the pond snail, *Lymnaea stagnalis*. *Journal of neurophysiology* *61*, 727-736.

Elliott, C.J., and Susswein, A.J. (2002). Comparative neuroethology of feeding control in molluscs. *J Exp Biol* *205*, 877-896.

Elliott, C.J.H., and Andrew, T. (1991). Temporal Analysis of Snail Feeding Rhythms - a 3-Phase Relaxation-Oscillator. *Journal of Experimental Biology* *157*, 391-408.

Elphick, M.R., Kemenes, G., Staras, K., and O'Shea, M. (1995). Behavioral role for nitric oxide in chemosensory activation of feeding in a mollusc. *J Neurosci* *15*, 7653-7664.

Emlen, J.M. (1966). The role of time and energy in food preference. *The American Naturalist* *100*, 611-617.

Fedirchuk, B., Wenner, P., Whelan, P.J., Ho, S., Tabak, J., and O'Donovan, M.J. (1999). Spontaneous network activity transiently depresses synaptic transmission in the embryonic chick spinal cord. *J Neurosci* *19*, 2102-2112.

Fiorillo, C.D., Tobler, P.N., and Schultz, W. (2003). Discrete coding of reward

probability and uncertainty by dopamine neurons. *Science* 299, 1898-1902.

Fouriez, G., and Wise, R.A. (1976). Pimozide-induced extinction of intracranial self-stimulation: response patterns rule out motor or performance deficits. *Brain research* 103, 377-380.

Glimcher, P.W. (2011). Understanding dopamine and reinforcement learning: the dopamine reward prediction error hypothesis. *Proceedings of the National Academy of Sciences of the United States of America* 108 *Suppl 3*, 15647-15654.

Grillner, S. (2006). Biological pattern generation: the cellular and computational logic of networks in motion. *Neuron* 52, 751-766.

Gross, G.W. (1979). Simultaneous single unit recording in vitro with a photoetched laser deinsulated gold multimicroelectrode surface. *IEEE transactions on bio-medical engineering* 26, 273-279.

Harris, C.A., Buckley, C.L., Nowotny, T., Passaro, P.A., Seth, A.K., Kemenes, G., and O'Shea, M. (2012). Multi-neuronal refractory period adapts centrally generated behaviour to reward. *PLoS ONE* 7, e42493.

Harris, C.A., and Kilarski, L.L. (2009). A Novel, Web-Based Approach To Public Participation in Neuromodulation Research. Paper presented at: 9th World Conference of the International Neuromodulation Society (Seoul, South Korea).

Harris, C.A., Passaro, P.A., Kemenes, I., Kemenes, G., and O'Shea, M. (2010). Sensory driven multi-neuronal activity and associative learning monitored in an intact CNS on a multielectrode array. *Journal of neuroscience methods* 186, 171-178.

Hill, E.S., Wang, J., and Frost, W.N. (2009). Large-scale optical recording reveals neurons that wander in and out of a rhythmic motor network. Paper presented at: 39th Annual Meeting of the Society for Neuroscience.

Hills, T., Brockie, P.J., and Maricq, A.V. (2004). Dopamine and glutamate control area-restricted search behavior in *Caenorhabditis elegans*. *J Neurosci* 24, 1217-1225.

Hills, T.T. (2006). Animal foraging and the evolution of goal-directed cognition. *Cogn Sci* 30, 3-41.

Hodgkin, A.L., and Huxley, A.F. (1939). Action potentials recorded from inside a nerve fibre. *Nature* 144, 710-711.

Hodgkin, A.L., and Huxley, A.F. (1952). A Quantitative Description of Membrane Current and Its Application to Conduction and Excitation in Nerve. *Journal of*

Physiology-London 117, 500-544.

Horn, C.C., Zhurov, Y., Orekhova, I.V., Proekt, A., Kupfermann, I., Weiss, K.R., and Brezina, V. (2004). Cycle-to-cycle variability of neuromuscular activity in *Aplysia* feeding behavior. *Journal of neurophysiology* 92, 157-180.

Ikegaya, Y., Aaron, G., Cossart, R., Aronov, D., Lampl, I., Ferster, D., and Yuste, R. (2004). Synfire chains and cortical songs: temporal modules of cortical activity. *Science* 304, 559-564.

Johansen, B.E. (2005). Exploring Reinforcement Processes using Intra-Cranial Self-Stimulation. 115-120.

Kabotyanski, E.A., Baxter, D.A., Cushman, S.J., and Byrne, J.H. (2000). Modulation of fictive feeding by dopamine and serotonin in *aplysia*. *Journal of Neurophysiology* 83, 374-392.

Kandel, E.R. (2001). The molecular biology of memory storage: a dialogue between genes and synapses. *Science* 294, 1030-1038.

Kemenes, G., Elliott, C.J.H., and Benjamin, P.R. (1986). Chemical and Tactile Inputs to the *Lymnaea* Feeding System - Effects on Behavior and Neural Circuitry. *Journal of Experimental Biology* 122, 113-137.

Kemenes, G., Staras, K., and Benjamin, P.R. (2001). Multiple types of control by identified interneurons in a sensory-activated rhythmic motor pattern. *J Neurosci* 21, 2903-2911.

Kemenes, I., O'Shea, M., and Benjamin, P.R. (2011). Different circuit and monoamine mechanisms consolidate long-term memory in aversive and reward classical conditioning. *The European journal of neuroscience* 33, 143-152.

Kim, K.M., Baratta, M.V., Yang, A., Lee, D., Boyden, E.S., and Fiorillo, C.D. (2012). Optogenetic mimicry of the transient activation of dopamine neurons by natural reward is sufficient for operant reinforcement. *PloS one* 7, e33612.

Kim, Y.C., Lee, H.G., and Han, K.A. (2007). Classical reward conditioning in *Drosophila melanogaster*. *Genes Brain Behav* 6, 201-207.

Kispersky, T., Gutierrez, G.J., and Marder, E. (2011). Functional connectivity in a rhythmic inhibitory circuit using Granger causality. In *Neural systems & circuits*.

Kojima, S., Hosono, T., Fujito, Y., and Ito, E. (2001). Optical detection of neuromodulatory effects of conditioned taste aversion in the pond snail *Lymnaea*

stagnalis. *J Neurobiol* 49, 118-128.

Kyriakides, M.A., and McCrohan, C.R. (1988). Central Coordination of Buccal and Pedal Neuronal-Activity in the Pond Snail *Lymnaea-Stagnalis*. *Journal of Experimental Biology* 136, 103-123.

Kyriakides, M.A., and McCrohan, C.R. (1989). Effect of Putative Neuromodulators on Rhythmic Buccal Motor Output in *Lymnaea-Stagnalis*. *Journal of Neurobiology* 20, 635-650.

Levi, R., Varona, P., Arshavsky, Y.I., Rabinovich, M.I., and Selverston, A.I. (2004). Dual sensory-motor function for a molluskan statocyst network. *J Neurophysiol* 91, 336-345.

Levi, R., Varona, P., Arshavsky, Y.I., Rabinovich, M.I., and Selverston, A.I. (2005). The role of sensory network dynamics in generating a motor program. *J Neurosci* 25, 9807-9815.

Libet, B. (1985). Unconscious cerebral initiative and the role of conscious will in voluntary action. *Behavioural and Brain Sciences* 8, 529-539.

Lindskog, M., Kim, M., Wikstrom, M.A., Blackwell, K.T., and Kotaleski, J.H. (2006). Transient calcium and dopamine increase PKA activity and DARPP-32 phosphorylation. *PLoS computational biology* 2, e119.

Lisman, J.E., and Grace, A.A. (2005). The hippocampal-VTA loop: controlling the entry of information into long-term memory. *Neuron* 46, 703-713.

Ljungberg, T., and Enquist, M. (1987). Disruptive effects of low doses of d-amphetamine on the ability of rats to organize behaviour into functional sequences. *Psychopharmacology* 93, 146-151.

MacArthur, R.H., and Pianka, E.R. (1966). On optimal use of a patchy environment. *The American Naturalist* 100, 603-609.

Marder, E., and Bucher, D. (2001). Central pattern generators and the control of rhythmic movements. *Current biology : CB* 11, R986-996.

Marder, E., and Bucher, D. (2007). Understanding circuit dynamics using the stomatogastric nervous system of lobsters and crabs. *Annu Rev Physiol* 69, 291-316.

Marra, V., Kemenes, I., Vavoulis, D., Feng, J., O'Shea, M., and Benjamin, P.R. (2010). Role of tonic inhibition in associative reward conditioning in *lymnaea*. *Frontiers in behavioral neuroscience* 4.

McCrohan, C. (1984). Initiation of feeding motor output by an identified interneurone in the snail *Lymnaea stagnalis*. *Journal of Experimental Biology* *113*, 351-366.

McLean, D.L., Fan, J., Higashijima, S., Hale, M.E., and Fetcho, J.R. (2007). A topographic map of recruitment in spinal cord. *Nature* *446*, 71-75.

Miller, E.W., Lin, J.Y., Frady, E.P., Steinbach, P.A., Kristan, W.B., Jr., and Tsien, R.Y. (2012). Optically monitoring voltage in neurons by photo-induced electron transfer through molecular wires. *Proceedings of the National Academy of Sciences of the United States of America* *109*, 2114-2119.

Nargeot, R., Baxter, D.A., and Byrne, J.H. (1997). Contingent-dependent enhancement of rhythmic motor patterns: an in vitro analog of operant conditioning. *The Journal of neuroscience : the official journal of the Society for Neuroscience* *17*, 8093-8105.

Nargeot, R., Le Bon-Jego, M., and Simmers, J. (2009). Cellular and network mechanisms of operant learning-induced compulsive behavior in *Aplysia*. *Current biology : CB* *19*, 975-984.

Niv, Y., Daw, N.D., Joel, D., and Dayan, P. (2007). Tonic dopamine: opportunity costs and the control of response vigor. *Psychopharmacology* *191*, 507-520.

Novak, J.L., and Wheeler, B.C. (1986). Recording from the *Aplysia* abdominal ganglion with a planar microelectrode array. *IEEE transactions on bio-medical engineering* *33*, 196-202.

Olds, J., and Milner, P. (1954). Positive reinforcement produced by electrical stimulation of septal area and other regions of rat brain. *Journal of comparative and physiological psychology* *47*, 419-427.

Passaro, P.A., Harris, C.A., Seth, A., O'Shea, M., and Husbands, P. (2008). Spike sorting and functional connectivity analysis using self-organizing maps and granger causality. In *Neuroinformatics 2008*.

Pine, J. (1980). Recording action potentials from cultured neurons with extracellular microcircuit electrodes. *Journal of neuroscience methods* *2*, 19-31.

Pouzat, C., Delescluse, M., Viot, P., and Diebolt, J. (2004). Improved spike-sorting by modeling firing statistics and burst-dependent spike amplitude attenuation: a Markov chain Monte Carlo approach. *J Neurophysiol* *91*, 2910-2928.

Prentice, J.S., Homann, J., Simmons, K.D., Tkacik, G., Balasubramanian, V., and Nelson, P.C. (2011). Fast, scalable, Bayesian spike identification for multi-electrode arrays. *PLoS one* 6, e19884.

Proekt, A., Brezina, V., and Weiss, K.R. (2004). Dynamical basis of intentions and expectations in a simple neuronal network. *Proc Natl Acad Sci U S A* 101, 9447-9452.

Qin, J., and Wheeler, A.R. (2007). Maze exploration and learning in *C. elegans*. *Lab Chip* 7, 186-192.

Quiroga, R.Q., Nadasdy, Z., and Ben-Shaul, Y. (2004). Unsupervised spike detection and sorting with wavelets and superparamagnetic clustering. *Neural computation* 16, 1661-1687.

Redgrave, P., and Gurney, K. (2006). The short-latency dopamine signal: a role in discovering novel actions? *Nature reviews Neuroscience* 7, 967-975.

Rose, R.M., and Benjamin, P.R. (1979). Relationship of the Central Motor Pattern to the Feeding Cycle of *Lymnaea-Stagnalis*. *Journal of Experimental Biology* 80, 137-163.

Schei, J.L., McCluskey, M.D., Foust, A.J., Yao, X.C., and Rector, D.M. (2008). Action potential propagation imaged with high temporal resolution near-infrared video microscopy and polarized light. *Neuroimage* 40, 1034-1043.

Schultz, W. (2007). Multiple dopamine functions at different time courses. *Annual review of neuroscience* 30, 259-288.

Schultz, W., Dayan, P., and Montague, P.R. (1997). A neural substrate of prediction and reward. *Science* 275, 1593-1599.

Selverston, A.I. (2010). Invertebrate central pattern generator circuits. *Philosophical transactions of the Royal Society of London Series B, Biological sciences* 365, 2329-2345.

Smith, J.C., Abdala, A.P., Rybak, I.A., and Paton, J.F. (2009). Structural and functional architecture of respiratory networks in the mammalian brainstem. *Philos Trans R Soc Lond B Biol Sci* 364, 2577-2587.

Soon, C.S., Brass, M., Heinze, H.J., and Haynes, J.D. (2008). Unconscious determinants of free decisions in the human brain. *Nat Neurosci* 11, 543-545.

Staras, K., Kemenes, G., and Benjamin, P.R. (1998). Pattern-generating role for motoneurons in a rhythmically active neuronal network. *The Journal of neuroscience* :

the official journal of the Society for Neuroscience *18*, 3669-3688.

Staras, K., Kemenes, I., Benjamin, P.R., and Kemenes, G. (2003). Loss of self-inhibition is a cellular mechanism for episodic rhythmic behavior. *Curr Biol* *13*, 116-124.

Stevenson, I.H., and Kording, K.P. (2011). How advances in neural recording affect data analysis. *Nature neuroscience* *14*, 139-142.

Stratton, P., Cheung, A., Wiles, J., Kiyatkin, E., Sah, P., and Windels, F. (2012). Action potential waveform variability limits multi-unit separation in freely behaving rats. *PLoS One* *7*, e38482.

Straub, V. (1999). In vitro study of a central pattern generator. In *School of Life Sciences (University of Sussex)*.

Streit, J., Tscherter, A., and Darbon, P. (2006). Rhythm generation in spinal cultures: is it the neuron or the network? In *Advances in Network Electrophysiology: Using Multi-Electrode Arrays*, M. Taketani, and M. Baudry, eds. (Springer).

Stringer, S.M., Rolls, E.T., Trappenberg, T.P., and de Araujo, I.E. (2003). Self-organizing continuous attractor networks and motor function. *Neural networks : the official journal of the International Neural Network Society* *16*, 161-182.

Tabak, J., Rinzel, J., and O'Donovan, M.J. (2001). The role of activity-dependent network depression in the expression and self-regulation of spontaneous activity in the developing spinal cord. *J Neurosci* *21*, 8966-8978.

Teyke, T., Rosen, S.C., Weiss, K.R., and Kupfermann, I. (1993). Dopaminergic neuron B20 generates rhythmic neuronal activity in the feeding motor circuitry of *Aplysia*. *Brain Res* *630*, 226-237.

Thomas, C.A., Jr., Springer, P.A., Loeb, G.E., Berwald-Netter, Y., and Okun, L.M. (1972). A miniature microelectrode array to monitor the bioelectric activity of cultured cells. *Experimental cell research* *74*, 61-66.

Tsai, H.C., Zhang, F., Adamantidis, A., Stuber, G.D., Bonci, A., de Lecea, L., and Deisseroth, K. (2009). Phasic Firing in Dopaminergic Neurons Is Sufficient for Behavioral Conditioning. *Science* *324*, 1080-1084.

Tsyganov, V.V., and Sakharov, D.A. (2000). Locomotor rhythms in the pond snail *Lymnaea stagnalis*: Site of origin and neurotransmitter requirements. *Acta Biologica Hungarica* *51*, 189-195.

Tuersley, M.D., and McCrohan, C.R. (1987). Food Arousal in the Pond Snail,

Lymnaea-Stagnalis. Behavioral and Neural Biology 48, 222-236.

Wagenaar, D.A., Hamilton, M.S., Huang, T., Kristan, W.B., and French, K.A. (2010). A hormone-activated central pattern generator for courtship. Curr Biol 20, 487-495.

Wagenaar, D.A., Pine, J., and Potter, S.M. (2006). An extremely rich repertoire of bursting patterns during the development of cortical cultures. BMC neuroscience 7, 11.

Vavoulis, D.V., Straub, V.A., Kemenes, I., Kemenes, G., Feng, J.F., and Benjamin, P.R. (2007). Dynamic control of a central pattern generator circuit: a computational model of the snail feeding network. European Journal of Neuroscience 25, 2805-2818.

Vehovszky, A., and Elliott, C.J. (2001). Activation and reconfiguration of fictive feeding by the octopamine-containing modulatory OC interneurons in the snail Lymnaea. J Neurophysiol 86, 792-808.

White, N.M. (1989). Reward or reinforcement: what's the difference? Neurosci Biobehav Rev 13, 181-186.

Wilson, D.M. (1961). The Central Nervous Control of Flight in a Locust. Journal of Experimental Biology 38, 471-490.

Winlow, W., and Haydon, P.G. (1986). A Behavioral and Neuronal Analysis of the Locomotory System of Lymnaea-Stagnalis. Comparative Biochemistry and Physiology a-Physiology 83, 13-21.

Wise, R.A. (1996). Addictive drugs and brain stimulation reward. Annu Rev Neurosci 19, 319-340.

Wise, R.A. (2006). Role of brain dopamine in food reward and reinforcement. Philosophical transactions of the Royal Society of London Series B, Biological sciences 361, 1149-1158.

Wise, R.A. (2009). Reinforcement. In Scholarpedia, pp. 2450.

Volkow, N.D., Wang, G.J., Newcorn, J., Telang, F., Solanto, M.V., Fowler, J.S., Logan, J., Ma, Y., Schulz, K., Pradhan, K., *et al.* (2007). Depressed dopamine activity in caudate and preliminary evidence of limbic involvement in adults with attention-deficit/hyperactivity disorder. Archives of general psychiatry 64, 932-940.

Yao, X.C., Foust, A., Rector, D.M., Barrowes, B., and George, J.S. (2005). Cross-polarized reflected light measurement of fast optical responses associated with neural activation. Biophys J 88, 4170-4177.

Yuste, R. (2008). Circuit neuroscience: the road ahead. Front Neurosci 2, 6-9.

Yuste, R., MacLean, J.N., Smith, J., and Lansner, A. (2005). The cortex as a central pattern generator. *Nature reviews Neuroscience* 6, 477-483.

Zhang, H.Y., and Sillar, K.T. (2012). Short-term memory of motor network performance via activity-dependent potentiation of Na⁺/K⁺ pump function. *Curr Biol* 22, 526-531.

Appendix

Science communication

Rapid advances in science and technology are increasing both the need and the opportunity for effective science communication and public participation in science (Maesele, 2007). Many research grants, including those from the Research Councils of the United Kingdom that supported the work presented in this thesis, come with provisions requiring grantees to engage the public in their research. This appendix describes a web-based science communication project I conducted during my doctoral studies. The first aim of the project was to provide accessible information about the research presented in this thesis and about the neuroscience of dopamine and reward generally. The second aim was to engage with the public about possible medical applications of rewarding brain stimulation (RBS, introduced in Section 1.2). The outcome of the project was presented at the 9th World Conference of the International Neuromodulation Society (Harris and Kilarski, 2009).

A.1 Communicating dopamine and reward neuroscience

There is today considerable public interest in dopamine and the neuroscience of reward. To make the most of this I produced two videos entitled ‘What is dopamine?’ and ‘Dopamine and the frontal lobes’. These describe in broad terms the neuroscience of dopamine and reward (see Section 1.2). They have been viewed more than a quarter million times since they were first uploaded in 2009 and are the first two videos returned by a YouTube search for the term ‘dopamine’. A third video entitled ‘Spontaneous and dopamine-driven brain activity’ was created in 2010. Here I used the JFugue 4.0.3 library to convert spike rate data from the MEA into musical tracks which I

combined with the output from the parameter display function in MC_Rack. This resulted in an audiovisual rendering of neural data recorded on the buccal ganglia and on the wider dorsal surface of the *Lymnaea* CNS. In addition to these videos I also co-host the dopamine page on Facebook, with one other person. Here we post articles and relevant media, and answer questions about dopamine and reward neuroscience. The page currently has more than 5000 subscribers.

A.2 The iPlant project

Deep brain stimulation is increasingly applied to the reward pathway in order to treat patients who suffer from obsessive-compulsive disorder (Goodman et al., 2010; Greenberg et al., 2010; Haq et al., 2011; Huff et al., 2010), depression (Bewernick et al., 2010; Malone et al., 2009; Schlaepfer et al., 2008) and other psychiatric conditions (Ackermans et al., 2008; Kuhn et al., 2007). The Reclaim implant for example, which is developed by Medtronic (US) and targets the nucleus accumbens, has recently received regulatory approval in the EU and US. This trend is expected to continue and has raised debate about the possibility of using deep brain stimulation implants to induce RBS in human patients (Oshima and Katayama, 2010; Synofzik et al., 2012). RBS has previously been used as a positive reinforcer to motivate rats to perform specific behaviours such as physical exercise (Burgess et al., 1991; Garner et al., 1991) and problem solving (Hermer-Vazquez et al., 2005). It has long been recognized that RBS might similarly be used to help human patients perform challenging but beneficial behaviours, but the associated concerns regarding safety and ethics are not well understood.

To engage with the public about the possibility of using RBS to assist human patients I and a collaborator ran a web project called 'iPlant' from 2007 to 2009. The project was organized around the concept of an iPlant - a hypothetical deep brain stimulation system for delivering RBS whenever a patient performs a challenging but beneficial behaviour such as physical exercise or learning. Use of the term iPlant to refer to such a system provided structure and focus for engaging with the public and allowed discussions about iPlants taking place online to be found and analysed (e.g. Figure A.1). The aim of the project was to provide concrete and accessible

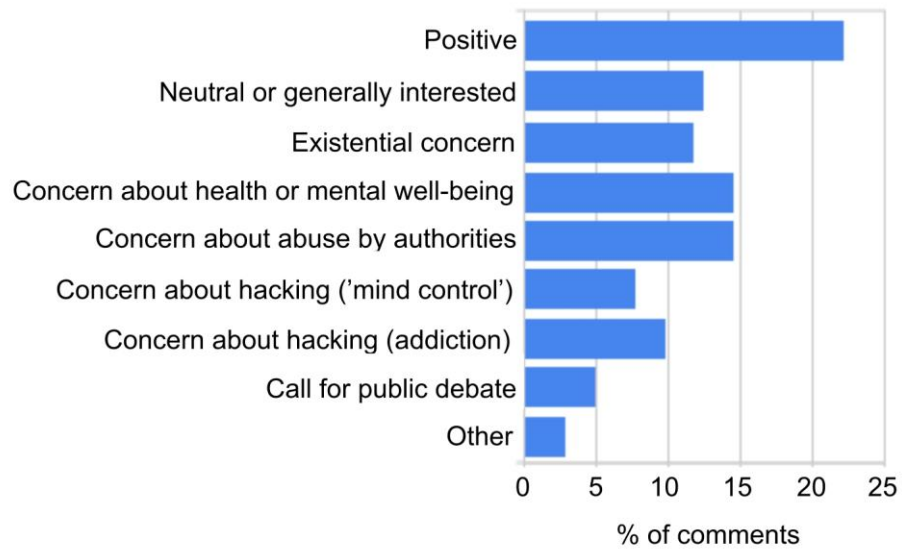


Figure A.1 Content of comments regarding a possible medical application of RBS

145 representative comments on the possibility of using RBS to help patients perform difficult but beneficial behaviours were collected in June and July 2009, and categorized based on their content. The comments were collected on forums and social media sites associated with the iPlant project, and on some independent weblogs. Most commentors brought up one of three concerns regarding safety (see text or www.iplant.eu).

information about how the RBS-based treatment would work and to engage with the public about the technology and associated issues. By such engagement, we hoped to gain a better understanding of the problems that might arise if RBS-based treatments were to be developed, and of how those problems might be addressed in accordance with public opinion.

Seven videos that describe RBS and its possible application to assist human patients were produced. Two of these are currently the first videos returned by a YouTube search for 'rewarding brain stimulation'. A website containing basic information and references about reward neuroscience, deep brain stimulation, RBS and the iPlant project was also created and is still maintained at www.iplant.eu. Written comments on the possibility of developing iPlants were collected on the site, on YouTube, on blogs and on various social media sites. These were used to develop the project further, e.g. to highlight and address recurring theoretical questions or issues regarding safety or ethics. Figure A.1 illustrates the diversity of the opinions we collected.

The project concluded that while deep brain stimulation-based RBS could probably be used to help motivate specific beneficial behaviours in patients, there are three recurring concerns regarding safety and ethics that would first have to be addressed. These hinge on the fact that iPlants depend on RBS being delivered if and only if a patient performs a specific behaviour. Commentors frequently raised the concern that patients would find ways to circumvent such restrictions and self-stimulate unconditionally and endlessly, or that malevolent individuals might take control of the behaviour of another person. A second class of concerns regards the possibility that governments or cultures might misuse iPlants by motivating citizens to engage in dangerous or demeaning behaviour, e.g. to conform to unreasonable standards of productivity. A third class of concerns highlights the possible negative impacts on health or natural self-discipline. Ways of addressing these concerns, often suggested by members of the public, have been made available online. The outcome of the project was presented at the 9th World Conference of the International Neuromodulation Society (Harris and Kilarski, 2009). Since that time the project has been more or less inactive, awaiting further developments in the field.

A.3 References

Ackermans, L., Temel, Y., and Visser-Vandewalle, V. (2008). Deep brain stimulation in Tourette's Syndrome. *Neurotherapeutics* 5, 339-344.

Bewernick, B.H., Hurlemann, R., Matusch, A., Kayser, S., Grubert, C., Hadrysiewicz, B., Axmacher, N., Lemke, M., Cooper-Mahkorn, D., Cohen, M.X., *et al.* (2010). Nucleus accumbens deep brain stimulation decreases ratings of depression and anxiety in treatment-resistant depression. *Biol Psychiatry* 67, 110-116.

Burgess, M.L., Davis, J.M., Borg, T.K., and Buggy, J. (1991). Intracranial self-stimulation motivates treadmill running in rats. *J Appl Physiol* 71, 1593-1597.

Garner, R.P., Terracio, L., Borg, T.K., and Buggy, J. (1991). Intracranial self-stimulation motivates weight-lifting exercise in rats. *J Appl Physiol* 71, 1627-1631.

Goodman, W.K., Foote, K.D., Greenberg, B.D., Ricciuti, N., Bauer, R., Ward, H., Shapira, N.A., Wu, S.S., Hill, C.L., Rasmussen, S.A., *et al.* (2010). Deep brain stimulation for intractable obsessive compulsive disorder: pilot study using a blinded, staggered-onset design. *Biol Psychiatry* 67, 535-542.

Greenberg, B.D., Gabriels, L.A., Malone, D.A., Jr., Rezai, A.R., Friehs, G.M., Okun, M.S., Shapira, N.A., Foote, K.D., Cosyns, P.R., Kubu, C.S., *et al.* (2010). Deep brain stimulation of the ventral internal capsule/ventral striatum for obsessive-compulsive disorder: worldwide experience. *Mol Psychiatry* 15, 64-79.

Haq, I.U., Foote, K.D., Goodman, W.G., Wu, S.S., Sudhyadhom, A., Ricciuti, N., Siddiqui, M.S., Bowers, D., Jacobson, C.E., Ward, H., *et al.* (2011). Smile and laughter induction and intraoperative predictors of response to deep brain stimulation for obsessive-compulsive disorder. *Neuroimage* 54 Suppl 1, S247-255.

Harris, C.A., and Kilarski, L.L. (2009). A Novel, Web-Based Approach To Public Participation in Neuromodulation Research. Paper presented at: 9th World Conference of the International Neuromodulation Society (Seoul, South Korea).

Hermer-Vazquez, L., Hermer-Vazquez, R., Rybinnik, I., Greebel, G., Keller, R., Xu, S., and Chapin, J.K. (2005). Rapid learning and flexible memory in "habit" tasks in rats trained with brain stimulation reward. *Physiol Behav* 84, 753-759.

Huff, W., Lenartz, D., Schormann, M., Lee, S.H., Kuhn, J., Koulousakis, A., Mai, J., Daumann, J., Maarouf, M., Klosterkötter, J., *et al.* (2010). Unilateral deep brain

stimulation of the nucleus accumbens in patients with treatment-resistant obsessive-compulsive disorder: Outcomes after one year. *Clin Neurol Neurosurg* 112, 137-143.

Kuhn, J., Lenartz, D., Huff, W., Lee, S., Koulousakis, A., Klosterkoetter, J., and Sturm, V. (2007). Remission of alcohol dependency following deep brain stimulation of the nucleus accumbens: valuable therapeutic implications? *J Neurol Neurosurg Psychiatry* 78, 1152-1153.

Malone, D.A., Jr., Dougherty, D.D., Rezai, A.R., Carpenter, L.L., Friehs, G.M., Eskandar, E.N., Rauch, S.L., Rasmussen, S.A., Machado, A.G., Kubu, C.S., *et al.* (2009). Deep brain stimulation of the ventral capsule/ventral striatum for treatment-resistant depression. *Biol Psychiatry* 65, 267-275.

Oshima, H., and Katayama, Y. (2010). Neuroethics of deep brain stimulation for mental disorders: brain stimulation reward in humans. *Neurol Med Chir (Tokyo)* 50, 845-852.

Schlaepfer, T.E., Cohen, M.X., Frick, C., Kosel, M., Brodesser, D., Axmacher, N., Joe, A.Y., Kreft, M., Lenartz, D., and Sturm, V. (2008). Deep brain stimulation to reward circuitry alleviates anhedonia in refractory major depression. *Neuropsychopharmacology* 33, 368-377.

Synofzik, M., Schlaepfer, T.E., and Fins, J.J. (2012). How Happy Is Too Happy? Euphoria, Neuroethics, and Deep Brain Stimulation of the Nucleus Accumbens. *AJOB Neuroscience* 3, 30-36.